VIBRATION TESTS OF STRUCTURES

Thesis by

Willard Otis Keightley

In Partial Filfillment of the Requirements

For the Degree of

Doctor of Philosophy

California Institute of Technology

Pasadena, California

1964

ACKNOWLEDGMENTS

The author is indebted to many persons for their personal assistance during the performance of the experimental work and the preparation of the manuscript. He is pleased at this time to acknowledge and to express his gratitude for this assistance.

Professors G. W. Housner and D. E. Hudson were the author's immediate advisors. Their guidance of the work, their personal efforts in certain phases of the work, and their suggestions and critical review of the manuscript are deeply appreciated.

Professor T. K. Caughey gave freely of his advice, and by his interest in the work was a source of encouragement. Professor C. W. McCormick provided certain digital computer solutions of indeterminate trusses, used in Part II. Mr. Robert Williams was of invaluable aid to the author on problems of instrumentation, and Mr. George Downs gave valuable advice on instrumentation. Mr. Kendrick Hebert was very helpful on problems on digital computing. Mr. Fred MacDonald and Mr. Ilhan Gozaydin spent many hours, often under an uncomfortably hot sun, assisting with the field work. Mr. N. N. Nielsen assisted with the field work at Dry Canyon Dam. The author is especially indebted to Mr. H. B. Hemborg of the Los Angeles Department of Water and Power. It was only through his active interest and cooperation that the tests at Encino and at Dry Canyon were made possible. The cooperation of Mr. Gene Boyd, resident engineer on the Encino Reservoir construction work, and of his staff is greatly appreciated. Mr. W. K. Cloud and Mr. C. Knudson, of the U. S. Coast and Geodetic Survey, made displacement measurements at Dry Canyon Dam. Mr. Jerry Morrill and Mr. Ron Dobner, of the U. S. Coast and Geodetic Survey,

furnished displacement measurements of the Encino Reservoir structure. Mr. David Leeds of the University of California, Los Angeles, contributed displacement measurements from Encino and from Dry Canyon. Mr. Don Laird aided in the construction of the laboratory structure described in Part IV, and Mr. R. W. Hanson assisted in testing the structure. Mrs. Etta Grinwis of Montana State College typed the final manuscript, and Mr. Fred Sanford was responsible for the ink tracings. Finally, the author wishes to express his appreciation to his wife for typing most of the original manuscript and for her forbearance and understanding during the entire project.

The financial burden of the field work was borne by the Earthquake Engineering Research Laboratory of the California Institute of Technology, with some transportation and assistance during the field installation of the shaking machines provided by the Department of Water and Power of the City of Los Angeles. The California State Division of Architecture kindly made available the shaking machines used for the tests at Encino and at Dry Canyon. Digital computer work was financed by the Division of Engineering and Applied Science of the California Institute of Technology. The author is grateful for the generous manner in which the work was supported.

During the course of this work the author received financial assistance from Science Faculty and Graduate Fellowships of the National Science Foundation and from the Ford Foundation Loan Fund for Engineering Teachers. This financial aid was important and is deeply appreciated.

ABSTRACT

Dynamic tests of three structures are described. In two cases linear vibration theory is applied to explain the behavior of the structures. In the third case a new method of analyzing the vibration records is introduced to define nonlinear properties of the structure.

Free and forced vibration tests were conducted on a reservoir outlet structure consisting of a reinforced concrete tower, 149 feet in height, with a steel truss bridge, 339 feet long, connected to the tower near the top. Measurements revealed five natural frequencies and mode shapes, and indicated the extent and significance of foundation movements. A detailed theoretical analysis of linear vibrations of the structure is carried out to show good agreement with the observations and to illustrate a general technique for the dynamic analysis of framed structures.

An earth dam 485 feet long by 60 feet in height by 450 feet thick at the base was subjected to a sinusoidal lateral exciting force at the top. Application of the theory of a truncated wedge vibrating in shear modes is made to determine an effective shear wave velocity in the earth fill and to estimate damping in the modes.

A general procedure is presented for experimentally determining the restoring and dissipating functions in lumped mass structures, linear or nonlinear. An experiment on a single degree of freedom laboratory structure with bolted joints is used to illustrate the method.

The question of instrumentation suitable for structural dynamic work is considered and recommendations are made on the basis of tests and examination of many commercially available components.

TABLE OF CONTENTS

LIST OF FIGURES

LIST OF TABLES

I. INTRODUCTION

Dynamic tests of structures are usually of two types: either an ad hoc test is made to determine how a particular structure responds to a particular force or an exploratory test is made, measuring the responses to applied forces, with the aim of discovering the dynamic properties of the structure so that its response to any force can be calculated. The latter type of test, of course, leads to results with the widest application and does most to advance the state of knowledge of the behavior of structures under dynamic loading. If every dynamic test were conducted with the aims of advancing the art of testing and improving the techniques of dynamic structural analysis, the need for dynamic testing would eventually be greatly diminished.

Excitation of Structures

The word "structure" usually refers to a building or to a large piece of construction, but in discussing dynamic testing, the word "structure" can be taken in a more general sense to mean any assemblage of material which possesses mass and resistance to deformation. Newton's laws of motion apply as well to an element of an electronic tube as to a large dam. The techniques of testing might be different for each, but the basic problem of dynamic testing is the same, namely, to apply a time-varying force, preferably known and controlled, and to measure response at significant points. Of the three structural tests described here, two pertain to very large structures, one weighing over two million pounds and one close to one billion pounds, whereas the third pertains to a structure weighing less than five hundred pounds. It was found that the experience of testing one of these structures was always pertinent and valuable for testing another structure.

The size of the structure to be tested often determines the type of testing program to be followed. Modern electrodynamic shaking machines which can be programmed can be used to subject small structures and models of large structures to uniaxial force or base excitation of almost any form imaginable. In Japan, models of dams have been subjected to simulated earthquake excitation by distributing many electrodynamic shakers over the model, each programmed to produce a force proportional to accelerations recorded in an earthquake.(1) Equipment is not presently available to excite large structures in such a manner, so recourse must be had in the second method of testing; that is, to apply some attainable force pattern at strategic places on the structure, and from the measured response to deduce relationships which will enable a calculation to be made of the time-history of motion of each point on the structure, resulting from any dynamic force.

The force of the wind has been used extensively as a source of excitation for buildings of more than a few stories. The magnitude and distribution of the force are, of course, unknown and uncontrolled, so the information which can be gained from such measurements is usually limited to one or two of the lowest natural frequencies and damping at very low amplitudes of vibration. References 2 and 3 show records of wind excited vibrations.

Earthquake excitation of large structures can induce oscillations large enough to yield information of structural behavior which would be very difficult to obtain in any other way. However, the infrequency with which intense earthquakes occur in any small area, and the fact that they cannot be predicted has resulted in very few records of structural response to earthquakes. References 4 and 5 contain records

of structural motions resulting from earthquakes.

The efforts of man to excite large structures vary widely in their nature and complexity. The simplest method is manual forcing, in which a person standing on the structure simply shifts his weight back and forth at the natural frequency of the structure. Manual forcing can be used only over a limited range of low frequencies to determine the natural frequencies and damping of rather flexible structures. A record obtained by this method is shown in Part II. Pullback excitation, in which the structure is pulled laterally with a cable which is suddenly released, has been used successfully on chimneys and elevated water tanks.[3] A similar result, obtained by an entirely different means, has been accomplished by Scruton and Harding, who applied a pulse to a large chimney by firing small rockets attached near the top.[6] Excitation of large structures by ground vibrations resulting from nearby blasting has been reported in Reference 7.

None of the foregoing methods is ideal for exciting large structures. In general the force cannot be well controlled in one or more of the following respects: time of occurrence, time-history, distribution in space, or magnitude. If accurate duplication of the force is not possible, the number of simultaneous records of the motions of different points on a structure is limited to the number of recording channels available.

The eccentric-mass vibration exciter offers many advantages over the methods described so far. It can deliver finely controlled uniaxial sinusoidal forces simultaneously at several points on a structure, at frequencies of interest for a wide range of large structures. The excellent control that is now available permits finely detailed studies of

structural response to sinusoidal force. In its present state of development the amount of force available from one machine of reasonable size is often insufficient at very low frequencies and the energy output is inadequate to cause any significant amount of structural damage to a large structure, but the eccentric-mass vibrator is by far the most effective means now available for studying structural vibrations of small to moderate amplitude.

Eccentric-mass vibrators seem first to have been used in Europe, in the 1920's, for geophysical work.[8] Some of the earliest uses in the United States are reported in Reference 9. Very large eccentric-mass vibrators, up to 20 tons force, have been used in Europe in the shipbuilding industry,[10] and in Japan for tests of dams.[11] The shaking machines used for the tests described in Parts II and III were recently developed at the California Institute of Technology for the California State Division of Architecture. Individually they are small compared to the largest machines which have been built, each being limited to $2\frac{1}{2}$ tons force and $1\frac{1}{2}$ horsepower. However, they possess an exceptionally fine speed control and four units are available to be synchronized to produce a larger force at one point, or to produce simultaneous forces at several points on a structure to more effectively excite higher modes. The machines are described in detail in References 12 and 13.

To excite massive structures into oscillations large enough to cause significant structural damage, some means other than eccentric-mass shaking machines must be used. Nearby air or ground blasts are possible sources of excitation but because of side effects they will undoubtedly not be used extensively. A promising avenue of investigation

is the firing at proper intervals of a number of rockets or explosive charges attached to the structure. Only a small effort has so far been devoted to developing this method of excitation.[6,14]

In Reference 15 Hudson has presented an excellent bibliography covering theory, means of excitation, and conduct of dynamic tests of large structures.

Measurement of Structural Response

The end products of a dynamic test are the records showing the response of the structure. In contrast to the few means available for exciting large structures, there are commercially available a multitude of measuring instruments which can be used in structural dynamic work. Appendix I is devoted to a discussion of such instrumentation.

Aim and Content of the Thesis

The aim of the thesis is to contribute to the art of conducting dynamic analyses of structures, both experimental and theoretical, as well as to add to the body of knowledge relating to the dynamic behavior of structures. In Part II a planar framework consisting of a tall concrete tower, two steel bridge spans, and a steel pier is studied. The theoretical analysis, based on Holzer's technique, is conducted in considerable detail and appears to be the first application of this method to framed structures. The experimental work on this framework was done with similar detail, and it illustrates what can be accomplished with readily available commercial instrumentation. The agreement between the theoretical and the experimental results is encouraging.

In Part III an earth dam is studied. Two vibrators were operated synchronously on the crest, and resonance curves showing many natural

resonances were recorded with the same instrumentation used in Part II. A theoretical analysis of the dam, made by considering it to be an elastic truncated wedge, fixed on the ends and on the bottom, yields a shear wave velocity for the material of the dam and predicts natural frequencies whose ratios, one to another, show surprisingly good agreement with the observed ratios. It may be noted that this analysis determines an average in situ value of the shearing modulus of the earth in the dam and, hence, is a promising technique for soil mechanics studies. Using the theory of normal modes, two resonance curves are constructed to estimate the damping in ten of the modes. The theoretical analysis of the dam allows one resonance curve, but not both, to be constructed to show fairly good agreement with the experimental curve.

Part IV is devoted to a new method for determining the masses and the constants defining the velocity-dependent and velocity-independent restoring functions of lumped-mass structures. The method is applicable to nonlinear as well as to linear structures. The method requires simultaneous records of the forces, accelerations, velocities, and displacements of all the mass points in the structure. Instantaneous values of these quantities are then entered into simultaneous equations of motion of the masses, which are solved by a least squares technique. A single-mass laboratory structure, weighing under 500 pounds, was constructed with bolted joints which slip. Excitation of the structure was provided by a small eccentric-mass oscillator and by a pendulum. Application of the method to the experimental records indicates that exceptionally good instrumentation is required and that, practically, the mass cannot be determined with accuracy, but rather the known value of the mass must be used as a criterion for judging the accuracy of the solution.

Statically measured hysteresis loops show good agreement with loops obtained from dynamic measurements.

Appendix I is devoted to instrumentation for structural vibrations. The properties desirable in an instrumentation system are listed, and descriptions and tests of commercially available components are presented.

Appendix II describes numerical integration with a second degree curve.

Appendix III discusses the separation of the components from records containing horizontal, vertical, and angular accelerations.

Appendix IV treats the static calibration of accelerometers.

Each of the main parts of the thesis is essentially complete in itself, including summary and conclusions. Cross references to other parts have been held to a minimum. Because of its length, Part II is divided into six subsections.

II. VIBRATION TEST OF A RESERVOIR OUTLET STRUCTURE

A. Introduction

Background of Test

Before a decision is made to conduct dynamic tests on a structure there should be asked the questions, "What might be learned by testing this structure?", "Will this knowledge which might be gained be worth the expense of the testing?", and "Will it be more profitable to test this structure rather than some other structure?" In answer to these questions with regard to testing the new Encino Reservoir tower the following observations can be made.

(a) The tower-and-bridge combination form a system simple enough to give hope of understanding all of the significant features of the dynamic behavior. The structure is essentially a planar framework composed of beam-like elements with distributed mass and elasticity. As such it is an excellent subject for attempting to extend to a framework the numerical technique recently applied to vibrations of tapered beams by Housner and Keightley.[16]

(b) The vibration test of the old Encino Reservoir tower left several questions unanswered.[2] The old tower has been demolished and is now replaced by the new structure. A test of the new structure should shed light on the unexplained phenomena.

(c) There is much practical interest in the dynamic characteristics of structures of this type. Knowledge gained from this structure will be useful in the earthquake resistant design of outlet structures, bridge piers, tall chimneys, and

similar structures.

(d) The test conditions at the site are ideal in several respects. The site is usually unoccupied and there is usually no machinery operating in the structure. This means that testing can proceed unimpeded by other activities in the structure, and the level of background vibration is very low. The structure will be available for testing for many years to come, unchanged in occupancy or by structural alterations. The filling of the reservoir will provide an excellent opportunity to measure at a large scale the influence of a surrounding liquid on a vibrating beam.

On the basis of these observations it was decided to proceed with dynamic tests of the structure.

Introduction - Description of the Structure

The new Encino Reservoir tower, pictured in Figures 2.1 and 2.2, Appendix V, is a reinforced concrete cylinder rising 149'-0" above its foundation, with an internal diameter of 13'-0" and wall thickness varying from 3'-6" at the base to 1'-0" near the top. Connecting the tower at a point 130'-0" above its base to the crest of Encino Dam is a steel truss access bridge 339'-0" long by 10'-8" deep by 6'-0" wide, consisting of two equal spans supported at their junction on a steel pier 61'-2" in height. Figure 2.3 gives the important dimensions of the structural elements.

The structure was completed in the spring of 1962 in a construction program which increased the capacity of Encino Reservoir. The design of the structure, accomplished by the owner, the Department of Water and

Power, City of Los Angeles, was governed by earthquake forces. The natural period of the tower, earthquake spectra, and the effective mass of the surrounding water were considered in the design. Professor G. W. Housner of the California Institute of Technology was consultant on the earthquake resistance aspects of the design.

The total weight of the tower above its foundation is approximately 2.14×10^6 pounds, based on a concrete density of 144.8 lb. per cu. ft. determined from three cores taken near the base, which showed densities of 144.2, 146.2, and 144.2 lb. per cu. ft. These cores, 2 23/32" diameter by 11 1/16", 10 35/64", and 9 39/64" long respectively, were vibrated as free-free beams with an Electro Products Laboratories Sonometer. Their fundamental frequencies were found to be 2415, 2700, and 2990 cps respectively, indicating moduli of elasticity of 4.19, 4.44, and 3.92×10^6 psi respectively, with an average value of 4.18×10^6 psi. The Poisson ratio of the concrete was not measured, but was assumed to be 1/6 in all the calculations.(17)

Over the lower half of the tower the area of vertical reinforcing steel is approximately 1.1% of the cross-sectional area of the concrete. This steel adds between 6% and 7½% to the moment of inertia of the cross section, computed on the basis of elastic action of the concrete-steel combination. In the upper half of the tower the vertical reinforcing steel varies between ½% and 1/5% of the cross sectional area, adding between 3% and 1¼% to the moment of inertia. At the base of the tower the moment of inertia in terms of concrete is 6875 ft.^{4} and the weight per foot of length is 2.63×10^4 pounds. The dead load compression stress at the base is approximately 80 psi. Just under the penthouse

floor the moment of inertia is 1849 ft.^{4} and the weight per foot is 9.9 x 10^3 pounds. In the lower 90' of the barrel are located six circular openings of 4'-0" diameter on which are mounted hydraulically operated butterfly valves. In the computations, adjustments were made to the mass of the tower to account for the openings and valves, but initially no adjustments were made to the moment of inertia of the cross section. Later, to improve the agreement between computed and observed frequencies, the moment of inertia used in the computations was decreased at sections through the openings.

The tower foundation is a reinforced concrete pad 48'-0" diameter by 10'-0" thick, penetrated by a 73½" diameter steel outlet pipe which runs horizontally beneath the dam at an angle of 16½° with the axis of the bridge. The foundation pad rests on a fine grained unweathered sandstone having a dry density of 125 pcf lb. per cu. ft. Unfortunately, no elastic constants were determined for this material.

The bridge is entirely of welded construction except for a 4" thick deck of Douglas fir. The approximate weight of each span is 50,000 pounds. The bridge is anchored to the tower and to its abutment structure on the dam with four 1 1/8" diameter anchor bolts, the shanks of which are surrounded by 1/8" thick micarta insulation sleeves which serve as an electrolytic corrosion preventive measure. Micarta insulation is also placed between the anchor bolt nuts and the truss, preventing any appreciable bearing force in excess of the weight of the bridge. At the steel pier, provision was made for temperature expansion of the bridge by elongating the holes in the bridge bearings, through which pass 1 1/8" diameter studs welded to the top of the steel pier. Each bridge

bearing at this point consists of a stainless steel sole plate which is bolted to the underside of the bottom chord, and rests on a graphite impregnated bronze plate, Lubrite, which in turn is separated from the top of the steel pier by 3/16" micarta insulation. The frictional forces developed by the weight of the bridge, therefore, are the only forces which prevent sliding of the bridge on its supports. At the tower and at the abutment both rubbing surfaces are steel. At the steel pier the surfaces are steel against Lubrite and Lubrite against micarta. The manufacturer states that the coefficient of friction between steel and Lubrite varies from 0.03 to 0.09. The dynamic coefficient of friction of steel on steel has been reported as between 0.03 and 0.09.(18)

The steel pier, midway between the tower and the crest of the dam, is of welded construction and weighs approximately 12,000 pounds. It rests on four reinforced concrete piers 2'-6" diameter by 14'-0" long, which are embedded in the compacted fill of the dam for most of their length and are all supported by one concrete mat, 14'-0" by 20'-0" by 2'-0", which is founded in the dam. The bridge abutment structure consists of a concrete foundation wall, 2'-8" thick by 6'-6" in height by 11'-4" long, which supports the bridge and rests on a concrete footing 4'-8" wide by 12" thick. A concrete entrance structure is tied to the foundation wall with dowels. The entire abutment assemblage rests on the dam and weighs approximately 1.8×10^5 pounds.

The dam itself at this point consists of a 40-year old earth dam, with a moist density of approximately 120 pounds per cubic foot, capped by 10' of compacted fill with a moist density of approximately 136 pounds per cubic foot. A 6" concrete slab covers the face of the dam and the bottom of the reservoir in the vicinity of the base of the tower.

B. Mathematical Analysis

Idealized Structure

For purposes of analysis the tower and the bridge were idealized as shown in Figure 2.4. The springs at the bases of T_{1a} and T_2 represent foundation compliance, termed "planting stiffness" by Jacobsen,[19] and in each case they allow rotation as well as vertical and horizontal translation. The substitution of springs for the surface of an infinite elastic medium is not theoretically correct, inasmuch as the springs return to the structure all of the energy put into them, whereas elastic waves in the infinite medium carry energy away from the structure. The only analytical technique which appears practical for the structure, however, is that of normal modes, which assumes a finite extent of perfectly elastic undamped material, or very special arrangements of viscous damping. For convenience of analysis, therefore, spring representation was used. It is shown in Reference 20 that if a moment, a harmonic function of time acting in a vertical plane, is applied to a rigid circular massless disc resting on an elastic half-space in which the Poisson ratio is zero, the rotation of the disc is closely proportional to and in phase with the applied moment for values of a_o less than 0.25, where a_o is the ratio of the circular frequency of excitation times the radius of the disc divided by the shear wave velocity in the elastic medium. If some average properties are assumed for the sandstone[21] and the foundation pad is assumed to be perfectly rigid, the value of a_o at 10 cps is 0.29, indicating that the assumption of elastic springs under the tower is not grossly in error over the range of testing frequencies.

The other springs in the structure allow relative movement between

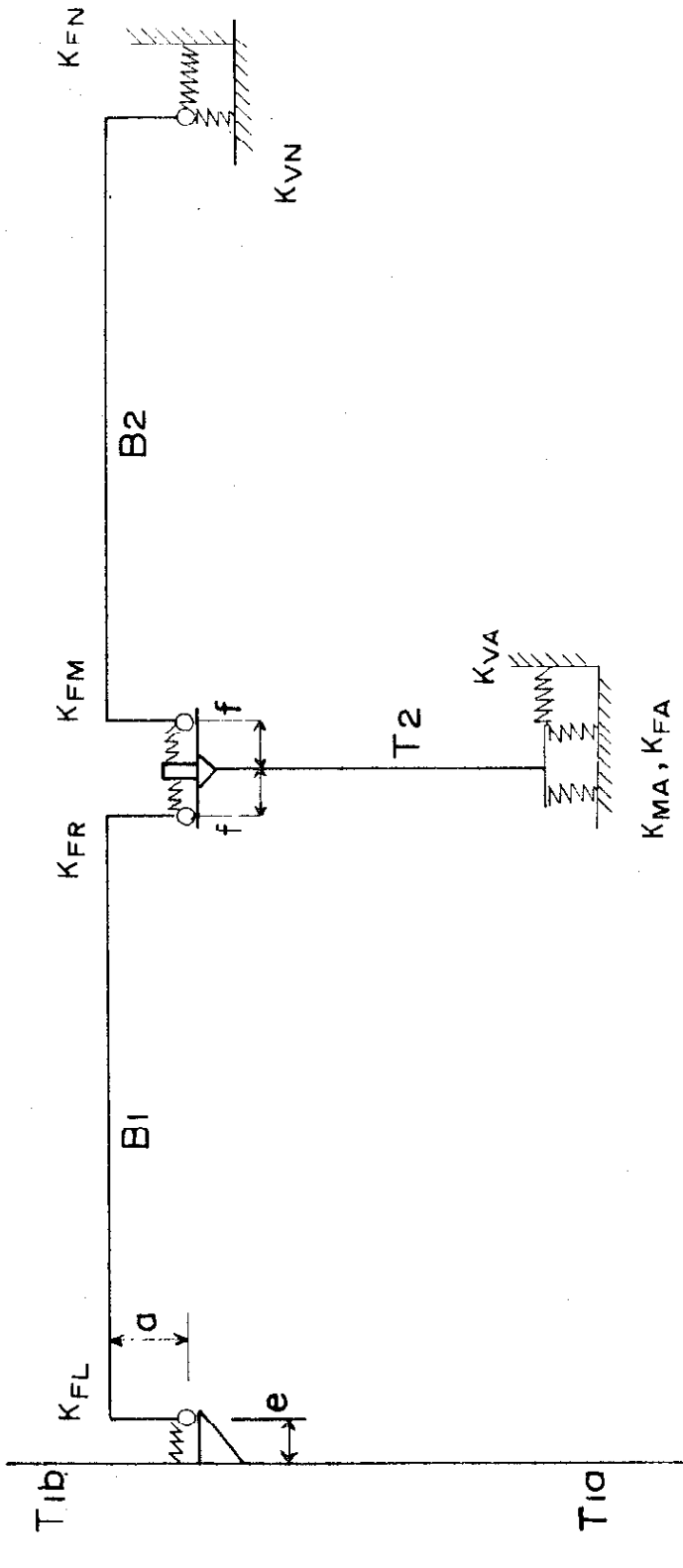

FIGURE 2.4
IDEALIZATION OF STRUCTURE

the bridge and its supports due to sliding. It is recognized that the force associated with the sliding motion is not the same as that associated with a spring deflection, but, once again the representation was used for expediency. In the analysis of the structure, the spring constants at the bases of T_{1a} and T_2 were adjusted until the computed motions of the idealized structure at these locations agreed with the observed motions in the first mode. The constants for the springs allowing bridge sliding were adjusted until the computed relative motions at the locations of the springs in the idealized structure agreed with the observed relative motions in the first mode.

The bridge spans, B_1 and B_2, are shown in Figure 2.4 to be straight members capable of carrying bending, axial, and shearing loads, and are connected to their supports by infinitely rigid arms of length $\underline{a}$, the distance from the bottom of the lower chord to the center of gravity of both chords, a distance of 72" in this case. For convenience of analysis the point of attachment of the bridge on the tower was assumed as $1\frac{1}{2}$" below the actual point on the tower. The center of mass of the bridge is located approximately 17.7" below the center of stiffness. The eccentricities $\underline{e}$ and $\underline{f}$ are 9'-0" and 1'-0" respectively.

In the analysis, the tower, T_1, is divided into two sections, the joint being at the level of the point of attachment of the bridge, the level of the bottom of the lower chord of the bridge and the assumed surface of sliding. The bottom of T_1 is taken to be the top of the foundation pad, and the bottom of T_2 is taken as the bottom of the steelwork. Both T_1 and T_2 are assumed to be capable of carrying bending, axial, and shearing loads.

Mathematical Analysis - Transfer Functions

The basis on which the analysis of the structure is founded is the transfer function, which is defined by the following question: If on the left end of an undamped elastic member, straight in this instance, there is imposed a harmonic exciting function ($A \sin\omega t$), where A is one, and only one, of the following: transverse shear V, bending moment M, angular displacement θ, transverse displacement Y, axial force F, or axial displacement U, then what values of these six quantities (transfer functions) are necessary at the right end of the member to hold it in dynamic equilibrium at the frequency ω? For straight uniform members, with shear and rotatory inertia neglected, transfer functions are easily derived from the differential equations of axial and transverse motion, but for nonuniform members digital techniques are the only practical approach.

The technique used here to find the transfer functions consisted of first dividing the member into a finite number of segments, ΔX in length, and concentrating the mass, m, in the half segments on either side of the division points at the division points. The material of the member between the division points was then assumed to be weightless and to possess constant area A, moment of inertia I, density ρ, modulus of elasticity E, modulus of rigidity G, and shear coefficient α, over the segment. Then, with reference to Figure 2.5, the following equations for the vibrating member may be written for small values of θ, it being understood that all terms are multiplied by $\sin\omega t$:

$$V_n = V_{n-1} + m_{n-1}\omega^2 Y_{n-1} \tag{2.1}$$

$$M_n = M_{n-1} + V_n \Delta X_n - F_n \theta_{n-1} \Delta X_n - \rho I_n \Delta X_n \omega^2 \theta_{n-1} \tag{2.2}$$

$$\theta_n = \theta_{n-1} + \frac{\Delta X_n}{2EI_n}(M_n + M_{n-1}) \tag{2.3}$$

$$Y_n = Y_{n-1} + \theta_{n-1}\Delta X_n + \frac{(\Delta X_n)^2}{3EI_n}(M_{n-1} + \frac{M_n}{2}) - \frac{\alpha \Delta X_n V_n}{GA_n} \tag{2.4}$$

$$F_n = F_{n-1} + m_{n-1}\omega^2 U_{n-1} \tag{2.5}$$

$$U_n = U_{n-1} - \frac{F_n \Delta X_n}{E A_n} - \frac{V_n \theta_{n-1} \Delta X_n}{E A_n} \tag{2.6}$$

These equations are then applied successively to the segments and division points of the member, proceeding from left to right. The final values of these quantities, on the right end of the member, are the desired transfer functions.

The main features of this technique have appeared in Reference 16 and its references, but several of the terms require explanation. On the right side of equation 2.2 the fourth term expresses the moment due to rotatory inertia of the segment between the division points. The segment is assumed to have distributed mass for this calculation. The third term in equation 2.2 indicates a coupling between axial and transverse vibrations. The force consists of a constant term and a time varying term, $A+B\sin\omega t$, which means that the product $F\theta$ is not of frequency ω, and hence the equation is not valid throughout a cycle of vibration. The effect of the dynamic component of F in this term is assumed to be small for all the members of this structure, and later it will be demonstrated to be small. In equation 2.2 then, F represents only axial force which does not vary in time. On similar grounds, V in equation 2.6 is assumed to represent only shear force which does not vary in time. Allowing these two limitations, the equations 2.1 through 2.6 are linear. The fourth term in equation 2.4 expresses the shearing deformation between

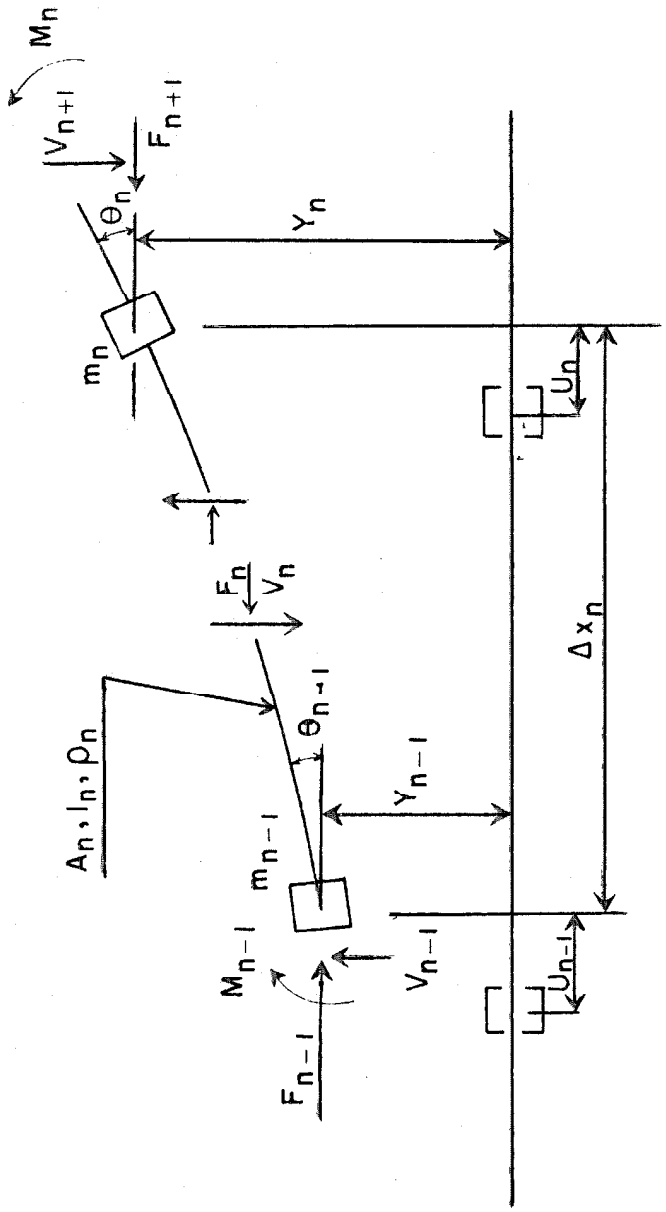

FIGURE 2.5
DISCRETE APPROXIMATION OF MEMBER

the division points. It should be noted that the moment of F times transverse deflection due to shear has been neglected.

In the most general case the introduction of one of the six quantities at the left end of the member results in six quantities at the right end, so there can be as many as 36 linearly independent transfer functions for one member. Each quantity, V, M, θ, Y, F, U, at the right end of the member is thus expressed as a combination of the six quantities at the left end of the member. As is explained later, the solution of the equations of equilibrium and continuity at the joints and at the boundaries of the structure permits the determination of the left end quantities and the natural frequencies.

Mathematical Analysis - Calculation of the Shear Coefficient

If the shearing deformation of the tower is assumed to be determined by the shearing stress at the neutral axis and this stress is given by

$$f = \frac{VQ}{Ib} , \qquad (2.7)$$

where V is the shearing force, Q is the first moment of the area on one side of the neutral axis taken about the neutral axis, I is the moment of inertia, and b is the total thickness resisting shear, then the coefficient α in equation 2.4 has the form

$$\alpha = \frac{2(D^2 + t^2/3)}{D^2 + t^2} , \qquad (2.8)$$

where D is the mean diameter of the shell and t is the wall thickness. Values of α for the tower shell vary between 1.94 at the bottom and 1.99 near the top.

From energy considerations, Sutherland and Goodman[22] give the formula

$$\alpha = \frac{A \int_A f^2 dA}{V^2} , \qquad (2.9)$$

where A is the cross sectional area, f is the unit shearing stress, and V is the shearing force. If, for an approximate analysis, the vertical component of shear stress in the shell is assumed to be constant over the area included within lines making 45° with the neutral axis, and zero elsewhere, equation 2.9 gives the value $\alpha = 2.0$, the same as given by equation 2.8 when $t/D = 0$.

Mathematical Analysis - Effect of Finite Length of Element

In equation 2.2, the term relating to rotatory inertia is exact only for beam elements of infinitesimal length. For elements of finite length, ΔX, the moment of inertia, I, about an axis through the cross sectional centroid at one end of the element is

$$I = \rho \Delta X \left(I_c + \frac{A(\Delta X)^2}{3} \right), \qquad (2.10)$$

where ρ is the mass density, and I_c is the moment of inertia of the cross sectional area, A, about the axis through the centroid. For a typical cross section of the tower the second term in the brackets, expressing the effect of the finite element length, increases I by 5% for an element 2'-0" long. If the element is assumed to rotate about a transverse axis midway between the ends of the element, the increase due to the second term is only 0.6%. It is shown later that rotatory inertia changes the first two frequencies by only a small amount, so the increase in I due to finite element length has only a very small effect on the first two frequencies.

It can be concluded from the data in Reference 16 that the effect of using a finite length of element, 2'-0", to approximate the 149' tower is to cause only a very small decrease in the computed values of the first two frequencies.

Mathematical Analysis - Approximations of Trussed Members

The substitution of solid members in Figure 2.4 for the trussed members T_2, B_2, and B_1, in the computations requires careful examination. A comparison of dynamic behaviors is called for, but because of the complexity of the problem of a vibrating truss, comparisons under static load only were made between the trusses and the solid members.

Professor C. W. McCormick of the California Institute of Technology has written a program for the Burroughs 220 digital computer to solve for the member forces and joint displacements of two dimensional structures subjected to static loads. With the aid of this program, static solutions of the trussed members were obtained relatively easily even though the bridge trusses were indeterminate because of welded joints and T_2 was additionally indeterminate because of framing.

In Table 2.1 displacements of T_2 and displacements of substitute structures caused by a transverse force at the top are shown for several different construction conditions. In all cases, the structures are considered fixed at the base. Column a gives displacements of the points of T_2 as shown in Figure 2.3 with all joints welded. Columns b and c are not pertinent to the problem but they were easily obtained at the time column a was computed and are of interest to structural engineers. They represent deflections of T_2 with all joints assumed hinged, both diagonals assumed effective in column b and only one diagonal assumed effective in column c. It is seen that the effect of the restraint due to welding is very small, but for this structure and loading the second diagonal in each panel adds appreciable stiffness. Column d gives the bending deflections of a solid tapered beam having a moment of inertia equal to the total area of all the legs of T_2 times the square of one

Panel Point	a	b	c	d	e	f	g
1	149	151	218		112	157	1.05
2	452	455	578	361	383	470	1.04
3	857	862	1034	750	760	889	1.04
4	1349	1356	1576	1212	1225	1396	1.03
5	1898	1909	2178	1732	1746	1961	1.03
6	2430	2444	2753	2237	2255	2512	1.03
7	3008	3032	3380	2791	2808	3113	1.03

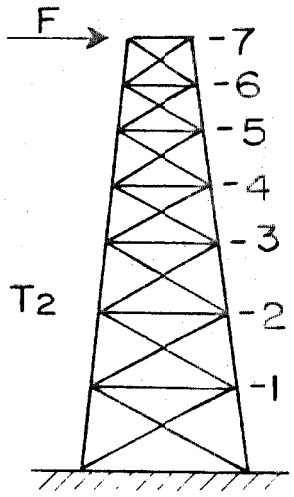

Column

a: T_2 as built, all joints welded.

b: All joints pinned.

c: All joints pinned, one diagonal removed.

d: Solid beam of Equivalent I, no shear deflection.

e: 7-segment solid beam, no shear deflection.

f: 7-segment solid beam, shear deflection included.

g: Ratio of column f to column a.

TABLE 2.1
DEFLECTIONS OF T_2

half of their separation distance. These deflections were obtained by evaluation of the exact expression for deflection of the beam and do not include the effect of shear.

In columns e and f, T_2 is considered to be made up of seven elements, each having a moment of inertia equal to the total area of all the legs times the square of one half of the distance separating the legs midway between the ends of the element. The computations were performed with the numerical procedure previously described, the frequency ω being zero. In column e, the displacements are due to chord shortening and lengthening only, whereas in column f the effects of changes in the lengths of the diagonals are included. For convenience, one average angle of intersection for all the diagonals was assumed, this being only a slight modification of the actual structure. The ratios of the displacements computed for the segmental beam including shear, column f, to those computed from the original trussed structure, column a, are shown in column g. In the region of greatest importance to vibrations of the entire structure, the approximate technique gives static deflections 3% high. In later computations the modulus of elasticity of T_2 was decreased by 3% as a compensation.

The action of T_2 under dynamic excitation is not, of course, simply that of a massless spring. The degree of its influence on the tower vibrations, however, is indicated by the facts that its total mass is approximately 0.56% that of the tower and, in the fundamental mode of the structure, the top of T_2 undergoes roughly one-half the displacement experienced by the top of T_{1a}. The static spring constant of T_2 is approximately 12,000 lb./in. for a transverse force at the top, whereas

it requires approximately 2.5×10^5 pounds at the top of T_{1a} to deflect it one inch. The relationship between T_2 and T_1 is therefore roughly that of two single degree of freedom systems connected in parallel, one having a mass 180 times greater and a spring 21 times stiffer than the other.

In order to estimate the effect of using only seven segments for the dynamic analysis of T_2, an analysis was made of a solid linearly tapered cantilever of rectangular cross section, whose depth, in the direction of motion, at the tip was one half the depth at the base, and whose breadth at the tip was twice the breadth at the base. These proportions result in a beam with a constant cross section throughout the length and with a moment of inertia at the tip equal to one quarter the moment of inertia at the base, roughly approximating T_2, although the rate of change of moment of inertia along the length is not the same as in T_2. Then, using the technique of Reference 16, the first and second frequencies were found for this beam, treated first as a beam of 100 segments and then as a beam of seven segments. The first and second frequencies of the seven-segment beam were, respectively, 0.988 and 0.959 times the first and second frequencies of the 100-segment beam, which were 6.7 cps and 36.5 cps.

To examine the representation of a trussed bridge span by a solid member, whose properties are shown in Figure 2.6 (a), two static loading conditions were considered, an axial force at the level of the centroid of the bottom chord, and a transverse force at the centerline of the span, shown in Figure 2.6 as cases (a) and (b). For the loading of case (a), deflections of a truss with hinged connections were computed

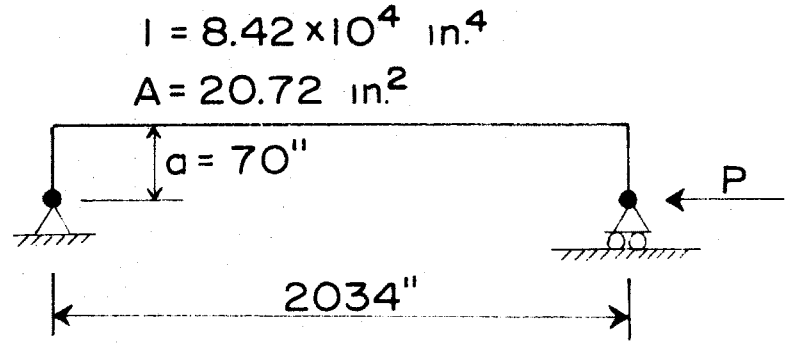

(a)

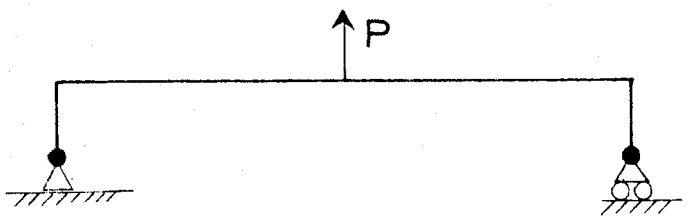

(b)

FIGURE 2.6
STATIC LOADS ON EQUIVALENT BEAM

by slide rule, and were found to agree with deflections of the welded truss, computed by Professor McCormick's program, to within $\frac{1}{2}\%$, indicating that the effect of rigid joints is very small. Then, using the moment-area relationships, several deflections of the solid member were computed by slide rule and were found to differ only in the third or fourth decimal place from those determined by the previously described numerical procedure applied to an 18-segment solid member. In Table 2.2, however, vertical deflections of the solid member under the loading of case (a), shown in column 2, are as much as 9% larger than the deflections found by Professor McCormick's analysis of the welded truss, shown in column 1. One sidelight of this surprising variation is illustrated in Figures 2.7 (a) and (b), where the bottom chords of two truss panels are shown under compressive loads. Although the deflection angle θ is the same in both instances, the ends of the panel in view (a) undergo relative vertical deflection not experienced in the panel in view (b). In the case of the bridge truss in the Encino Reservoir structure, if the upper ends of all the diagonals pointed toward midspan the centerline deflection under loading condition (a) would be increased by approximately 25%. The shortening of the distance between the supports of the truss is always the same as for the solid member, however, regardless of the configuration of the diagonals. This means that if both the truss and the solid member are considered as massless springs resisting the deflection of the tower, their effects on vibrations of the structure are identical. This static spring constant for compression of the bottom chord is 2.78×10^5 lbs. per inch for one bridge span. It is found later that the longitudinal force existing in the bridge when the entire structure is vibrating at

Panel Point	Loading Condition (a) Figure 2.6 Actual Truss Col. 1	18-Segment Beam Col. 2	Loading Condition (b) Figure 2.6 Actual Truss Col. 3	18-Segment Beam Col. 4
1	95.1	90.1	738	741
2	169.7	169.6	1586	1576
3	233.3	238.5	2425	2378
4	286.3	296.7	3221	3127
5	328.7	344.4	3948	3810
6	360.5	381.5	4591	4406
7	381.7	408.0	5129	4898
8	392.3	423.9	5551	5272
9	392.8	429.2	5798	5508
Shortening of bottom chord	216.1	216.3	784	859

TABLE 2.2

STATIC DEFLECTIONS OF BRIDGE

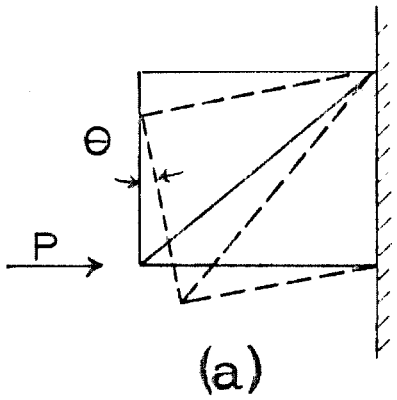

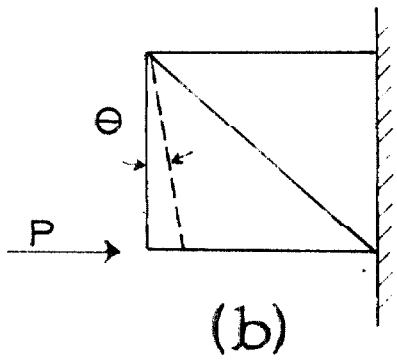

FIGURE 2.7
ILLUSTRATIVE TRUSS PANELS

its fundamental frequency is only about 0.6 the static force which produces the same shortening of the distance between bridge supports. The transverse inertia of the bridge is responsible for most of this difference between the static and dynamic spring constants.

Vertical deflections of the centroid of the chords are shown for loading condition (b), the concentrated load in the center of the span, in columns 3 and 4 of Table 2.2. Column 3 pertains to the actual truss, and column 4 pertains to the solid beam. The centroid of mass of the bridge is approximately 17.7" below the centroid of the chords and its vertical deflections differ only by a fraction of 1% from the deflections shown in column 3. Midspan deflection of the solid beam under this loading condition is seen to be 5% too small, whereas the shortening of the distance between the supports of the solid beam is seen to be $9\frac{1}{2}$% too large.

To provide a compromise for the several discrepancies, the eccentricity of the centroid in the solid beam representation was reduced to 95% of its theoretical value and the two loading cases were recomputed, the differences between deflections in the revised solid beam and in the actual truss appearing in Figure 2.8. Except at the supports, horizontal deflections of the solid beam are compared with horizontal deflections of the center of mass of the actual truss. The large discrepancies in these horizontal deflections result from the fact that the axis of the modified solid beam lies 14.2" above the center of mass of the truss. At the points where the 28% discrepancies occur in cases (a) and (b), the actual horizontal deflections are only 11% and $5\frac{1}{2}$% respectively of the vertical deflections which occur at midspan, so the

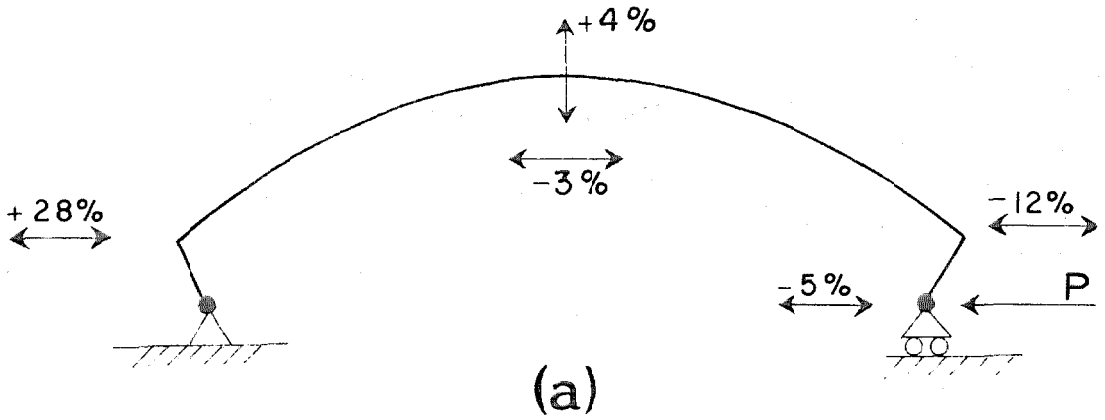

FIGURE 2.8
DISCREPANCIES IN DEFLECTIONS
FOR TWO LOADING CONDITIONS

$$\% = 100\left(\frac{\text{EQUIV. BEAM DEFL.} - \text{TRUSS DEFL}}{\text{TRUSS DEFL.}}\right)$$

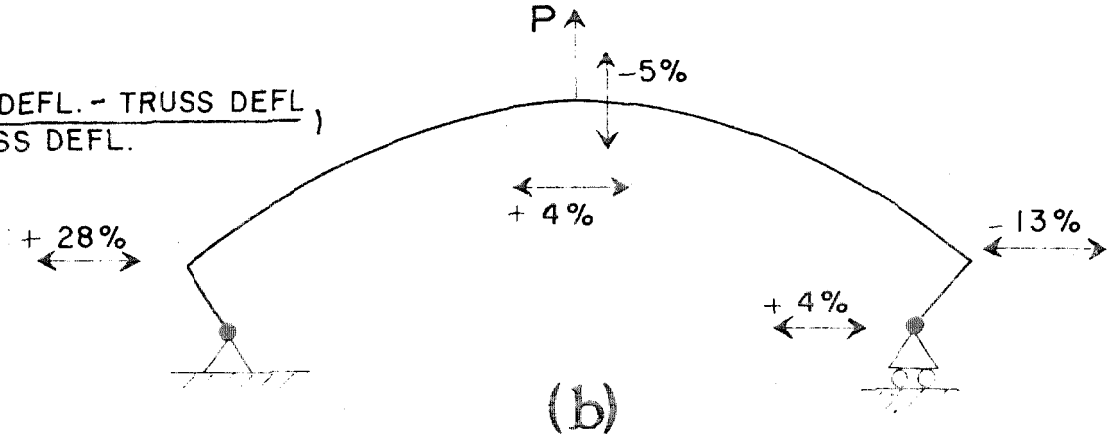

effects of the discrepancies on vibrations of the structure are not as great as their numerical values would indicate. The effect of the inertia of the bridge on the fundamental mode shape and on two frequencies of the structure is shown later in Table 2.6.

If the energy method were to be used for finding the fundamental frequency of the entire structure, some assumption would have to be made regarding the fundamental mode shape. Often a gravity loading is used to approximate a fundamental mode shape, but in the case of a bridge span the deflected shape due to an axial force at the level of the bottom chord might be considered. The importance of the proper choice of static loading for approximating the fundamental mode shape is illustrated by comparing the ratio of the vertical deflection at the centerline of the span to the shortening of the distance between the supports for four loading conditions: case (a) and case (b) of Figure 2.6, a uniform gravity loading, and the dynamic loading of the fundamental mode of the modified solid beam with the support conditions shown in Figure 2.6. These ratios are respectively 1.99, 6.74, 4.77, and 5.78. The first two natural frequencies of the modified solid beam with the support conditions shown in Figure 2.6 are 3.03 and 9.46 cps. If the hinges are maintained at both ends, but the ends are held a fixed distance apart, the first two frequencies are 3.78 and 9.51 cps. It is shown later that these frequencies of the bridge are very close to certain frequencies of vibration of the entire structure.

Mathematical Analysis - Solution of the Framework

To illustrate the principle used to find the natural frequencies of the intake structure Figure 2.9 shows an elastic framework, assumed

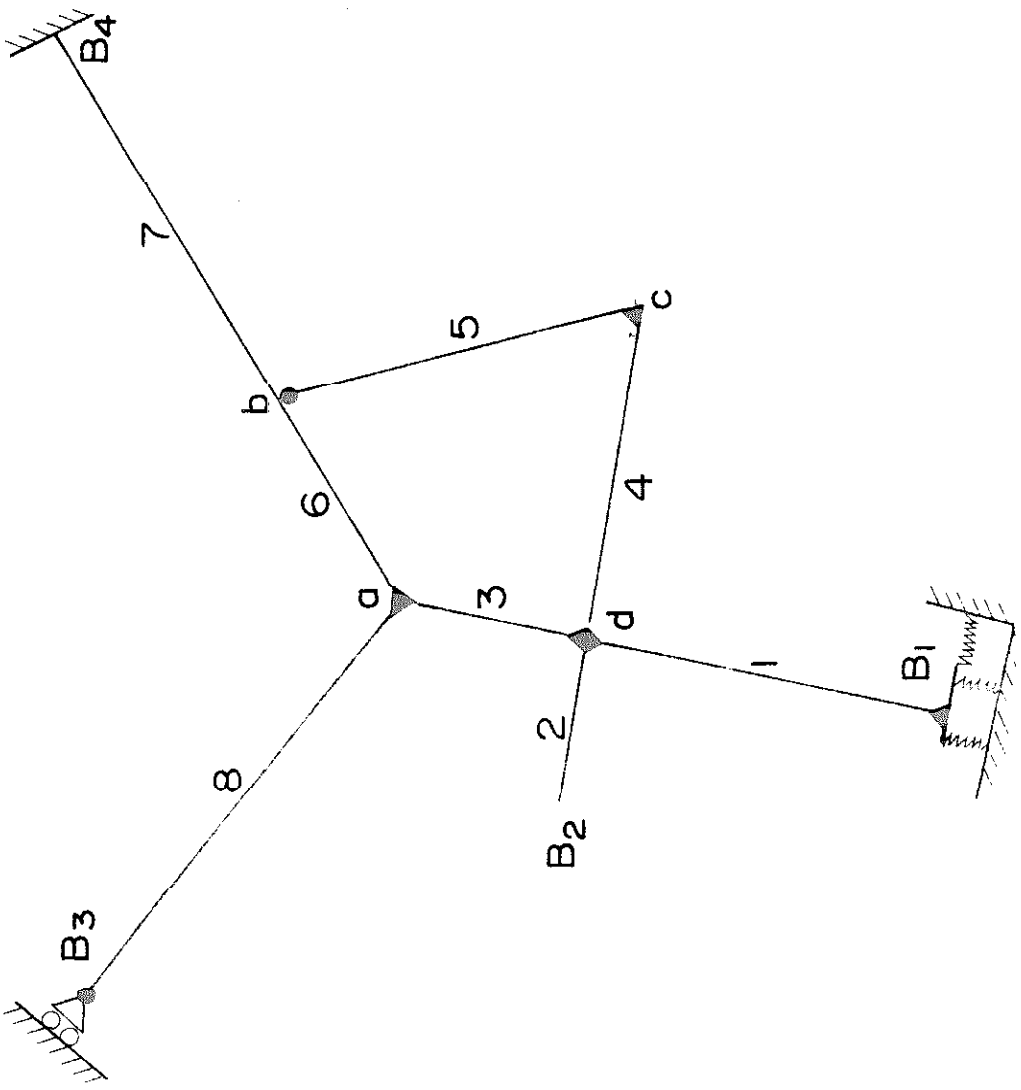

FIGURE 2.9
ILLUSTRATIVE STRUCTURE

to be vibrating in the plane of the paper with all parts in phase at a frequency ω. Let the number of members be designated by N_m, the number of internal joints by J, the number of boundary points by B_p, and the number of members framing into an internal joint by N_j. In Figure 2.9 there are eight members, four internal joints, four boundary points, and framing into joints a, b, c, d there are three, three, two, and four members respectively.

The dynamic forces and distortions in each member will be known only if all six of the quantities V, M, Θ, Y, F, U sin ω t are known at the left end of the member. Because normal mode vibration involves relative, not absolute distortion, an arbitrary value may be assigned to one of the six quantities in one of the members, meaning that the total number of unknowns is $(6N_m-1)$, equal to 47 in this case. At each internal joint there may be written three independent equations of equilibrium and 3 (N_j-1) independent equations of continuity, giving a total of $3J + 3\sum_{j=1}^{J} (N_j-1) = 3\sum_{j=1}^{J} N_j$ equations, equal to 36 in this case.* When there are added to this the three equations available at each boundary point, 3 B_p, 12 in this case, the total number of independent equations becomes $3\sum_{j=1}^{J} N_j + 3 B_p$, equal to exactly six times the number of members in the framework. There are thus always (6M) equations for (6M-1) unknowns regardless of the statical determinacy or indeterminacy of the framework. The overdetermined set of equations can be satisfied only for particular frequencies of vibration, the natural frequencies of the structure.

---

* Where members join at a boundary point, the number of independent equations available is the same as if the particular joint were counted only as an internal joint.

Figure 2.10 shows the lettering scheme that was used in writing the equations of equilibrium and continuity of the Encino Reservoir structure. The letters at the ends of the bridge spans refer to quantities at the lower ends of the rigid arms in Figure 2.4. Only those quantities of interest are shown. For instance, at the bottom of T_{1a} and T_2, no displacements are shown because the displacements at these points are simply proportional to the forces, the constants of proportionality being the constants of the springs connecting the structure to the ground. Hence, it is not necessary to compute separate transfer functions for displacements occurring at these points. At the right ends of the bridge spans no rotations are shown because the rotations that occur there are not used in the dynamic analysis.

For the numerical analysis, the lower portion of the tower, T_{1a}, was divided into 2'-0" segments, whereas 1'-0" segments were used for T_{1b}. The trussed members, B_1, B_2, and T_2, were divided at their panel points as indicated previously. Then proceeding from left to right on the bridge spans and from bottom to top on the vertical members, the transfer functions, at a given frequency, ω_1, were computed for all the quantities shown at the left and bottom ends of these members. As an example, at the left end of B_2, Θ_M was assigned the value $\Theta_M = 1 \cdot \sin \omega_1 t$, and V_M, Y_M, F_M and U_M were all made zero. Using the step-by-step procedure described earlier it was found that at the right end of B_2, Y_N had the value $Y_N = C_4^{33} \sin \omega_1 t$. In the identification scheme used, the six quantities V, M, Θ, Y, F, U are identified by the numbers 1, 2, 3, 4, 5, 6 respectively, and the members are identified by the numbers shown in Figure 2.10, B_1 and B_2 having the same number since their properties are identical. The first superscript stands for the member

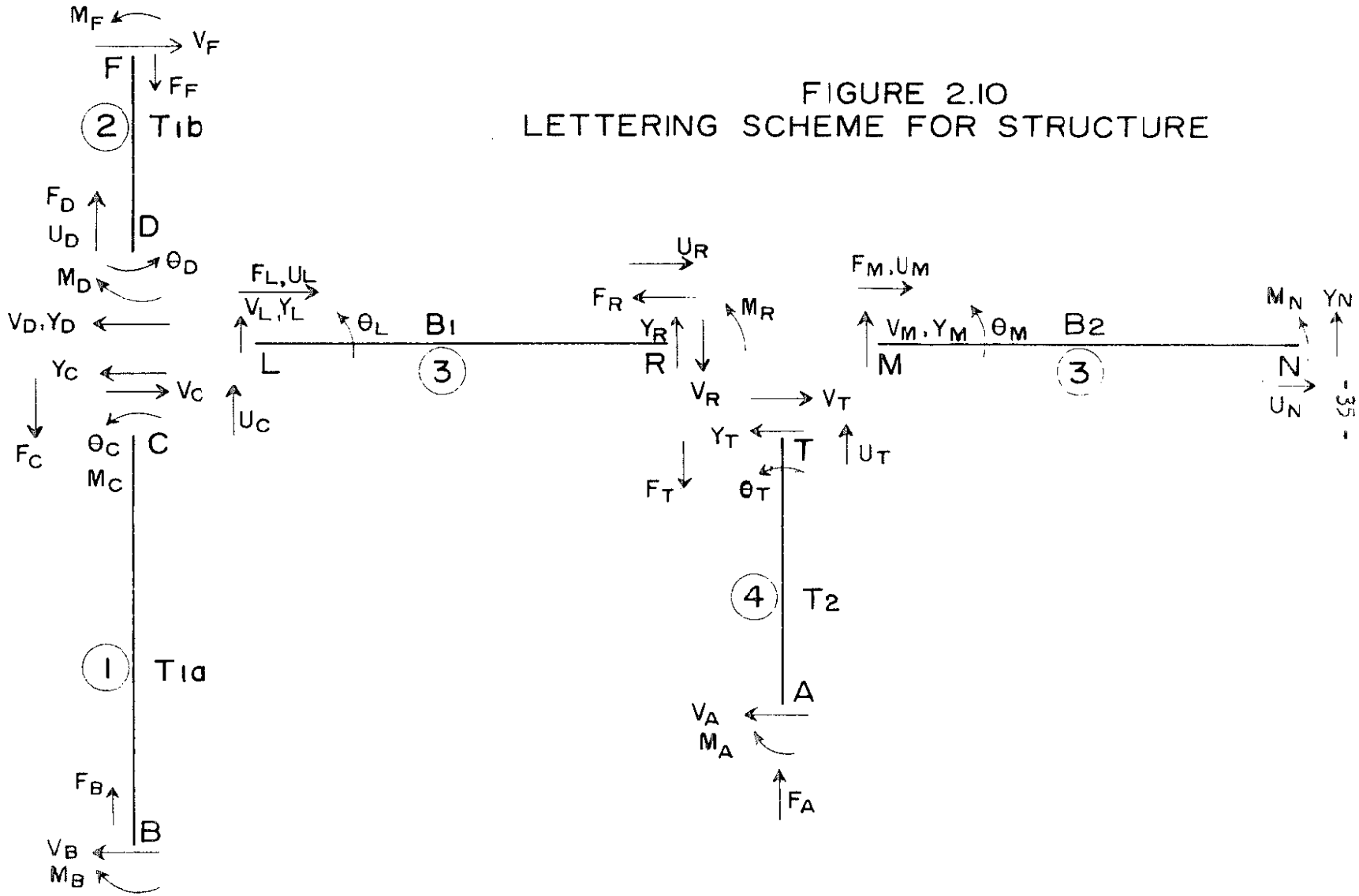

FIGURE 2.10
LETTERING SCHEME FOR STRUCTURE

number, the second superscript for the quantity introduced at the left or bottom, and the subscript stands for the quantity determined at the right or top of the member. The value of C_4^{33} is directly proportional to the amplitude of θ_M and is dependent in a more complex manner on the value of ω_1.

When the transfer functions had been computed for all the quantities shown at the left and bottom ends of the members in Figure 2.10, each having been assigned in turn the value $(1 \cdot \sin \omega_1 t)$, it was then possible to express the quantities at the opposite ends of the members in terms of the quantities at the left and bottom ends. For instance, in T_{1a}

$$V_C = C_1^{11} V_B + C_1^{12} M_B + C_1^{15} F_B .$$

For this member C_1^{15} is found to be zero. The shear V_B was assigned the value of unity, thus determining the scale for all the other quantities in the structure. The equations of equilibrium and continuity were then written in matrix form, AB = C, where A is a 21 x 21 matrix of the transfer functions, B is a 21 x 1 matrix of unknowns, and C is a 21 x 1 matrix containing transfer functions and zeros. This matrix equation is shown in Figure 2.11, Appendix V, where for convenience the unknown quantities in B are shown above their corresponding columns in A. Although there are a total of 29 unknowns in this structure, only 21 equations were written, it being recognized that M_L and M_M are zero and the three displacements at the bottom of both T_{1a} and T_2 are directly related to the forces there. The one remaining equation to be satisfied is the requirement that there be no moment, M_T, at the top of T_{1b}. By successive approximation, the value of ω_1 was adjusted until this condition was met.

The method is seen to be an extension of the Holzer or Myklestad-Prohl method.[16] The limitation of its use is determined by the number of simultaneous linear algebraic equations which can be solved quickly and accurately. A subroutine used for the Burroughs 220 computer in the computing center of the California Institute of Technology will solve a maximum of 99 equations, representing a structure of perhaps 17 members, in approximately 20 minutes. This means that it would require somewhat more than 20 minutes for each guess at the natural frequency, a prohibitively long time. A subroutine available for the I.B.M. 7090 computer will solve a set of 75 equations in approximately one minute, the time required increasing approximately as the cube of the number of equations. Inasmuch as the accuracy of a solution depends upon the determinant of the matrix to be inverted, the question of accuracy is an individual problem for each different framework. The accuracy of the computations for the Encino Reservoir structure is discussed in Section E.

If the technique is revised slightly, the response of the undamped structure to an applied sinusoidal force at any point can be found. Suppose it is desired to find the response resulting from the force produced by the shaking machine, bolted to the penthouse floor. Since the axis of this force is only about two feet above the junction of T_{1a} and T_{1b}, it will be satisfactory to replace the effect of the force on the structure by a force and a moment located at the junction of T_{1a} and T_{1b}. The equilibrium equations, Figure 2.11, Appendix V, at this joint, must then be modified to allow for the presence of this external shear and moment. In addition, the equation $M_F = 0$ is added to the set of simultaneous equations, and V_B is no longer assigned the value unity

but becomes an unknown. This means that one equation and one unknown have been added to the set of equations, so a solution of the set is still possible. The column matrix (C) now contains only zeros except for the two equations of equilibrium involving the shear and the moment at the top of T_{1a}. The solution of this set of simultaneous equations then yields the values of all the quantities at the left and bottom ends of the members, from which the amplitudes of response of all the points on the structure are easily found. If the external force is located at some distance from the end of a member it is necessary to cut the member at the location of the force, adding six additional unknowns and six additional equations.

Mathematical Analysis - Computer Program

The numerical work in this analysis was accomplished on the Burroughs 220 digital computer. Data for the computation of the properties of each member were entered into the computer, which, after calculating the values, stored them on an auxiliary magnetic tape unit. The main program was then entered, after which the computer called out for each member in turn the data stored on magnetic tape, calculated the values of the transfer functions for a given frequency and stored them in memory. When the transfer functions had all been computed, the computer solved the 21 simultaneous equations of equilibrium and continuity, and from these answers computed the moment at the top of T_{1b}. This moment, Δ, used as a criterion for the natural frequency, was printed out for the operator to see. A new trial frequency was entered and the computation process was repeated to produce a new value of Δ. Then using these two values of Δ, at the operator's discretion, the

computer interpolated for a new trial frequency and repeated the cycle automatically until the value of Δ was as small as desired. The computer then calculated the mode shape associated with the frequency and printed out the quantities V, M, Θ, Y, F, U for each division point of each member.

The feeding in of the data tape, computation and storage of the member properties, storage of subroutines in memory, and the feeding in of the program tape required approximately 115 seconds. From this point on the time to produce one value of Δ for a given frequency was 38 seconds. The program occupied approximately 3750 words of the 5000 word memory available.

Mathematical Analysis - Tests of the Method

To test the general procedure, a framework was constructed of five identical members connected end-to-end to form a uniform cantilever beam, each member containing 20 division points. With shear, rotatory inertia and dead load compression neglected, the first two mode shapes of this structure, normalized so that the tip deflection was unity, were found to differ from their corresponding Bernoulli-Euler values only by a digit in the fourth decimal place.

To test the correctness of the terms involving shear deflection and rotatory inertia, the fundamental frequencies were found for several simply supported beams with different ratios of $\propto E/G$ and I/AL^2. The ratios of these frequencies to those computed with shear and rotatory inertia neglected agreed with the values found by Sutherland and Goodman.[22] In addition, the first three frequencies were found for a cantilever beam with the ratio $\propto E/G$ equal to 3.20 and I/AL^2 equal to

0.0036. The ratios of these frequencies to the frequencies computed with shear and rotatory inertia neglected also agreed with the values reported by Sutherland and Goodman.*

To check the effect of axial force on bending vibrations, the first two frequencies of a uniform cantilever beam with a constant axial compressive force $F = 0.14\ EI/L^2$, shear deflection and rotatory inertia neglected, were found to be 0.974 and 0.993 respectively, times the frequencies which occur when the axial force is not present. An approximate formula, due to Timoshenko,[25] for the ratio of the first frequencies gives the value 0.975. Timoshenko's formula does not apply to the second frequency, however.

Because the only members subjected to known dead load shear are the bridge spans, and a rough calculation showed that the term involving dead load shear in equation 2.6 has an effect of the order of 0.1% of that due to axial force, the effect of dead load shear on the simultaneous longitudinal and transverse vibration was not included in any of the computations.

C. Equipment and Testing Procedure

Manual Forcing

It was found that the fundamental mode of the structure, with and without the bridge attached, could be excited by one man shifting his weight back and forth while standing on the penthouse floor. A portion of a record of manually excited vibration of the tower only is shown in

---

* The results of Sutherland and Goodman have been reprinted in References 23, 24. It should be noted that the cantilever beam charts in these publications have been printed with an error in the decimal place of the abscissa, resulting in the abscissa appearing ten times too large.

Figure 2.12, Appendix V. At the natural frequency of the tower with the bridge attached, approximately 2.1 cps, it was difficult to maintain the proper phase relationship between the force and the motion of the structure for more than a few seconds, but this proved to be long enough to build up accelerations as high as 0.002 g on the penthouse floor. Inasmuch as the person exciting the structure could not feel the tower's motion it was necessary for him to watch the oscillograph trace while doing the forcing. A metronome, set to the frequency of the structure, was tried as an aid to maintaining the proper rhythm, but at 2.1 cps the visual signal of the oscillograph proved more effective than the audible signal. Attempts at forcing at one half the frequency of the structure were less successful than those made at the natural frequency. At 2.1 cps, one man forcing alone was more effective than two men trying to synchronize their motions.

The important structural properties which relate to manual forcing are the natural frequency of the structure, the stiffness, and the damping. From the experience on the Encino tower it would appear to be difficult for anyone but a person with exceptional rhythm to maintain oscillations at above 3 cps. Exciting very low frequencies, however, should not be difficult if a timing signal is used. The stiffness referred to, of course, is dynamic stiffness, but if the fundamental mode is being excited, the static stiffness may be used for estimating the amplitudes of motions that can be expected. As mentioned previously, the free standing tower was calculated to have a static stiffness of approximately 3×10^6 lbs. per ft. when applied force and the deflection measurement were both located on the penthouse floor. The highest damping observed

during the manually forced vibrations was 1.17% critical.

Attempts to get clean traces of wind or manually excited transverse vibrations of the structure, perpendicular to the bridge, were not successful for two reasons. First the wind acting on the side of the bridge caused considerable background vibration, and second, the structure had natural frequencies in the transverse direction of 1.43, 1.56, and 1.76 cps, and the person forcing the structure was never able to tune the frequency of his motion fine enough to produce a record without beats.

Equipment and Testing Procedure - Structural Vibration Exciter

Machine excited vibration tests of the structure were conducted with the shaking machine which is shown in Figure 2.13, Appendix V, and which is described in detail in References 12 and 13. Briefly, the machine consists of two eccentric masses which rotate in opposite directions in horizontal planes, alternately adding and cancelling their centrifugal forces to produce a horizontal sinusoidal force directed along one axis. Because the eccentric weights do not lie in the same horizontal plane, a small sinusoidal moment, 0.28 foot-pounds per pound of force, is produced in a vertical plane perpendicular to the axis of the sinusoidal force. The machine produces a maximum sinusoidal force of approximately 800 pounds at 1.0 cps, the force increasing as the square of the frequency. The maximum frequency at which the machine can run is 10 cps and the maximum allowable force is 5000 pounds, which necessitates decreasing the amount of eccentric weight at higher speeds. With power from a large city power system, the speed control held the frequency of the force on the lightly damped Encino Reservoir structure

within 0.004 cps at lower speeds and within 0.016 cps at higher speeds, the frequency being measured over one second intervals by a digital device that counted 300 pulses per revolution of the eccentric weights. Although the machine itself was bolted to the penthouse floor, it was possible to orient the sinusoidal force in any direction by removing one of the drive chains and rotating one of the weight buckets by the proper amount before reassembling the chain.

Two groups of eccentric weights, each of which can be stacked four layers deep in the weight buckets are used in the shaking machine. One layer of the smaller weights produces 46.7 lbs. force at one cps, whereas one layer of the larger weights produces 144 lbs. force at one cps, the force in all cases increasing as the square of the frequency. The weight combinations are designated by two numbers, the first indicating the number of layers of large weights, and the second indicating the number of layers of small weights. Thus, a (1 - 2) loading means the force produced is 238 lbs. at one cps. Inasmuch as the weight buckets in the machine used at Encino are counterweighted, no force other than that due to the reported weight loading is introduced, and a force due to a (0 - 2) loading is exactly twice the force due to a (0 - 1) loading.

A special loading consisting of a 4.02 lbs. weight at a 16 11/16" radius in each bucket was used in an attempt to excite low level oscillations in which the friction at the bridge bearings would be sufficient to prevent sliding of the bridge. This loading, designated as (L.L.), produced a force of 13.7 lbs. at one cps, 29% that of the (0 - 1) loading.

Equipment and Testing Procedure - Instrumentation

The instrumentation consisted of two Statham Instruments Corporation strain gage accelerometers, model A5-2-350, one Consolidated Electrodynamics Corporation reluctance-type accelerometer, type 4-260, a William Miller Company model C-3 carrier amplifier, and a Consolidated Electrodynamics Corporation direct writing oscillograph, model 5-124. These components are described in Appendix I, so only a few details are given here. The strain gage accelerometers, of $\pm$ 2 g range and 100 cps natural frequency, each contained a 4-arm bridge of unbonded strain gage wire. An accelerometer is shown in Figure 2.14, Appendix V, mounted on a 6 3/4 lb. steel block which was placed on horizontal surfaces at various places in the structure where accelerations were to be measured, friction only holding the block to the surface. On the side of the tower, the accelerometers were bolted to plates which were bonded to the tower wall with a quick setting epoxy adhesive.

The carrier amplifier, which produced a 3000 cps carrier wave adjustable up to 10 volts, possessed an exceptionally low noise-to-signal ratio, so that a sinusoidal acceleration of 0.001g could be recorded by a galvanometer of 100 cps natural frequency as a wave of 5 1/2" peak-to-peak amplitude with a trace width, under the best conditions, of 0.05", composed chiefly of 60 cps signal. In places where high frequency accelerations were present, such as close to the shaking machine and on the bridge at higher frequencies, or where measured accelerations were extremely small, a galvanometer of 18.5 cps natural frequency, and lower sensitivity, was sometimes used to reduce the higher frequency components in the record. The oscillograph recorded all the traces on a light

sensitive roll of paper, 7" wide, which developed under daytime lighting conditions within a few seconds. A cardboard shield was placed over the front of the oscillograph to prevent the record from fading due to exposure to sunlight. In Figure 2.15, Appendix V, looking along the bridge towards the dam, the amplifiers and the oscillograph are partially exposed behind the amplidyne control unit for the shaking machine. The small black object in the center of the bridge deck is an accelerometer on a portable mounting block oriented to sense vertical accelerations.

A magnetic pickup is shown clamped to the top plate of the machine in Figure 2.13, Appendix V. For each revolution of the weight buckets, this pickup produced one pulse which, when recorded by the oscillograph with a 3000 cps galvanometer, was used to indicate the phase relationship between the force and the response.

The instrumentation was satisfactory for measuring vibrations excited by the shaking machine and for manually excited vibrations measured on the penthouse floor. The measurement of base motions caused by manual excitation, however, would have required approximately ten times more sensitivity than was available. The 100 cps natural frequencies of the accelerometers and the galvanometers provided a good picture of phase lag and of the non-linear behavior of the bridge at higher frequencies, but there were many instances in which the reduction of high frequency components by the use of lower frequency elements would have been desirable. Some accelerometers of greater sensitivity and lower natural frequency are described in Appendix I.

Equipment and Testing Procedure - Testing Procedure

The forced vibration tests on the structure required 15 days in the

field, but because the site was remote from the campus and the electronic equipment had to be transported and set up each day, only an average of four or five hours of each day were actually devoted to testing. The entire field operation was conducted by only two men, so that a considerable amount of the testing time was consumed in moving accelerometers and in handling cables. The recording and control equipment were located 25 feet out from the tower on the bridge so as to be safely away from the shaking machine in case it should rupture or break loose from its mountings. The motion of the equipment sitting at this point on the bridge was so great in the higher modes of the bridge that writing on the oscillogram was difficult. At all the natural frequencies the horizontal, vertical, and torsional movements of the bridge were very noticeable to the operators, and in fact it was this personal observation that limited the amplitudes of the applied force. Although a force of 4700 pounds amplitude was applied at 10 cps, at the fundamental frequency in the direction of the bridge, 2.11 cps, the maximum force was limited to 825 lbs., resulting in penthouse floor motion of 0.024" amplitude. In the direction perpendicular to the bridge, at the fundamental frequency of 1.76 cps, the force was limited to 294 pounds, resulting in a penthouse floor motion of 0.045" amplitude. Although these amplitudes look very small on paper and the stresses in the structure associated with them are computed to be negligible, at 130' above the ground the motions seemed to be as large as a rational person would care to experience. The visible motions at the anchorages of the bridge were the chief cause of concern to the operators.

Equipment and Testing Procedure - Suggestions for Dynamic Testing

In testing the Encino Reservoir structure a considerable amount of time was wasted because of lack of experience in dynamic testing. The following recommendations are made as a result of the experience gained in this testing program.

1. Analyze the structure to the fullest extent possible with the best available information prior to the test. Attempt to calculate all of the natural frequencies and mode shapes which will be encountered. If the calculations had been carried further before the field work was started at Encino, much confusion about mode shapes would have been eliminated. From this initial analysis it can be established that certain measurements should not be attempted, i.e., measurements of motion in one direction in the presence of a much larger motion in the perpendicular direction.

2. As a first step in the field work make simultaneous records of steady state vibrations from as many points as possible, chosen on the basis of the prior analysis. Rundown records, produced by suddenly cutting off the power from the exciter and recording the response as the machine coasts to rest, are of some value for estimating frequencies, but if several modes are present the rundown records are complicated and difficult to evaluate. The rundown records shown in Figure 2.16, Appendix V, show beats after each natural frequency has been passed. The top trace is vertical acceleration at panel point 13 on B_1, the center trace is vertical acceleration at panel point 5 on B_2, and the lower trace is horizontal acceleration on the penthouse floor.

Scan the frequency range closely, especially in the vicinity of

resonances, and take care to get the peak readings. This means, of course, that the record must be visible in the field. Then, if the situation permits, retire from the field for as long as necessary to evaluate the oscillograms and to plot the resonance curves. This work should reveal the natural frequencies and the approximate mode shapes, or at least indicate what measurements should be made to determine them. Refine the analytical work at this time in the light of the first set of data.

3. On returning to the field for more precise data about the mode shapes, take several records at close intervals covering the range immediately above and below the suspected natural frequencies. Make each record long enough to indicate if the vibration is steady state. The use of two or more channels for defining mode shapes is absolutely essential.

4. Do not disregard the effects of temperature, humidity, structural changes, and the passing of time on the dynamic behavior of the structure. Do not overestimate coefficients of friction. Changes in natural frequencies and mode shapes from one test to another can result from any of these items.

5. If the static 2 g calibration is used, calibrate at least once in the middle of the day as well as at the beginning and the end of the day. Take a few dynamic readings with several instruments together on one point as a check of consistency among the channels. If sensitivity of the instrumentation varies with line voltage, monitor line voltage continuously with a voltmeter of good quality. The use of one of the galvanometers of the oscillograph to provide a measure of line voltage

on each record is suggested as a convenient method.

6. Although measuring the oscillogram amplitudes, reducing the data by slide rule, and manually plotting the resonance curves is a tedious task, it is the recommended method. A computer program was written to reduce measured trace amplitudes of Encino data to accelerations and then to put out a tape which was used to drive an automatic plotting machine, but the time spent in preparing the trace amplitudes for the computer and in carrying out the computer work and the machine plotting proved to be more than the time required by the manual method. Machine plotting was found to be less precise and less versatile than manual plotting.

D. Vibrations of the Free-Standing Tower.

Table 2.3 indicates the effects of shear deflection, rotatory inertia, dead load compression, and of rotational and translational foundation compliance on the first two computed frequencies and on the fundamental mode shape of the tower without the bridge attached. Dimensionless terms relating to these phenomena do not enter into a frequency formula in a simple manner, so the effects occurring here cannot exactly be applied to other cases, but the trends resulting from each can be observed. In all cases foundation compliance constants and the modulus of elasticity of the concrete are assumed to have the same values in the second mode as in the first mode.

In Table 2.3 the increases in the fundamental frequency, f_1, and the increase in the ratio of the second frequency to fundamental, $f_2/f_1 = F$, as a result of neglecting shear deflection in the tower are seen to be approximately proportional to the value of α, the shear coefficient. If shear is neglected in calculating the frequencies of the tower, f_1 is

Conditions	f_1 cps	f_2 cps	f_2/f_1 = F	V_B #	M_B ft#	Θ_B RAD	Y_B ft	Y_{Top} ft	$Y_{76'}$ ft	Row
Basic Conditions	1.948	9.340	4.795	$3.56_6 \times 10^6$	$4.09_8 \times 10^8$	0	0	1.239	0.345	a
Same as row a, except $\alpha = 0.64$	1.971	9.871	5.008	$3.63_6 \times 10^6$	$4.18_8 \times 10^8$	0	0	1.242	0.341	b
Same as row a, except $\alpha = 0$	1.983	10.164	5.126	$3.66_6 \times 10^6$	$4.22_8 \times 10^8$	0	0	1.243	0.338	c
Same as row c, except neglect rotatory inertia	1.990	10.403	5.228	$3.68_6 \times 10^6$	$4.23_8 \times 10^8$	0	0	1.243	0.338	d
Same as row d, except neglect dead load compression	1.992	10.405	5.223	$3.69_6 \times 10^6$	$4.23_8 \times 10^8$	0	0	1.243	0.338	e
Same as row a, except $K_{MB} = 1 \times 10^{-12}$ RAD/ft #	1.894	9.009	4.757	$3.43_6 \times 10^6$	$3.90_8 \times 10^8$	3.90×10^{-4}	0	1.233	0.358	f
Same as row a, except $K_{MB} = 2 \times 10^{-12}$ RAD/ft #	1.844	8.735	4.737	$3.30_6 \times 10^6$	$3.72_8 \times 10^8$	7.44×10^{-4}	0	1.228	0.369	g
Same as row a, except $K_{MB} = 1 \times 10^{-11}$ RAD/ft #	1.544	7.572	4.904	$2.51_6 \times 10^6$	$2.71_8 \times 10^8$	2.71×10^{-3}	0	1.201	0.431	h

Basic Conditions: $E = 4.18 \times 10^6$ psi, $\alpha = 1.95$, base rigid, shear deflection, dead load compression, rotatory inertia included, Y on penthouse floor = 1 ft.

TABLE 2.3

VIBRATIONS OF NEW ENCINO TOWER WITHOUT BRIDGE

(continued on next page)

Conditions	f_1 cps	f_2 cps	f_2/f_1 = F	V_B #	M_B ft#	θ_B RAD	Y_B ft	Y_{Top} ft	$Y_{76'}$ ft	Row
Same as row a, except $K_{VB} = 1 \times 10^{-9}$ ft/#	1.944	9.103	4.683	3.569×10^6	4.080×10^8	0	3.569×10^{-3}	1.238	0.348	i
Same as row a, except $K_{VB} = 1 \times 10^{-8}$ ft/#	1.905	6.963	3.655	3.624×10^6	3.987×10^8	0	3.624×10^{-2}	1.229	0.370	j
Same as row a, except $K_{MB} = 2 \times 10^{-12}$ RAD/ft# $K_{VB} = 1 \times 10^{-9}$ ft/#	1.840	8.535	4.639	3.304×10^6	3.712×10^8	7.424×10^{-4}	3.304×10^{-3}	1.227	0.372	k
Same as row a, except $E = 3.83 \times 10^{+6}$ psi $K_{MB} = 1 \times 10^{-11}$ RAD/ft#	1.503	7.320	4.870	2.362×10^6	2.560×10^8	2.560×10^{-3}	0	1.203	0.427	l
Same as row a, except $E = 3.83 \times 10^6$ psi $K_{MB} = 2.227 \times 10^{-12}$ RAD/ft# $K_{VB} = 9.73 \times 10^{-10}$ ft/#	1.759	8.176	4.648	3.020×10^6	3.392×10^8	7.700×10^{-4}	2.938×10^{-3}	1.227	0.372	m
Same as a, except $K_{MB} = 3.88 \times 10^{-12}$ RAD/ft# $K_{VB} = 7 \times 10^{-10}$ ft/#	1.757	8.210	4.673	3.082×10^6	3.420×10^8	1.327×10^{-3}	2.157×10^{-3}	1.220	0.389	n
Observed Values	1.76	8.17-8.26	4.65-4.70			$7.7^* \times 10^{-4}$	$3.0^* \times 10^{-3}$			o

*θ_B and Y_B observed under (0-1) loading with bridge attached.

TABLE 2.3 (continued)

VIBRATIONS OF NEW ENCINO TOWER WITHOUT BRIDGE

increased by 1.8% and F is increased by 6.9%. The neglect of rotatory inertia further increases f_1 by 0.4% and F by 2.1%. If dead load compression is not included in the computations f_1 is increased by 0.1%, but F is decreased by 0.1%. Changes in the fundamental mode shape, as indicated by the ordinates shown at the 76' and the 149' levels on the tower for a 1'-0" deflection at the penthouse floor, which is 131' above the base, are very small, and changes in the base shear and moment, V_B and M_B, do not exceed 4% if shear deflection, rotatory inertia, and dead load compression are omitted from the calculations.

The rotational and translational foundation compliance constants in Table 2.3, K_{MB} and K_{VB}, are shown as they were used in the computations, as the reciprocals of spring constants. Respectively K_{MB} and K_{VB} relate moment at the bottom of the barrel to rotation at that point and shear at the bottom of the barrel to horizontal translation at that point. It is shown later that horizontal translation depends on both the moment and the shear at the base. Rotational foundation compliance in this instance changes f_1 and the ratio of base rotation times height of the tower divided by tip deflection, designated as S in Table 2.5, by amounts roughly proportional to the value of the compliance constant K_{MB}, the constants of proportionality decreasing to approximately 75% of their original values when S reaches 0.33. The frequency ratio F shows first a slight decrease and then an increase as K_{MB} increases.

Translation compliance affects f_1, F, and the ratio of base translation divided by tip deflection, designated as T in Table 2.5, closely in proportion to K_{VB} for values of T up to at least 0.035. The effects of foundation compliance, on P and R, where P is the ratio of the change in f_1, divided by f_1, and R is the ratio of the change in F divided by

K_{VB}	K_{MB}	f_1	f_2	$f_2/f_1 = F$	Y_B	θ_B
0	0	0.03357	0.2104	6.267	0	0
0.1	0	0.03353	0.2069	6.171	0.00176	0
1.0	0	0.03312	0.1763	5.323	0.0174	0
5.0	0	0.03134	0.1120	3.574	0.0863	0
0	0.1	0.03355	0.2102	6.265	0	0.00126
0	1.0	0.03334	0.2089	6.267	0	0.0125
0	5.0	0.03234	0.2036	6.278	0	0.0597
0	50.0	0.02553	0.1755	6.871	0	0.3910

I = 0.0036, L = 1.0, A = 1.0,

ρ = 1.0, E = 1.0, Shear Deflection and Rotatory Inertia Neglected.

Y at Base = $K_{VB} \cdot V_B$

θ at Base = $K_{MB} \cdot M_B$

Y at Tip = 1.0

TABLE 2.4

EFFECTS OF FOUNDATION MOVEMENTS ON THE FREQUENCIES OF A UNIFORM CANTILEVER BEAM

$Y_B/Y_T = T$	P/T	R/T		$\frac{\theta_{BL}}{Y_T} = S$	P/S	R/S
2.88×10^{-3}	-0.71	-8.1	DATA FROM	4.71×10^{-2}	-0.59	-0.17
2.95×10^{-2}	-0.75	-8.1	TABLE 2.3	9.00×10^{-2}	-0.59	-0.13
				3.36×10^{-1}	-0.62	+0.07
1.76×10^{-3}	-0.78	-8.7	DATA FROM	1.26×10^{-3}	-0.57	-0.17
1.74×10^{-2}	-0.77	-8.6	TABLE 2.4	1.25×10^{-2}	-0.57	0.00
8.63×10^{-2}	-0.77	-5.0		5.97×10^{-2}	-0.57	+0.03
				3.91×10^{-1}	-0.61	+0.25

P = (change in f_1) $\div$ f_1, R = (change in F) $\div$ F, θ_B = θ at base,

Y_B = Y at base, Y_T = at tip

TABLE 2.5

EFFECTS OF FOUNDATION MOVEMENTS ON FREQUENCIES OF CANTILEVER BEAMS

F, are summarized in Table 2.5. Also appearing in Table 2.5 are similar data from a completely different cantilever beam, for which the effects of foundation compliance are tabulated in Table 2.4. The ratios P/T, P/S, and R/T in Table 2.5 appear to be sufficiently consistent to be useful for estimating changes in f_1 and F resulting from moderate foundation movements. The important relationships between these changes and the values of K_{VB} and K_{MB} have not been developed here, however.

An approximation of the ratio P/S for a uniform cantilever beam with S very small can be made by equating the potential and the kinetic energies of the vibrating beam. Let Y_m designate the deflection of the beam when the base rotation θ_B is zero and let Y designate the total deflection when base rotation occurs. A study of the fundamental Bernoulli-Euler mode shape of the uniform cantilever beam shows the deflection in terms of the tip deflection, Y_{mt}, is approximately given by

$$Y_m = Y_{mt}\,(x/L)^n, \quad n = 1.56. \tag{2.11}$$

For values of S up to 0.06 or so, computer mode shapes indicate

$$Y = Y_m + \theta_B x. \tag{2.12}$$

The kinetic energy then is given by

$$\text{K.E.} = 1/2 \int_o^L \rho A \omega^2 Y^2 dx = 1/2 \int_o^1 \rho A \omega^2 Y_{mt}^2 \left[z^{2n} + 2z^{n+1}S\right] L dz$$
$$= \frac{\rho A \omega^2 L Y_{mt}^2}{2(4.12)} \left[1 + 2.315S\right], \tag{2.13}$$

where $z = (x/L)$ and the higher powers of S have been neglected.

The potential energy in the beam is given by

$$\text{P.E.} = \frac{\int_o^L M_x^2 dx}{2EI} + 1/2\, M_B \theta_B \,, \tag{2.14}$$

where M_B is the base moment, and M_x is the bending moment at any section,

expressed by

$$M_x = \int_x^L \rho A \omega^2 \left[Y_{mt} (\xi/L)^n + \theta_B \xi \right] \left[\xi - x \right] d\xi$$

$$= Y_{mt} \rho A \omega^2 L^2 \left[\frac{1}{n+2} + \frac{Sz^3}{6} + \frac{S}{3} + \frac{z^{n+2}}{(n+1)(n+2)} - \frac{z}{n+1} - \frac{Sz}{2} \right] . \qquad (2.15)$$

If these calculations are carried out, there results

$$P.E. = \frac{\rho^2 A^2 Y_{mt}^2 \omega^4 L^5}{2\ EI} \left[0.01968 + 0.04853S \right] +$$

$$+ 1/2\ Y_{mt} \rho A \omega^2 L^2 \left[0.2809 + 0.3333S \right] \theta_B . \qquad (2.16)$$

Now $\theta_B = \frac{SY_{mt}}{L}$, so the second term in equation 2.16 becomes

$$1/2\ Y_{mt}^2 \rho^2 A^2 \omega^4 L^5\ S(0.2809)\ \left(\frac{EI}{\rho A \omega^2 L^4}\right).$$

Inasmuch as the frequency of vibration is close to the natural frequency of a cantilever with a perfectly rigid mounting, the term in parenthesis is approximately 1/12.36, and the potential energy becomes

$$P.E. = \frac{\rho^2 A^2 Y_{mt}^2 \omega^4 L^5\ (0.01968)}{2\ EI}\ (1 + 3.620S). \qquad (2.17)$$

Then solving for ω^2 from equations 2.13 and 2.17

$$\omega^2 = \frac{12.33EI}{\rho AL^4}\ (1 - 1.305S),$$

indicating that for small S, ω_1 is proportional to (1-0.65S). The data in Table 2.5 show that ω_1 is closely proportional to (1-0.57S), indicating that the computation is rather sensitive to the assumed mode shapes.

Comparison of frequencies in rows h and 1 of Table 2.3 illustrates the fact that if foundation compliance is present, the natural frequencies are no longer proportional to the square root of the modulus of elasticity.

Small oscillations of the tower without the bridge attached were observed in the first part of February, 1962. Accelerations of 0.002 g and less on the penthouse floor were excited by wind and by manual forcing.

The observed frequencies, shown in row o of Table 2.3 were used to estimate the foundation compliance constants, K_{MB} and K_{VB}. Unfortunately, the level of excitation of the free standing tower was so low that it was not possible to measure foundation motions, so, as noted in Table 2.3, the foundation motions listed in row o along with the frequencies of the tower without the bridge attached were actually observed after the bridge had been erected. Computer work shows that the base moment and the base shear in the free-standing tower are smaller by approximately 3% and 8% respectively than the base moment and the base shear in the tower with the bridge attached, if the foundation is considered rigid in both cases. The use of the base motions shown in row o for the free-standing tower is, therefore, reasonable.

In row n of Table 2.3 calculated with the value of E measured by the sonic method in July, the calculated frequencies are seen to agree with the observed frequencies, but the base rotation is 85% greater and the base translation is 27% smaller than their observed values. The concrete in the tower, however, was poured between July and December, 1961, so it is probable that the modulus of elasticity was lower in February, 1962, when the frequencies were measured, than in July, 1962, when the test cores were taken.(26) Adjusting E downward to 3.83×10^6 psi, an $8\frac{1}{2}$% decrease, yields frequencies and base motions, row m, matching the observations, and points out the fact that without an accurate knowledge of the value of E, no check is possible between the computations and the measurements. As mentioned previously, the sonically determined values of E showed a spread of $12\frac{1}{2}$% centered about the average, and they pertained to only one pour of concrete at the base of

the tower. Just how realistically the sonic value of E in small cores represents the effective modulus of elasticity of the concrete in the tower vibrating at its natural frequency, where the wave length is several hundred times longer and the stress conditions are different, has yet to be proved. Carefully conducted tests on free standing towers will eventually reveal the answer.

In the direction perpendicular to the length of the bridge, the first two frequencies of the tower without the bridge attached were observed in February, 1962, to be 1.73 and approximately 8.1 cps, the second frequency less accurate than the first because, being excited to a lesser extent by the wind, the records were shorter and usually contained the fundamental along with the second frequency. After the bridge had been erected, the observed base rotation and translation per 1'-0" motion on the penthouse floor were 7.2×10^{-4} radians and 2.3×10^{-3} ft. respectively, compared with 7.7×10^{-4} radians and 3.0×10^{-3} ft. respectively in the direction parallel to the bridge. Using the observed base motions and the reduced value for E, 3.83×10^{6} psi, the natural frequencies in the direction perpendicular to the bridge were computed as 1.77 and 8.2 cps slightly higher than the observations. To reduce the computed frequencies to the observed values would require an increase of base rotation by approximately 37% and an increase of base translation by approximately 28%, thus giving some measure of the accuracy of the computed compliance constants in this case.

The amplitudes of displacement on the penthouse floor at the time the frequencies of the free standing tower were measured were

approximately 0.0004", whereas at the time the base motions were measured these amplitudes were approximately 0.016" in the direction parallel to the bridge and 0.030" in the direction perpendicular to the bridge. To examine the possibility of a trend in foundation compliance with amplitude, base motions were measured when the penthouse floor motion in the fundamental mode parallel to the bridge was approximately double the 0.016" mentioned above. The observed ratios of θ_B and Y_B to penthouse floor motion at this increased amplitude were both smaller than their previous values by 7%. In the second mode of the tower it was found that tripling the amplitude resulted in an increase in the ratios of θ_B and Y_B to the deflection of a point 74' above the base by 2% and 4% respectively.

At this point the accuracy of the field measurements should be discussed to shed light on the agreement between computations and measurements. Free vibration frequencies were measured in the field by Mr. Jerry Morrill and Mr. Ron Dobner of the U. S. Coast and Geodetic Survey with a Sprengnether Blast Recorder, no. 1720, with its own timing lines at 0.2 seconds and with an auxiliary time signal at 0.50 seconds from a very accurate clock. The two timing signals showed always perfect agreement to the naked eye. Any errors in the observed frequencies therefore, are due to reading the record and it is felt that the observed frequencies of free vibrations are in error by no more than 0.02 cps. Over the full length of decaying records of the type in Figure 2.12, Appendix V, very slight increases in frequency were noted at the smaller amplitudes, approximately 0.01 cps difference between the ends of the record. These variations could be caused by slight gusts of wind or by a

modulus of elasticity of the concrete that decreases with increasing amplitude. The reported frequencies of free vibrations are those measured at the smallest amplitudes.

Base motions of the tower with the bridge attached were measured during the machine forced vibration tests with accelerometers placed on top of the tower foundation against the inside of the tower walls. In computing the base rotation, θ_B, it was assumed that the cross section of the tower at the foundation level remained plane during rotation. The level of the accelerations used to determine the base rotation was approximately 4×10^{-5}g, much below the lowest level at which a calibration was ever attempted. This level of acceleration produced a trace of approximately 0.16" double amplitude, a value which was probably read from the oscillogram with $\pm$ 5% accuracy. Six separate measurements of vertical base motions, five on one day and one on another day, for θ_B, close to the fundamental frequency, showed a spread from 7.1×10^{-4} to 7.8×10^{-4} radians per foot of penthouse floor deflection in the direction parallel to the bridge. The value used, 7.7×10^{-4}, was measured the most carefully and by the most reliable procedure. Only one measurement was made of θ_B in the direction transverse to the bridge. Trace amplitudes of horizontal base translation were only 0.07" to 0.09" peak-to-peak, so the reading error might be as much as $\pm$ 10%. The measurements of horizontal base translation showed a spread of 10% centered about the average. Without actually calibrating the measuring equipment at this low level of measurement the accuracy of the measurements is of course in doubt. A comparison of these records of base motion with some records made simultaneously with the Sprengnether instrument showed

agreement within 3%, but the Sprengnether records were only 0.08" peak-to-peak, so the reading error might be much larger than 3%.

E. Vibrations of the Entire Structure

Adjusting the Parameters

In Table 2.6 rows (a) through (e) show the effects of foundation compliance, bridge inertia, and bridge sliding on two computed frequencies and on the computed fundamental mode shape of the tower with the bridge attached. The modulus of elasticity used in these computations was the average sonic modulus, 4.18×10^6 psi. The foundation movements used were those observed in the fundamental mode under the (0 - 1) loading condition, and the compliance constants determined for this condition were then held constant when the higher frequency f_{T2} was computed. When bridge sliding was introduced, row (e), it was found necessary to alter the foundation compliance constants slightly from their values in row (d) in order to maintain the proper ratios of base motions to motions on the penthouse floor. As mentioned previously, bridge sliding was represented in the computations as the deflections of springs placed between the ends of the bridge spans and their supports, the sliding motion being proportional to the longitudinal forces transferred at these points. The actual sliding movements associated with the (0 - 1) loading condition are described later.

The frequency f_1 in Table 2.6 is the lowest frequency of the structure. The frequency designated f_{T2} is the frequency of the second mode in which the tower plays a significant part. Two other modes, primarily of bridge motion, occur with frequencies between f_1 and f_{T2}, but inasmuch as the tower is the element of primary interest here, f_{T2} is used for making comparisons.

Row	f_1 cps	f_{T2} cps	f_{T2}/f_1	Deflections in Fundamental Mode Shape for Unit Deflection on Penthouse Floor: Point 1	2	3	4	5	6	7
a	2.261	9.165	4.05	0.054	0.432	0.432	1.208	1.405	0.519	1.639
b	2.442	9.238	3.78	0.054	0.434	0.434	1.209	0.950	0.484	0.955
c	2.183	8.452	3.97	0.075	0.457	0.457	1.197	1.369	0.515	1.563
d	2.182	8.452	3.97	0.075	0.457	0.457	1.197	1.367	0.515	1.565
e	2.142	8.441	3.92	0.075	0.456	0.456	1.198	1.151	0.515	1.360
f (0-1)	2.11	8.09	3.83	0.076	0.46	0.46	1.22	1.09	0.51	1.33
f (L.L)	2.16	8.20	3.81		0.45	0.45	1.20	1.00		1.46
g	2.115	8.27	3.91	0.075	0.456	0.456	1.198	1.143	0.513	1.342

TABLE 2.6

TWO FREQUENCIES AND FUNDAMENTAL MODE SHAPE OF ENTIRE STRUCTURE

(Explanation of Table 2.6 on Following Page)

EXPLANATION OF TABLE 2.6

Row

a: $E_c = 4.10 \times 10^6$ psi, no sliding of bridge, rigid foundations, shear and rotatory inertia included.

b: Same as row a except inertia of bridge and inertia of T_2 neglected.

c: Same as row a except base of T_1 allowed to rotate and translate to agree with observations. $\theta_B = 7.7 \times 10^{-4}$ radians, $Y_B = 3 \times 10^{-3}$ ft.

d: Same as row c except base of T_2 allowed to move to agree with observations. $\theta_A = 3 \times 10^{-4}$ radians, $Y_A = 1 \times 10^{-3}$ ft., $U_A = 5 \times 10^{-4}$ ft.

e: Same as row d except motions observed with (O-1) load allowed at bridge bearings.

f: Observed data. Top line for (O-1) load, lower line for (L.L.) load.

g: Same as row e except I reduced for gates in tower, $E_c = 4.10 \times 10^6$ psi.

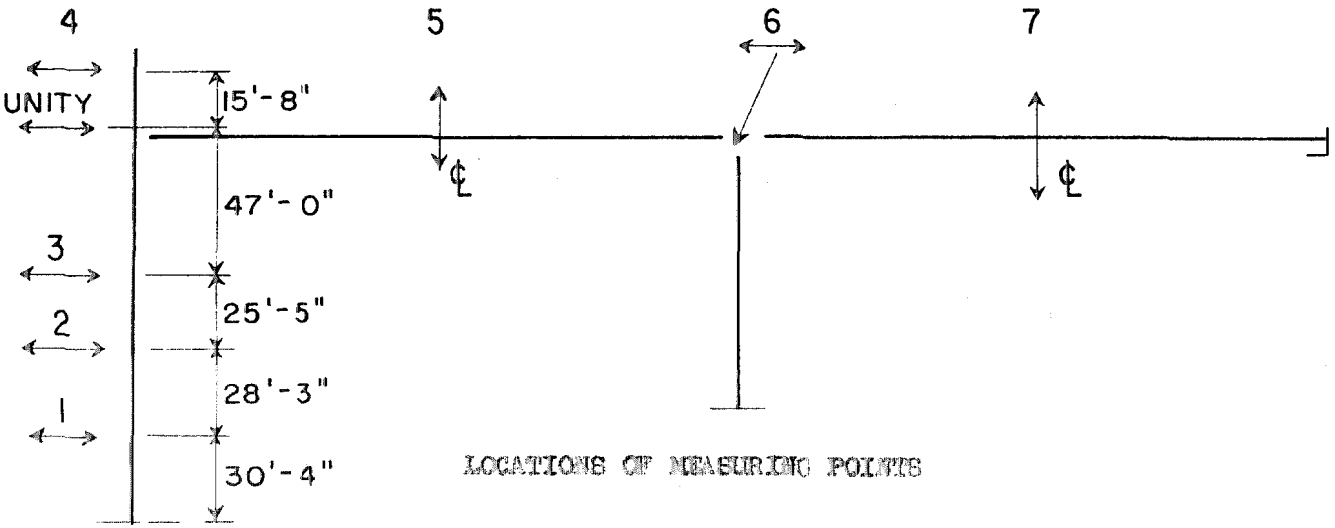

LOCATIONS OF MEASURING POINTS

By comparing row (b) of Table 2.6 with row (a) it is seen that neglecting the mass of the bridge and of T_2 in the calculations increases the fundamental frequency of the structure by 8%, decreases the deflections at the centerlines of the bridge spans by 30% to 40%, but increases f_{T2} by only 0.8%. The chief effects of foundation movements of T_1 are seen from rows (a) and (c) to be a softening of the mode shape of T_1 below the bridge connection, a 4% decrease in f_1, an 8% decrease of f_{T2}, and a softening of the deflection curves of the bridge spans. Base motions of T_2 are seen from row (d) to have a very small effect on the structure. Bridge sliding, row (e), has a very minor effect in the mode shape of the tower, but markedly reduces the centerline deflections of the bridge spans, and reduces f_1 by 0.04 cps.

Row (f) shows the observed frequencies and the fundamental mode shape for the (0 - 1) loading condition. These data should agree with row (e) if the measurements were exact and the idealization of the structure in the computations were perfect. The computed frequency f_1 is seen to be 1.5% high and f_{T2} is 4.2% high. The computed mode shape differs from the observed mode shape generally by amounts within the consistency of the field measurements, $\pm$ 5%.

In attempting to explain the discrepancies between rows (e) and (f), principally the discrepancy in f_{T2}, several observations can be made concerning the idealization of the structure for computational purposes. First, no reduction in the moment of inertia of the tower was made to allow for the gates in the side of the tower. If I is reduced by the product of the cross sectional area removed times the square of the distance to the neutral axis, assumed through the center of the cross section, then over eight 2'-0" sections in T_{1a} the moment of inertia

should be reduced by approximately 13%. Since the openings are lined over 12" of the tower wall's thickness with a steel ring it is questionable if this reduction in I is actually justified.

Second, the moment of inertia of the cross section through the penthouse door was computed by subtracting, over the height of the door, the product of the area removed by the door times the square of the distance from the tower centerline. This results in a value of I over the height of the door slightly too low, but realistically, the reduction should extend for some distance above and below the door. Extending the reduction for 2'-0" above and below the door, and decreasing I by 13% over eight sections in T_{1a} results in f_1 and f_{T2} having computed values of 2.13 and 8.35 cps, both closer to the observed frequencies.

Third, the representation of the trussed members by solid flexural members results in sizeable errors in bridge deflection under static loading, as was shown previously. The effect of the bridge and of T_2 on the frequencies in which the tower plays a significant role may be seen by comparing row (a) of Table 2.3 with row (a) of Table 2.6, the base of T_{1a} being rigidly fixed in both cases. It is seen that connecting the bridge to the tower increases f_1 by 16% and reduces f_{T2} by less than 2%. Errors in representation of the trussed members, therefore, can be expected to result in errors in f_1 and in the bridge deflections, but the effect on f_{T2} will be small. A comparison of rows (c) and (e) of Table 2.6 shows that bridge sliding has a very small influence on f_{T2}.

A fourth observation is that the foundation compliance constants were assumed in the second mode to remain unchanged from the values they had in the first mode. It has been mentioned previously in connection with vibrations of the free-standing tower, that slight increases and

slight decreases in base rotation and base translation were noted with increasing load level and no definite trend could be identified. Under (0 - 1) loading at the frequency f_{T2}, base rotation and base translation of T_1 were approximately twice and three times their respective values under (0 - 1) loading at the frequency f_1, so no large changes in the compliance constants at f_{T2} should be expected. Allowing the base translation constant K_{VB} to increase by 10% reduced the frequency f_{T2} by only 0.016 cps.

Finally, the effective value of the modulus of elasticity might reasonably vary by as much as 20% from the value determined by the sonic method from the three cores taken near the base. The constancy of E with stress level, however, is suggested by the constant ratio between amplitude and force level at frequencies at some distance from the natural frequencies, and by the relatively constant fundamental frequency at loadings between (0 - 1) and (0 - 4). Reducing the sonic value of E by 2% and using the reduced values of I mentioned above for T_1 yields a value for f_1 of 2.11 cps, agreeing with the observed value, and a value for f_{T2} of 8.27 cps, 2½% high. The fundamental mode shape associated with these frequencies, showing slightly better agreement with the observations, is shown in row g of Table 2.6.

Although other adjustments, deviating from the known and assumed properties of the structure, could possibly result in all the quantities tabulated in Table 2.6 agreeing with the observations, the intention here is to indicate what accuracy might be attained using known and measured properties of the structure. With the exception of a later modification of base translation, no further adjustments were attempted.

In the report of the test of the old Encino Reservoir tower,[2] which was replaced by the present structure, it was stated that the observed amplitude at midheight in the fundamental mode was approximately twice its computed value. Inasmuch as the computational method used here is very similar to that used for the old tower, the good agreement here between the computed and observed values at midheights suggests the discrepancy was the result of some instrumental difficulty.

Vibrations of the Entire Structure - Computing the Natural Frequencies

In the description of the mathematical technique it was stated that the natural frequencies were found by trial and that the natural frequencies were those for which the moment, M_F, at the top of T_{1b}, called Δ, went to zero when all the other boundary and joint conditions had been satisfied. A plot of M_Fv frequency is shown in Figure 2.17 for the structural conditions associated with row (e) of Table 2.6. The five natural frequencies and their associated mode shapes derived from the structural conditions of row (g) are shown in Figure 2.18. The frequencies are identified as f_1, f_{B1}, f_{B2}, f_{T2} and f_{B3}, the subscript B identifying those modes in which the bridge plays the dominant part, and the subscript T identifying those modes in which the tower is active. The computed mode shapes are shown by solid lines in these figures whereas observed ordinates are shown by small circles.

The Δ v f curve ($\Delta = M_F$) in Figure 2.17 looks unusual with its many branches extending to infinity, but it can be explained on the basis of forced vibration of the undamped structure. Consider the inverse problem of finding the shear, V_B, at the base of T_{1a} resulting from a moment, $M_F = (1 \cdot \sin \omega t)$, applied at the top of T_{1b}. Since the

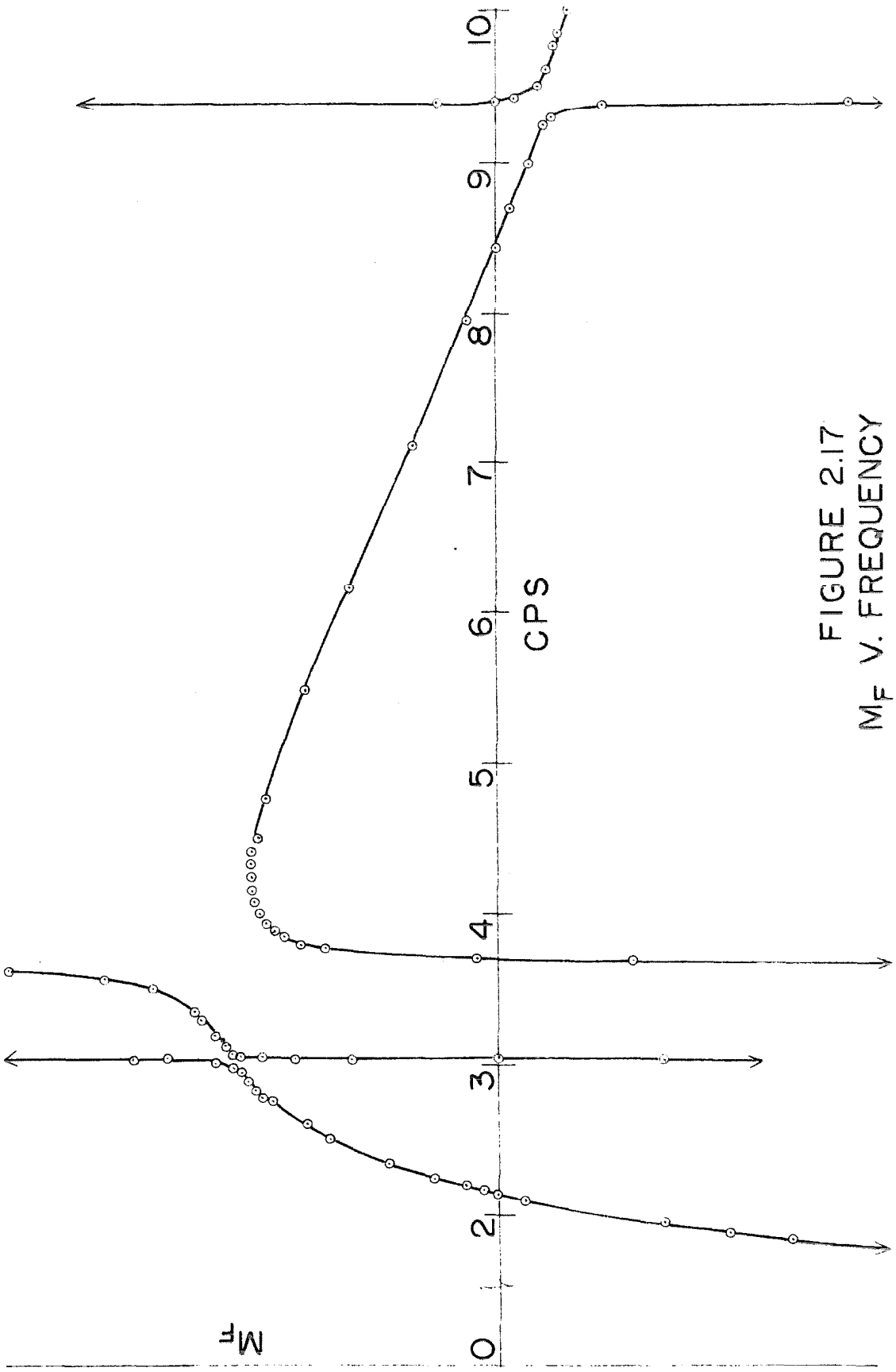

FIGURE 2.17
M_F V. FREQUENCY

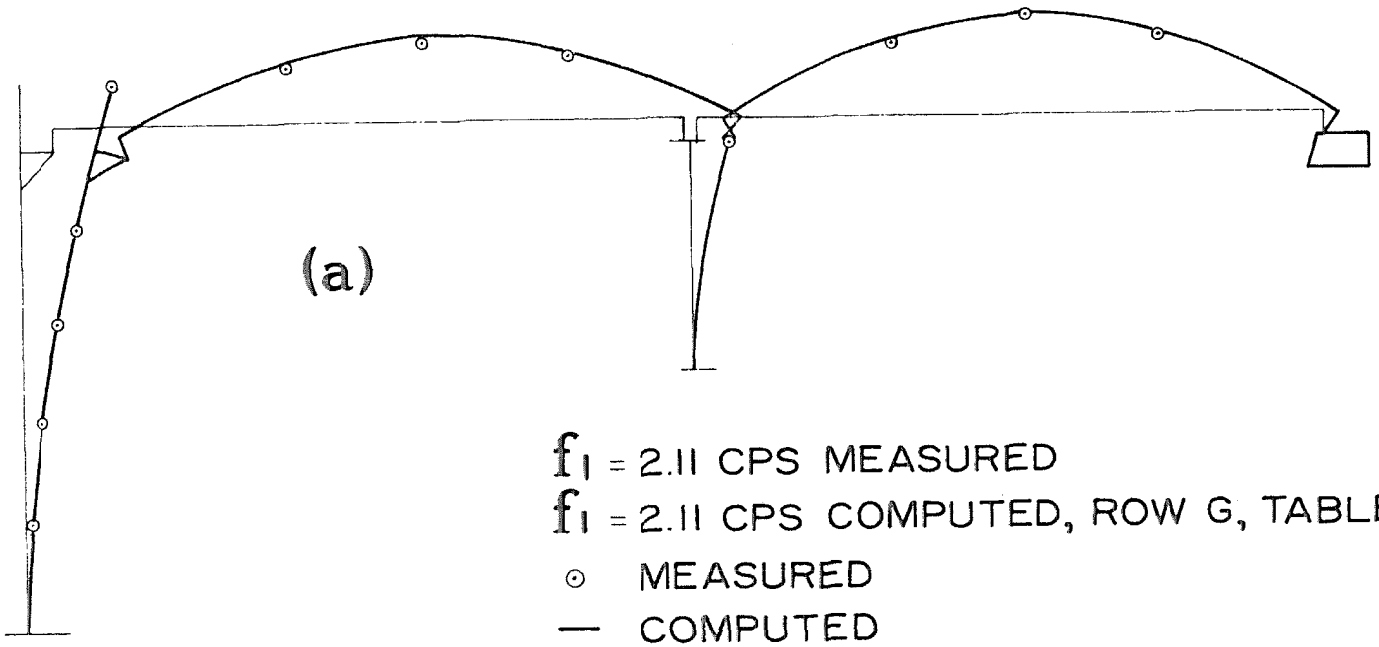

FIGURE 2.18
LONGITUDINAL MODE SHAPE

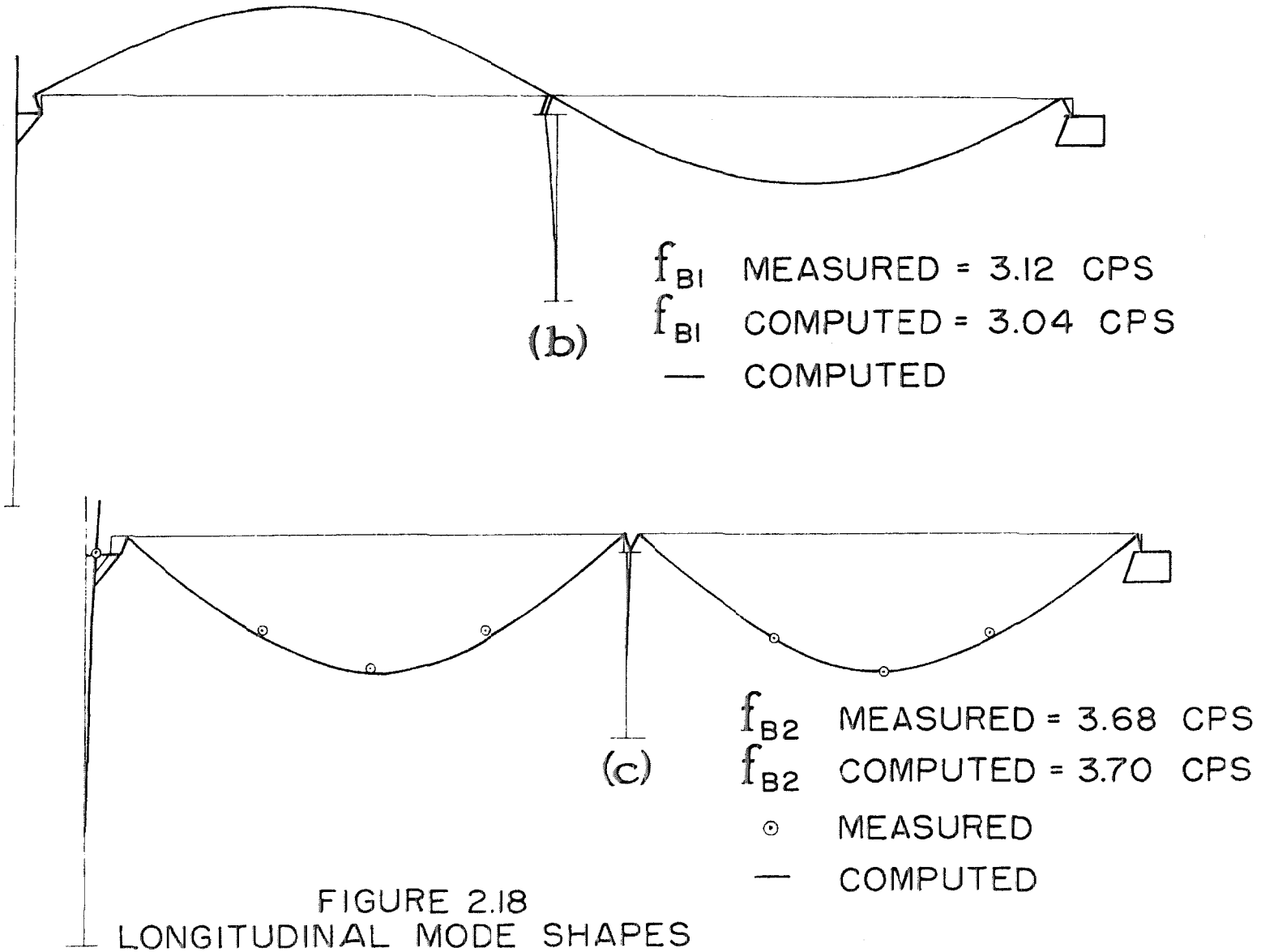

FIGURE 2.18
LONGITUDINAL MODE SHAPES

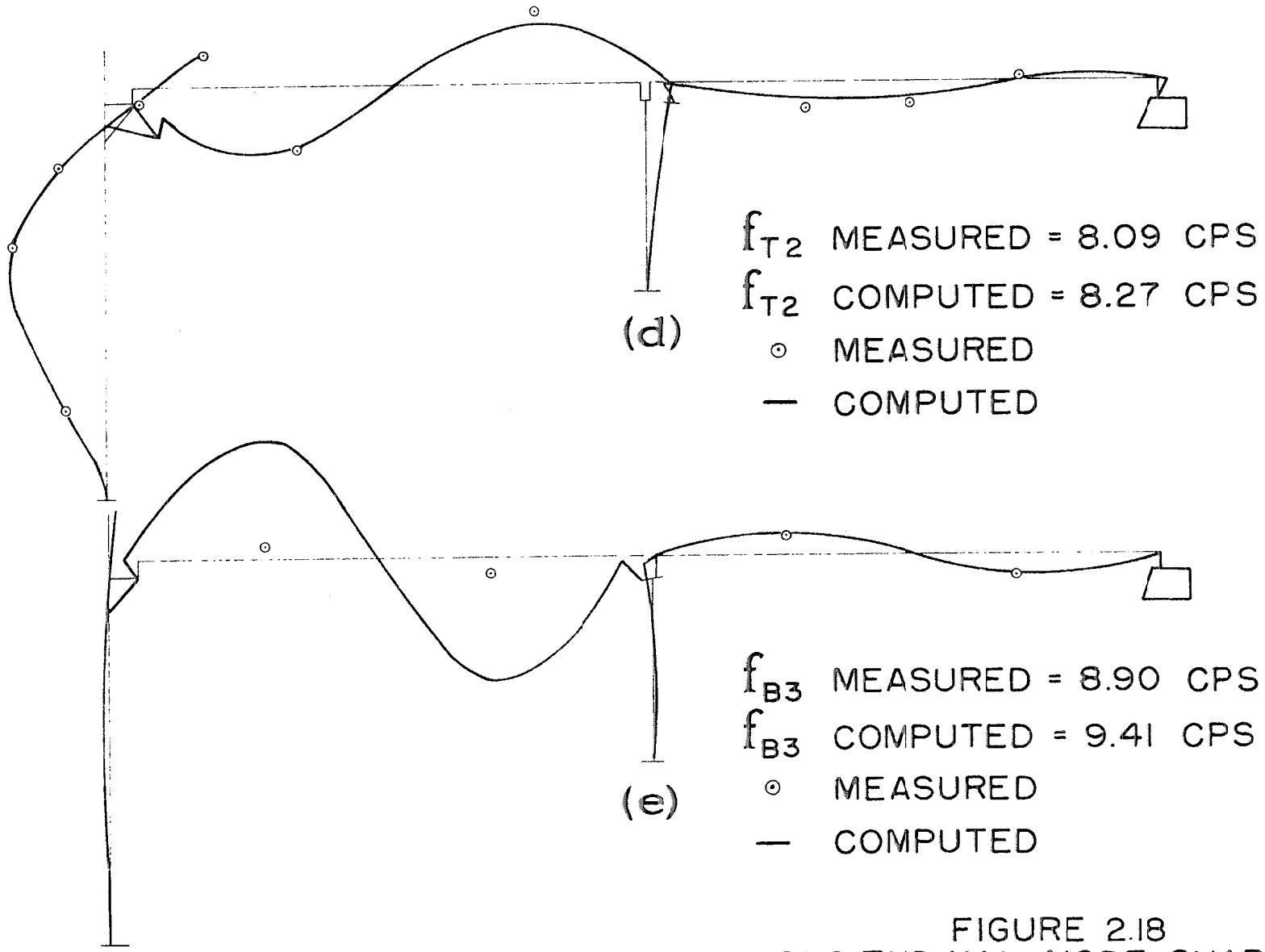

FIGURE 2.18
LONGITUDINAL MODE SHAPES

structure is undamped, V_B and all other forces and motions in the structure will always be in phase with M_F if a minus sign is attached to the amplitudes of those quantities which have a phase difference of 180°. Thus, the conditions for equations 2.1 through 2.6 are established, namely that all parts of the structure are moving in phase. The amplitude of V_B will vary from very small values at some frequencies, up to infinite values at all the natural frequencies of the structure, and, if desired, a curve of this response could be plotted with the sign of the amplitude of V_B changing each time a natural frequency is crossed. For discussion this curve will be called the signed resonance curve.

Consider now the question, "What values of M_F will result in the amplitude of V_B being always equal to unity?" It is seen that the answer is given by values of M_F which are the reciprocals of the ordinates of the signed V_B resonance curve. In the description of the technique used for the Encino Reservoir structure it was stated that V_B was always set to unity, so Figure 2.17 represents simply the reciprocal of the signed resonance curve of V_B due to $M_F = (1 \cdot \sin \omega t)$. If the negative arms of Figure 2.17 are plotted positively, the curve becomes the reciprocal of the resonance curve plotted in the usual manner. An infinite value for Δ on this particular curve simply means that V_B goes through zero at that particular frequency.

The very steep zero crossings in Figure 2.17 might easily be missed unless the frequency range were scanned very carefully. These sharp breaks in the curve are associated with modes in which M_F and V_B have little influence. In other words, the application of M_F produces very little of these modes except at their own frequencies, and the occurrence of these modes produces a very small amount of V_B. As an example,

consider the case in which the bridge is on rollers at zero eccentricity from the centerline of the tower. In this case, application of M_F at the top of the tower does not excite the bridge at all, and V_B results only from the excitation of modes in the tower. If a sufficiently broad scale in f is used there is no difficulty in plotting the resonance curve and its reciprocal. If then a slight eccentricity of the bridge reaction from the centerline of the tower is allowed, the resonance curve of V_B would look very similar to the previous case, except that when a frequency involving the bridge is approached V_B would rapidly become infinite. The more the coupling between the bridge and the tower, the more gradual the approach toward infinity and hence the flatter and more obvious the zero crossing of the Δ v f curve. For weakly coupled structures, the best technique for finding all the modes seems to be to write the equations so that the quantity made unity and the quantity called Δ appear on opposite sides of the weak couplings. To be certain that all the modes have been found it might be necessary to try several locations for these quantities. Figure 2.19 shows a Δ v f curve for the same structure with V_B again set equal to unity, but Δ is now M_R, the moment at the right end of B_1. The crossings here are more easily recognized from a coarse scanning of the frequency spectrum. The natural frequencies indicated in Figure 2.19 are just the same as those in Figure 2.17.

In connection with the description of the method it was pointed out that the response of the structure to a sinusoidal force at any point could be obtained by revising the set of simultaneous equations to include the change of shear, moment, or thrust across the section at which the force is located. The natural frequencies of the structure would then,

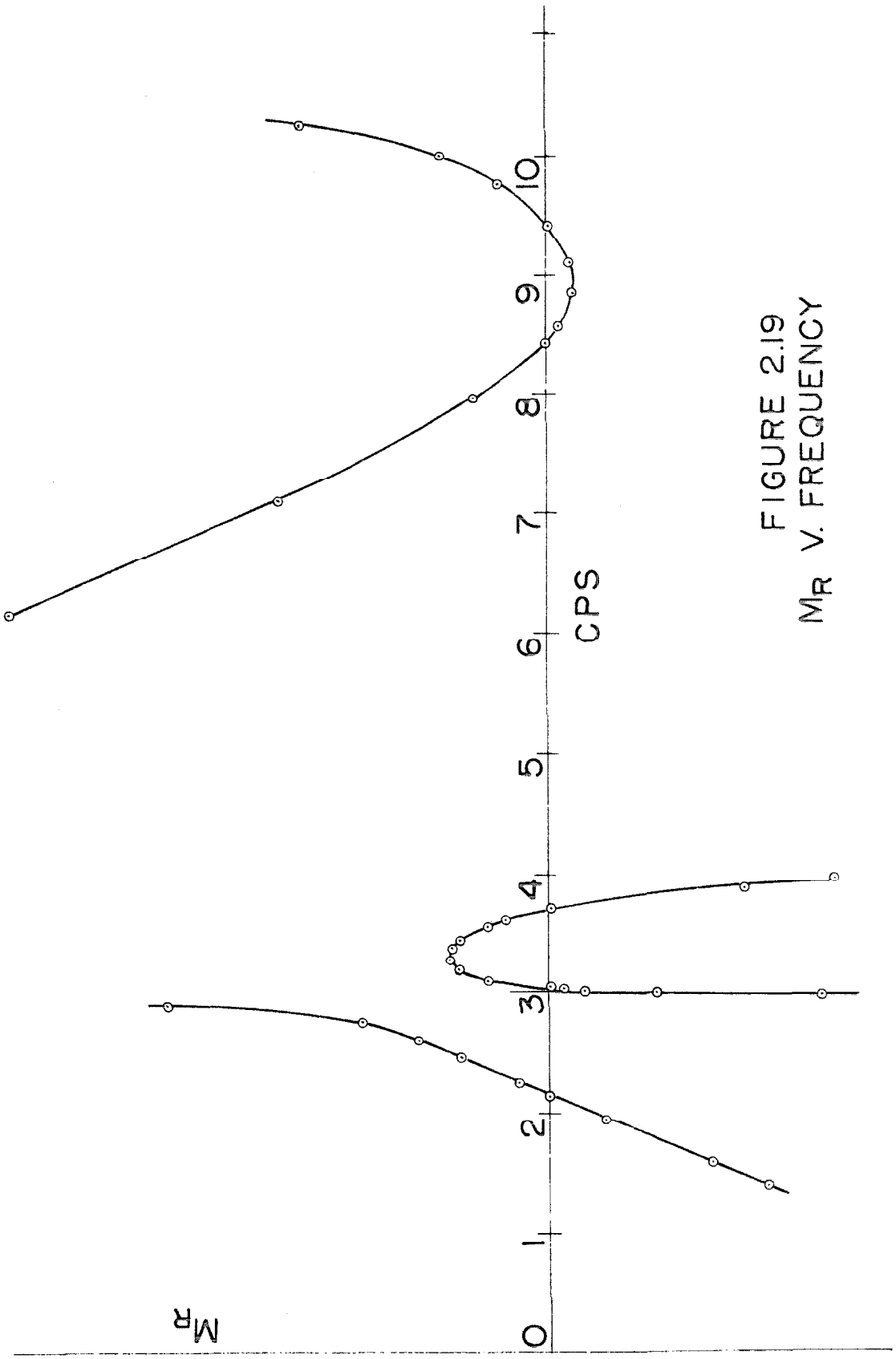

FIGURE 2.19
M_R V. FREQUENCY

of course, be indicated by the frequencies at which the amplitudes tended toward infinity, but overflow in the computer in the vicinity of the natural frequencies might cause difficulty in accurately defining the frequencies. At the expense of increasing the number of equations to be solved, the desired results could still be obtained and the natural frequencies could be accurately found if the following procedure were followed. Suppose it is desired to find the response of a point on the bridge, resulting from the shaking machine operating on the penthouse floor. If the bridge is cut at the point where the response is desired, and the deflection on the left end of the member on the right side of the cut is called unity, six new equations and six new unknowns have been introduced, inasmuch as the shear at the base of T_{1a} must now be considered an unknown. Then if Δ is made to be the change in shear or moment at the top of T_{1a} caused by the shaking machine, Δ now answers the question, "What shaking machine force is necessary to produce unit deflection at the selected point on the bridge?" The Δ v f curve is thus the reciprocal of the resonance curve sought. If only general bridge response is desired, the shear at the end of one of the spans might be set to unity and no additional equations are involved.

Vibrations of the Entire Structure - Experimental Resonance Curves and Mode Shapes

Resonance curves of the acceleration on the penthouse floor for several force levels are shown in Figure 2.20. Resonance curves for three points on the bridge and for a point on the side of the tower 84'-0" above the base are shown in Figure 2.21, Appendix V. In all cases the force was applied on the penthouse floor in the direction of

the length of the bridge. The accelerations on the tower were measured in the direction of the length of the bridge, whereas the accelerations plotted for the bridge were measured in the vertical direction. Different symbols used for data points on any one curve indicate that the data were taken on different days.

Although there is scatter in the penthouse floor data around the peaks of the fundamental frequency, f_1, and the peak for the (0 - 4) loading condition is broad, there appears to be no change in f_1, 2.10-2.12 cps, for loading levels between (0 - 1) and (0 - 4). Under the light loading (L.L.), approximately 29% of the (0 - 1) loading, f_1 occurred at 2.16 cps as shown by the detailed plot in Figure 2.22. These data, representing accelerations on the penthouse floor, were obtained when some temporary friction clamps to prevent bridge sliding at the center pier were in place across the joint between B_1 and B_2. The effectiveness of the clamps was not adequately evaluated, however. The computations in Table 2.6 indicates an increase of 0.04 cps in f_1 if bridge sliding is prevented, suggesting that less sliding occurred under the (L.L.) loading with the clamps in place. At acceleration levels of 1% to 10% of the acceleration produced by the (0 - 1) loading at the fundamental frequency, the observed frequency of free vibrations varied between 2.16 and 2.20 cps, the latter value higher than would be expected if no bridge sliding occurred. Possibly an increasing value of the modulus of elasticity at lower stress levels could account for the higher frequency, but this is in contradiction to the invariance of f_1 at loadings from (0 - 1) to (0 - 4). The increase in the fundamental frequency with lower stress level which was noted in the test of the old Encino intake tower was attributed at that time to an increase

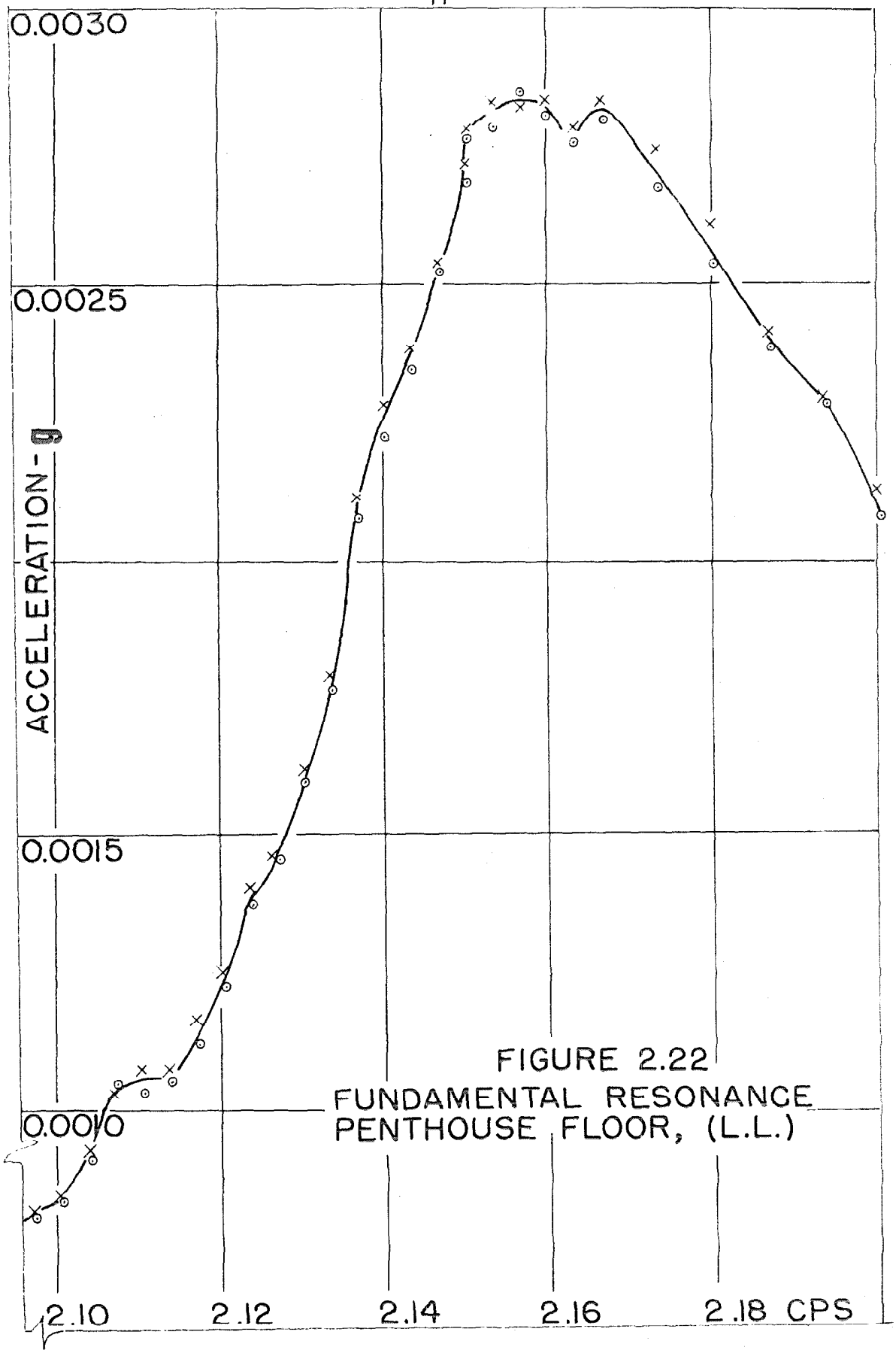

FIGURE 2.22
FUNDAMENTAL RESONANCE
PENTHOUSE FLOOR, (L.L.)

in E at a lower stress level.

Only once was f_1, under the (0 - 1) loading, observed to vary up or down by more than 0.01 cps between July and October, 1962, and this is believed to result from an error in reading the frequency or else to a sudden change in the line voltage supplying the amplifiers. The slightly higher values of f_1, noted on the resonance curves for the centerlines of B_1 and B_2, Figure 2.21, Appendix V, are the result of this data believed to be in error.

Close examination of the acceleration records from any three points on the structure at the frequency f_1, sensed and recorded with elements of approximately 100 cps natural frequency, always showed phase agreement that looked perfect to the eye. Although the unsteady paper drive and the presence of high frequency components in the records made accurate phase measurement impossible, at the frequency of the highest amplitude, 2.113 cps, the response of the structure was measured to lag the force by approximately 114°, of which 4° might be accounted for in the accelerometer and the recording galvanometer. Tests of the amplifier itself by the method described in Appendix I showed phase lag of 5° in the amplifier at 15 and at 30 cps. The pulse which indicated the phase of the force, recorded with a galvanometer of 3000 cps natural frequency, was probably not out of phase by more than $\pm$ 2° due to improper placement of the magnetic pickup which produced the pulse. Since the low level of damping in the structure could not account for this amount of phase lag at the peak amplitude, even considering the fact that the trace amplitudes increase as the fourth power of the frequency, no explanation is readily apparent. Phase lag of 90° occurred at approximately 0.01 cps below the frequency of the peak, where the amplitude was

3% to 4% lower than the peak amplitude. A record of accelerations at the frequency f_1 is shown in Figure 2.23 (a), Appendix V, the top trace being measured at the 84'-0" level on the side of the tower, the center trace at 146'-8" above the base, and the bottom trace on the penthouse floor. The bottom trace represents an amplitude of approximately 0.0075 g. The pulse indicating the phase of the force occurred 90° after the force reached its maximum. The traces in this record contain more high frequency components than were usually present because the chains on the shaking machine had just been tightened. The mode shape at the frequency f_1 is illustrated in Figure 2.18 (a).

At the second peak, frequency f_{B1}, on the bridge resonance curves, the mode shape was judged from the oscillograms to be one in which the bridge spans were moving up and down in opposition to each other at 90° phase with the motion of the tower, which still showed chiefly the fundamental mode. That this was essentially the case is seen from Figure 2.18 (b), where the computed motion on the penthouse floor is only 1% of the motion on the centerline of the bridge spans. The observed frequency f_{B1} was 3.12 cps compared with the computed value of 3.04 cps. The nature of this mode is indicated by the fact that the computed frequency of the bridge with no end restraint was given as 3.03 cps. In this mode the bridge is vibrating almost independently of the tower, its total length between the abutment and the tower remaining almost constant throughout a cycle. The horizontal force between the bridge and the tower in this mode is only approximately 2% of the horizontal force in the fundamental mode for equal centerline deflections of B_1.

Because the resonance peaks on the two spans did not occur at

exactly the same frequency due to the presence of the fundamental mode, and the peaks were very sharp, it was not possible to define a mode shape of the bridge at the frequency f_{B1}.

The field measurements were carried out before the computer work was completed, and this fact very well illustrated the advantages of carrying out both analytical and experimental investigations of the dynamic properties of a structure. The resonance peak at 3.12 cps was observed in the field, but it was only through this prior knowledge of its existence that its zero crossing in Figure 2.17 was found. On the other hand, the resonance at 3.68 cps, f_{B2}, was interpreted from field observations to be a torsional mode on B_1, and it was not until the computer showed otherwise that it was realized that a natural mode did exist in the plane of the structure.

Standing on the bridge, the sensation at 3.68 cps was that of torsion, so in addition to measurements of accelerations on the penthouse floor and on the centerlines of the bridge spans, which showed fairly good phase agreement, measurements were made on both trusses at the midspan of B_1. A curve of the differences of these two accelerations showed very definitely a resonance in torsion at 3.68 cps on B_1, but one such measurement on B_2 at the resonant frequency showed very little torsion. Just why the torsion should have induced large vertical motions midway between the trusses was not clear.

Probably the observed torsion on B_1 is the result of the resistances to longitudinal motion on the ends of one truss being unequal to the resistances on the other truss. Squeezing of the bottom chords then tends to cause one truss to arch upward more than the other. The trusses

of B_1 were observed to be practically free of torsion at the fundamental frequency of the structure, however, an observation which appears to be contradictory to the suggestion of unequal sliding resistances on the trusses. Using the forces and displacements given by the computer for the modes at the frequencies f_1 and f_{B2}, it was calculated that there occurred in the field, under the (0 - 1) loading at the frequency f_{B2}, a longitudinal force in B_1 of approximately 1.5 times the longitudinal force that occurred at the frequency f_1. This does not seem to be a large enough difference to account for the torsion. The only other significant difference between the two cases is that when the bottom chord of the truss is compressed in the mode shape at frequency f_1, rotation of the truss puts increased pressure on the outer edges of the bridge bearings, whereas when the truss is compressed at the frequency f_{B2}, the pressure is on the inner edges of the bearings. Whether this change of the location of pressure is significant is not known. Although it is not very obvious from Figure 2.18 (c), the bending moment at the frequency f_{B2} is negative on the ends of the bridge spans. This mode closely corresponds to the first mode of a bridge span with the ends held a fixed distance apart. The frequency reported previously for this support condition was computed to be 3.78 cps.

In July, 1962, f_{B2} was determined from torsion measurements on B_1 to occur very close to 3.60 cps, yet in October the peaks of both vertical acceleration and of torsion occurred at 3.68 cps, an increase of 0.08 cps. The frequency f_{B3} increased by approximately 0.07 cps over this period, but f_{B1} varied by no more than 0.01 cps, and f_1 showed no change at all. These observed increases of f_{B2} and f_{B3} were thought to be the result of an increase in the sliding resistance between July and October due to

corrosion of the sliding surfaces. To illustrate the effect of sliding resistance on the frequencies, the springs at the ends of the bridge spans in the computer model of the structure were made infinitely stiff, and all the other constants were held unchanged. The frequency f_1 was found to be increased by 0.04 cps, f_{B1} by 0.01 cps, f_{B2} by 0.22 cps, f_{T2} by 0.01 cps, and f_{B3} by 0.05 cps by the increased sliding resistance. These computed increases do not in all respects agree with the observations, indicating that the idealization of the sliding phenomenon by the deformation of elastic springs is not accurate for a range of conditions, and suggesting that some other unrecognized changes took place during the three months. It will be interesting to observe the changes in the frequencies of the structure as time passes, although the filling of the reservoir with water will add a complicating factor.

The resonance peak on the bridge at 3.88 cps was determined from field observations to result from vibrations in the direction perpendicular to the bridge, and a lateral mode shape of the bridge, shown later, was measured under the longitudinal excitation. The computer did not indicate a resonance in the vicinity of this frequency.

At the frequency f_{T2}, 8.09 cps, the accelerations on the penthouse floor lagged those measured at the 84' level by approximately 20°, the reason being, of course, that the record on the penthouse floor contained a much larger percentage of first mode than the record made close to the midheight of the tower. The resonance peak near the midheight ocurred at approximately 8.11 cps, although variations of 0.03 cps on either side were sometimes observed. The records allowed the mode shape of the tower to be reasonably well determined, but the records from the

bridge were in general very rough at the higher frequencies, often hardly sinusoidal, so that what is plotted as an observed mode shape of the bridge at f_{T2}, Figure 2.18 (d), was obtained by using a good amount of judgment in interpreting some of the records. An example representative of the poorer quality of the records at the higher frequencies is shown in Figure 2.23 (b), Appendix V, for the frequency 8.13 cps. The upper trace shows vertical acceleration at a point on B_2, 13 panels from T_2, the middle trace is from a point on B_1, five panels from T_1, and the lower trace shows horizontal acceleration on the penthouse floor. A record of better quality, made on a different date, is shown in Figure 2.23 (c), Appendix V, for the frequency 8.12 cps. Here the upper trace is from a point on B_1, five panels from T_1. This was recorded with a galvanometer of 18 cps natural frequency, whereas all the other traces were recorded with galvonometers of 100 cps natural frequency. The center trace is from a point on B_1, five panels from T_2, and the lower trace is from the penthouse floor. Rattling of the bracing elements on the bridge occurred at the higher frequencies and is presumed to be responsible for some of the roughness in the records. The quality of the records at the higher frequencies was not constant from day to day.

The bridge mode at f_{B3} was interpreted in the field as being one in which the bridge was vibrating independently of the tower. The frequency observed in October, 1962, was 8.90 cps, whereas in July the frequency was observed to be approximately 8.83 cps, increased resistance to the bridge sliding being assumed to be partially responsible for the change in frequency. Using the spring constants for bridge sliding

determined for the fundamental mode, the computed frequency f_{B3} was found to be 9.41 cps, 6% high, and the computed mode shape, Figure 2.18 (e), is seen to have drastically different relative amplitudes from the observed mode shape. The effect of the bridge springs on the relative amplitudes of the two spans was investigated by making all the bridge springs infinitely stiff, which resulted in the amplitude of B_1 only 18% greater than the amplitude of B_2. It is probable then that bridge sliding resistance different from that which was assumed at this frequency is responsible for the large difference between the computed and observed mode shapes. The fact that the computed second frequency, 9.46 cps, of one bridge span supported with one end on rollers as in Figure 2.6, is higher than the observed frequency of the bridge with some end restraint, 8.90 cps, indicates that the flexural beam representation of the truss is significantly in error in the second mode.

Although no computations were made for vibrations of the structure in the direction perpendicular to the bridge, accelerations were measured on the penthouse floor for the force applied transversely, and the mode shapes of the bridge were determined for vibrations in the lateral direction. The resonance curves for lateral acceleration on the penthouse floor are plotted in Figure 2.24, Appendix V, and the lateral mode shapes of the bridge are shown in Figure 2.25. The two strong resonances on the penthouse floor, at 1.76 and 8.13 cps for the (0 - 1) loading, are very close to the frequencies observed for the tower without the bridge, 1.73 and 8.1 cps, indicating that the effect of the bridge is not very great at these frequencies. Under the (L.L.) loading the fundamental of the tower in the lateral direction was found to be

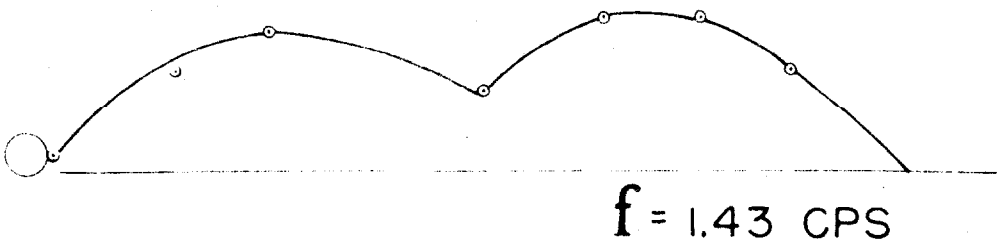

FIGURE 2.25
LATERAL MODE SHAPES

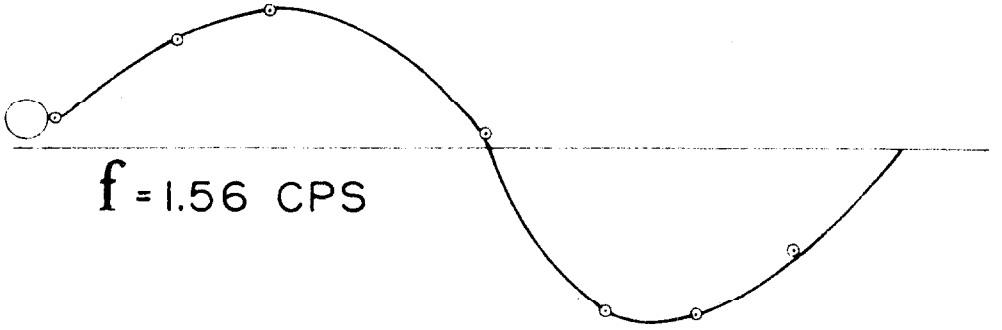

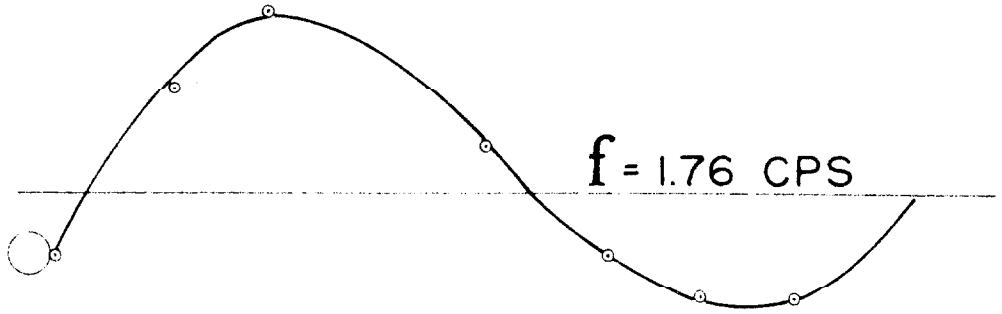

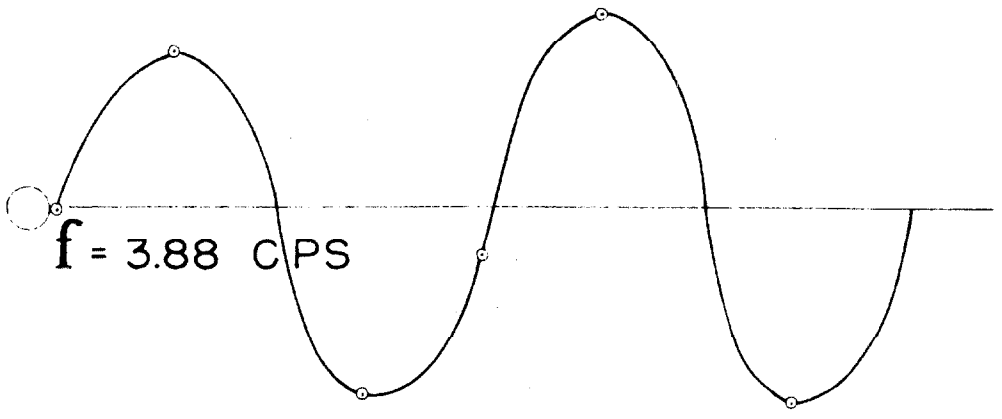

at 1.76 cps and the second mode of the structure was found at approximately 8.17 cps. The modes at 1.43 and 1.56 cps are essentially modes of the bridge, and they involve larger relative motions of the bridge than the mode at 1.76 cps. Because of the sharpness of the two lower resonance peaks considerable scatter was present in the mode shape data, the averages of which are shown in Figure 2.25. As was mentioned previously, the mode at 3.88 cps was determined when the shaking force was applied parallel to the axis of the bridge. The cause of the unevenness in the resonance curves in Figure 2.24, Appendix V, at 2.93 cps was not determined.

Vibrations of the Entire Structure - Damping

Equivalent viscous damping determined from the decay of free oscillations of the first mode of the tower without the bridge attached was found to be approximately 0.007 critical at an average acceleration level on the penthouse floor of 0.0004 g. With the bridge attached, at an average acceleration level of 0.00043 g in the direction of the length of the bridge the damping was measured from free vibrations as 0.0118 critical and at 0.00068 g average amplitude the damping increased to 0.0126 critical. Using the method reported by Hudson,[2] in which the damping is determined by the ratio of the peak amplitude to the amplitude at the horizontal tangent of an acceleration resonance curve resulting from a force which increases as the square of the frequency on a one degree of freedom system, the equivalent viscous damping in the first mode for the (0 - 1) loading condition in the direction of the length of the bridge, approximately 0.0063 g amplitude, was determined to be 0.016 critical. For the (0 - 4) loading, 0.011 g amplitude, the damping

was found to be 0.036 critical. The maximum dynamic stress at the base of the tower under the (0 - 4) loading was calculated to be only 7.5 psi, so the concrete always remained in compression. These data are tabulated in Table 2.7 along with data from two other towers. No relationship between damping and the ratio of tip deflection to height among the three towers can be seen from Table 2.7.

Damping in the mode at 8.09 cps, f_{T2}, is more difficult to determine because of the presence of the first mode and the presence of the mode at 8.90 cps which obscures the horizontal tangent at f_{T2}, but if the curves are sketched in, the amplitude ratio indicates damping around 0.018 critical.

Damping in the modes in which the bridge plays the dominant role is difficult to determine because of the superposition of response of the several modes. It is seen that just above 8.90 cps, f_{B3}, the response at panel point 5 on B_2 is lower than the response just above 8.09 cps, resulting from a phase difference of 180° in the two modes at this point. Sketching in the curves, and taking into account the phase difference indicates damping in the mode at 8.90 cps of approximately 0.018 critical.

In the direction perpendicular to the bridge, the damping for the (0 - 1) loading at 1.76 cps is approximately 0.010 critical, and for the (0 - 2) loading it is approximately 0.015 critical. At 1.56 cps, a mode principally of bridge motion, the damping appears to be less than 0.01 critical. At 8.13 cps under (0 - 1) loading, sketching in the curves indicates damping of approximately 0.028 critical.

Vibration of Entire Structure - Foundation Motions

Rotation and translation of the base of the tower were discussed

Structure	Deflection at Top ÷ Height	Acceleration Level at Top* - (g)	Viscous Damping Coefficient % Critical
Free vibration of 425' concrete chimney, lower half brick lined, f_o= 0.61 cps †	1.1×10^{-4} and lower	-	0.9
Free vibration of new Encino Tower without bridge f_o= 1.76 cps height = 149'	7.1×10^{-7}	4×10^{-4}	0.7
Free vibration of new Encino Tower with bridge f_o = 2.18 cps	4.9×10^{-7}	4.3×10^{-4}	1.18
Free vibration of new Encino Tower with bridge f_o = 2.18 cps	7.8×10^{-7}	6.8×10^{-4}	1.26
Forced vibration of new Encino Tower and bridge (0-1) loading	7.7×10^{-6}	6.3×10^{-3}	1.6
Forced vibration of new Encino Tower and bridge (0-4) loading	1.3×10^{-5}	1.1×10^{-2}	3.6
Forced lateral vibration of new Encino Tower and bridge, f_o = 1.76 cps	1.7×10^{-5}	9.7×10^{-3}	1.0
Forced vibration of old Encino Tower, f_o = 2.4 cps height = 104'	5.8×10^{-5}	4.3×10^{-2}	2.8

TABLE 2.7

DAMPING OF TOWERS

*Average amplitudes for free vibration data

†Cited in Reference 6

in connection with vibrations of the free-standing tower. It was found that under the (0 - 1) loading in the first mode, the rotation and the horizontal translation, measured on top of the foundation pad, were both in phase with the motion of the tower above. Every set of measurements for vertical translation, however, indicated that in the first mode the center of the foundation moved downward when the tower deflected toward the dam, just the opposite of the expected. The vertical force at the base of T_1 resulting from the bridge reaction on the tower is given by the computer as 1×10^5 lbs. uplift per foot of penthouse floor deflection toward the dam, when uplift is prevented. If the sandstone is assumed to have a modulus of elasticity of 2×10^6 psi and Poisson's ratio of 0.3,[21] and the foundation pad is assumed rigid, then using the data from Reference 20 the vertical uplift of the base should have been roughly 7×10^{-6} feet per foot of penthouse floor motion, and should have lagged the applied force on top of the pad by 3° in the first mode. The observed motion, obtained by taking the difference of vertical accelerations on opposite sides of the foundation pad inside the tower, was of the order of 6×10^{-4} feet per foot downward. The records at the base were very small, so the magnitude of this vertical motion showed considerable scatter, but the sense was always consistent. For vibrations in the lateral direction, the vertical accelerations on opposite sides of the base were of equal magnitude, indicating no vertical motion of the center of the tower's base.

The only reasonable explanation of this contradiction is that the underlying rock is not of uniform rigidity or that the $73\frac{1}{2}$" diameter pipe which penetrates the 10'-0" thickness of the foundation pad sufficiently lowers the stiffness of the one side of the pad so that, under

the moment at the base of the tower, deformation in the pad itself shifts the center of rotation of the top of the pad away from the dam. From the observations, the center of rotation was shifted approximately three feet from the center of the tower. Because of this observed unsymmetrical deflection, no vertical motion at the base of T_1 was allowed in the computer solution.

Rotation at the base of T_1 was responsible for only 9.3% of the deflection at the top of the tower, whereas it was reported that almost 40% of the top deflection of the old Encino tower was caused by base rotation.[2] Although the sites of the two towers are approximately 700 feet apart and it is not known if the rock at the two sites has the same characteristics, it is interesting to compare foundation moduli computed for the two cases. If both foundation pads are regarded as rigid discs, the quantity to be compared is $M_L/\theta R^3$, where M_L is the moment acting at the bottom of the disc, θ is the rotation, and R is the radius of the disc.[20] In the foundation of the new tower, M_L is approximately 10% greater than M_B, the moment on top of the pad, the difference being equal to V_B times the pad thickness. In the foundation of the old tower this increase is approximately 7%. The value $M_L/\theta R^3$ is roughly 7.3×10^7 lbs. per sq. ft. for the old tower, whereas for the new tower the value is 3.8×10^7 lbs. per sq. ft., little more than half as great.

That the foundation under the old tower appears more rigid is not surprising inasmuch as the foundation stiffness considered here actually includes the bending and shearing stiffnesses of the pads. The pad under the new tower, 48 feet in diameter by 10 feet thick, is much more flexible than the pad under the old tower, which was 22 feet in

diameter by 5 feet thick and supported a tower barrel 17 feet in outside diameter. It should be kept in mind that only one measurement under questionable conditions supported the value of base rotation calculated for the old tower, and the difference in frequencies noted for the old tower in two perpendicular directions indicates that the outlet pipe, which was not considered in the calculations, affected the base motions. However, if base rotation under the old tower had been smaller than assumed, meaning that less than 40% of the top motion was caused by base rotation, then the foundation under the old tower would appear stiffer here, further emphasizing the flexibility of the pad under the new tower. The modulus of elasticity calculated for the rock under the old tower, assuming a perfectly rigid pad, is of the order of 5×10^5 psi, rather low.[21]

Until more experimental evidence is gathered and until the problem of a thick elastic disc, with a rigid center support, resting on an elastic half-space is solved, the following approximation for comparing foundation moduli from base rotations is proposed. Through the foundation pad insert an imaginary cone of central angle 90°, whose intersection with the top of the pad coincides with the outside line of the tower on the pad. Use the radius of this cone at the bottom of the pad as the radius of the rigid disc referred to in Reference 20, unless the actual radius of the pad is smaller. Applying this suggestion to the foundation of the new tower gives a value for $M_L/\theta R^3$ of $6.6 \times 10^7 lb/ft^2$, closer to the value found for the old tower. Rotation θ here, of course, includes the suspected internal deformation of the pipe through the base.

Horizontal translation of the pad under the new tower, resulting from base shear in the first mode, should have amounted to roughly

1×10^{-3} feet per foot of penthouse floor motion, on the basis of the modulus of the rock estimated from the test of the old tower. If the rock surface had rotated the 7.7×10^{-4} radians per foot observed on top of the pad, the horizontal translation on top of the pad resulting from this rotation would have amounted to 7.7×10^{-3} feet per foot. The measured translation was only 3×10^{-3} feet per foot, however, suggesting that the deformation within the outlet pipe raised the center of rotation to within 3' of the top of the pad and/or submergence of the pad in the surface of the rock resulted in raising the center of rotation. The data gathered from vibration in the transverse direction, in which the outlet pipe should have little effect, suggests the latter possibility. In that instance, θ_B and Y_B had observed values of 7.2×10^{-4} radians and 2.3×10^{-3} feet respectively per foot of penthouse floor motion. The shear and the moment at the base in the transverse vibration probably differ by no more than 10% of their respective values in the direction parallel to the bridge, and using the values for the latter case results in the center of rotation being located approximately 2' below the surface of the pad. A check with the resident engineer on the construction revealed that the sandstone was excavated to a level one foot above the finish top of the pad, the pad excavation was made and the concrete was poured, and finally the sandstone around the pad was trimmed flush with the top surface of the pad. The classical problem here, then, is one of an elastic disc with a rigid center support, embedded in the surface of an elastic medium.

The preceding paragraphs have indicated that horizontal translation at the bottom of the barrel is more a function of base moment than of

base shear. Further evidence of this was obtained by comparing relative base motions in the first mode of the tower with the relative base motions in the mode of frequency f_{T2}. The magnitudes of base rotation and translation observed in the field under (0 - 1) loading at f_{T2} were approximately twice and three times their respective values at f_1, but as previously mentioned, tests at different amplitude levels in the two modes were contradictory in predicting any trend in the relative movements. In any case, linearity of the rock within 10% is expected at these higher amplitude levels. In order for computed relative base motions in both modes to agree with the observed relative base motions not only must the picture of foundation conditions be correct, but also the computer's model of the tower must be correct, so such a comparison is a severe test of the whole analytical procedure. Observed base rotation and translation at f_{T2} were 4.2×10^{-3} radians and 2.8×10^{-2} feet per foot of motion at a point 84'-0" above the base.* The computed values, based on translation at the base being proportional to base shear only, were 4.3×10^{-3} radians and 5.2×10^{-2} feet respectively, the rotation showing good agreement, but the translation almost double the observed value.

A new compliance constant was then introduced, K_{MYB}, relating base translation to base moment. The constant K_{VB} was set to zero, all other constants were left unchanged, and K_{MYB} was then given a value so that the computed base motions in the first mode agreed with those observed under the (0 - 1) loading. Then the mode at f_{T2} was computed with this

*The point 84'-0" above the base was used as a reference for the mode of frequency f_{T2} because the motion at this point was less affected by fundamental mode content than the motion on the penthouse floor.

value of K_{MYB}, and Θ_B and Y_B in this mode were found to be 4.3×10^{-3} radians and 1.7×10^{-2} feet per foot of motion at the 84' level. The computed value of Y_B here is 32% small, whereas when base translation was assumed proportional to base shear only, the computed value of Y_B was 85% greater than the observed value at frequency f_{T2}. The frequency f_{T2} was raised by 0.11 cps, to 3.6% above the observed, by this change but the mode shape at f_{T2} showed slightly better agreement with the observed mode shape. Thus it is evident that relating the base translation to some combination of the shear and the moment at the lower end of the barrel can produce computed relative base translations and rotations that agree with the observations in both modes, but the computed second frequency of the tower will be approximately 3% too high. In the light of this information, it appears that the effective modulus of elasticity of the tower is perhaps 6% below the assumed value of 4.10×10^6 psi and the bridge is slightly stiffer than has been assumed in the first mode. These two changes would bring the computed frequencies f_1 and f_{T2} and their mode shapes into agreement with the observations. Other changes to the bridge would be necessary to bring the computed bridge modes and frequencies into agreement with the observations, however.

Measurements to detect if base rotation occurred about axes parallel and perpendicular to the outlet pipe, which made an angle of $16\frac{1}{2}°$ with the axis of the bridge, indicated that the major and minor axes of stiffness were determined by the bridge, not by the pipe. Measurements made on the penthouse floor led to the same conclusion.

Foundation movements of T_2 were determined by measuring acceleration on top of the four concrete piers supporting it. The horizontal

translation averaged 1.3×10^{-3} feet, the vertical motion averaged 5.1×10^{-4} feet uplift, and the rotation averaged 2.9×10^{-4} radians per foot of penthouse floor motion. The records of these motions were extremely small, from 0.02" to 0.06" peak to peak, so 50% variation in the values given is not unexpected. It is very likely that rotation here is not proportional to base moment only nor is translation proportional to base shear only, but the minor effect of these base movements of T_2 on the structure as a whole indicate that the effects of errors in the compliance constants would not be noticed.

Figure 2.26 summarizes the observed base motions and the computed base forces and moments for a penthouse floor deflection of one foot in the first mode. Bridge sliding, discussed in the next section, is also shown as well as the computed longitudinal forces at the ends of the bridge spans. The letters T and C indicate respectively the tendency for a joint to separate or to close when the structure is deformed as shown. The actual maximum amplitude experienced on the penthouse floor was approximately 0.024", so actual forces and motions did not exceed 0.2% of the values shown in Figure 2.26. The dynamic axial forces which were neglected in equation 2.2 are now seen to be very small compared to the dead load compression forces in T_1 and T_2, amounting to only 0.8% in T_2 and to a much smaller value in T_1. On the bridge, the dynamic axial force neglected in equation 2.2 has an effect of roughly 0.05% of the effect of shear in equation 2.2, so it is obvious that at these small amplitudes the coupling between axial and lateral vibrations is not measurable.

Ground movements on the dam and on the reservoir bottom were measured by Mr. David Leeds with the Kanai microtremor apparatus when

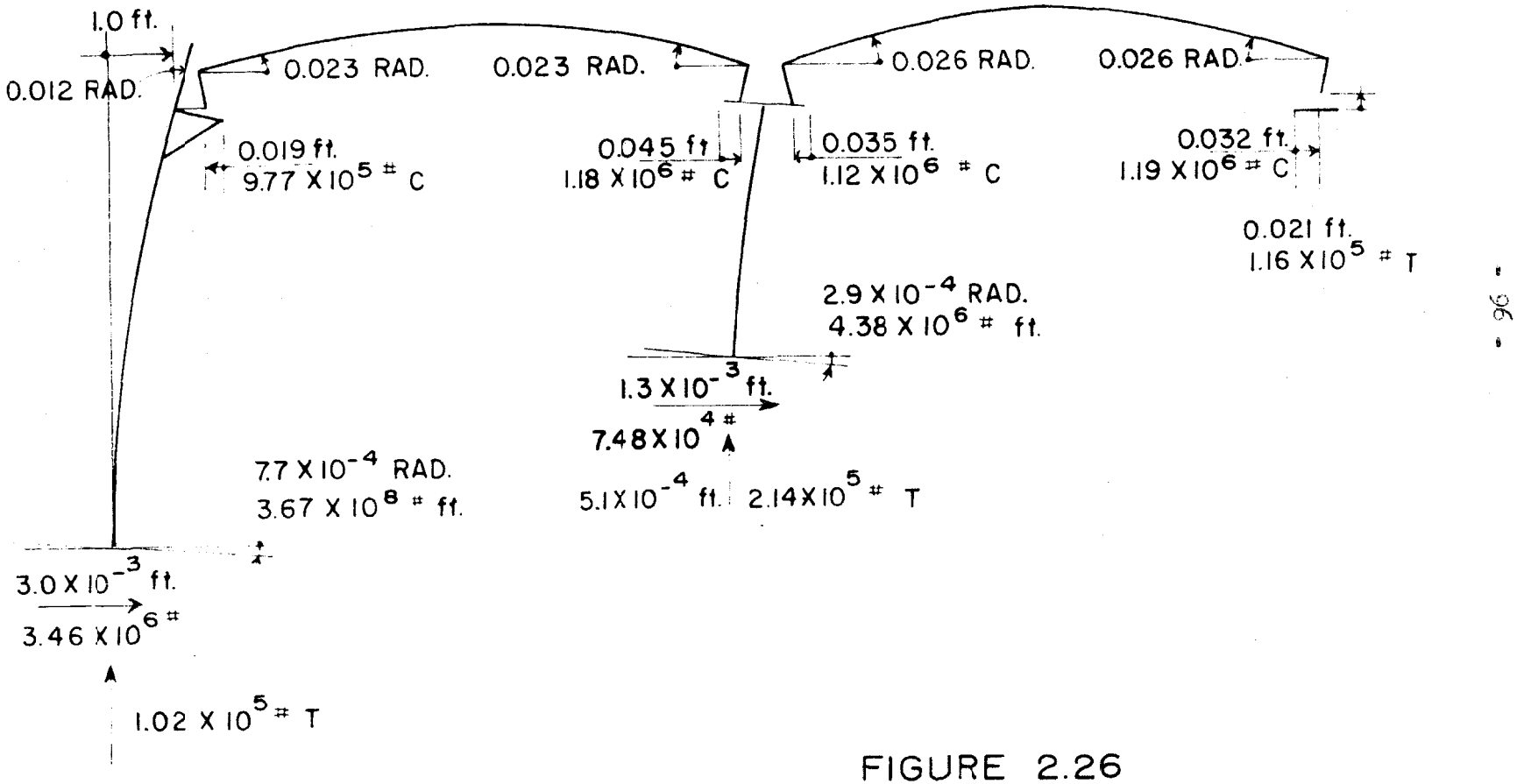

FIGURE 2.26

RELATIVE MOVEMENTS AND FORCES IN THE FIRST MODE

(ACTUAL MAXIMUM AMPLITUDE 0.024 INCHES)

the structure was vibrating at the fundamental frequency. On the floor of the abutment structure, when the computed reactions of the bridge on the abutment were 2000 lbs. longitudinal thrust accompanied by 200 lbs. uplift force, the measured horizontal motion next to the end of the bridge was roughly 7×10^{-5} inches in amplitude, amounting to 0.35% of the motion on the penthouse floor. Fifty feet away from the abutment, in directions both parallel and perpendicular to the length of the dam, the horizontal motion parallel to the length of the bridge was measured as only 3% to 4% of the motion on the abutment. Traces of these low level motions were considerably modified by background noise to the extent that their amplitudes were close to the lower limit at which quantitative measurements of the forced motions of the dam could be made. On the bottom of the reservoir, not yet capped by the 6" concrete slab, 25' from the tower in an extension of the plane containing the bridge and the tower, the horizontal motion was found to be only 2% of the horizontal motion measured adjacent to the base of the tower. The vertical motion at this point, measured with an accelerometer, was found to be approximately 20% of the vertical motion measured next to the outside wall of the tower.

Vibrations of the Entire Structure - Sliding at the Bridge Bearings

Relative movements between the ends of the bridge spans and their supports were determined by measuring accelerations on both sides of the joints, and by placing a dial indicator, reading in units of 10^{-4} inches, across the joints. The accelerometer shown resting on the lower chord at the abutment in Figure 2.14, Appendix V, is typical of the accelerometer mountings. The dial indicator, used for measurements at T_2 and at the bridge bearing on the tower, was clamped to the bridge with its shaft

between 3" and 4" above the surface on which sliding was assumed to occur.

If relative rotations of the members on opposite sides of the joints are neglected, the sliding computed from the dial indicator measurements showed good agreement with the sliding computed by taking the difference of the accelerometer readings on the two sides of the joints. Across the joint between the two spans at T_2, under the (0 - 1) loading at the frequency f_1, the dial indicator showed an amplitude of sliding of the west truss of B_1 relative to the west truss of B_2 of 1.38×10^{-3} inches, 8.1% of the penthouse floor motion, whereas the acceleration differences indicated 7.8%. Across the joint between the east trusses of the two spans the readings were 7.0% and 6.0% respectively.

If it is assumed that the points of attachment of the instruments at the ends of the bridge spans underwent the rotations shown by the computer work, Figure 2.26, and that the center of this rotation was located on the sliding surfaces, the relative motion across the joint indicated by the dial readings should be reduced by 17%, whereas the relative motion indicated by the accelerometer readings should be reduced by approximately 40%, chiefly the result of the rotation of the accelerometers in the earth's gravitational field. The good agreement between the relative motion determined by the two sets of measurements was taken as an indication that the bridge bearings did not rotate about a point on the sliding surface. It is recognized now that by taking two acceleration readings at each point, one with the accelerometer reversed 180° about a vertical axis, the effect of rotation in the earth's gravitational field could have been measured. Unfortunately, this

solution was not realized in the field. The relative motions in the first mode which were used to determine the springs allowing sliding in the computer study were 0.045 and 0.035 times the penthouse floor motion for the joints B_1-T_2 and T_2-B_2 respectively.

An interesting phenomenon was observed with the dial indicator across the joint B_1-B_2. While the amplitude of the dial reading was fairly constant, the center reading about which the needle swung gradually shifted back and forth 0.002" or so in each direction, indicating that the gap between the spans gradually opened and then closed. No regularity of this movement was observed. Probably what was occurring was that as the ends of the spans were sliding back and forth on the plates below, one end of a span would seize and thus force all the restoring motion to occur at the opposite end of the span, causing the span to "walk", first in one direction for several steps and then in the other direction. In the light of this observation, scatter in the data around the resonance peaks is not surprising.

At the tower anchorage of B_1, the sliding movement was measured with the dial indicator as amounting to 1.9% of the penthouse floor motion at the fundamental frequency under the (0 - 1) loading. If rotation of the bridge bearing about a point on the sliding surface is assumed, the measured sliding is reduced by 45%. For the computer work it was assumed that this rotation did not occur.

At the abutment anchorage of B_2 the horizontal motion of the bottom chords of the trusses, next to the anchor bolts, was determined by acceleration measurements to be 3.2% of the penthouse floor motion and the vertical motion at this point was found to be 2.1% of the penthouse floor motion at the frequency f_1 under the (0 - 1) loading. Since the

trace amplitudes of horizontal acceleration were approximately six times what would be expected due to rotation of the accelerometer in the earth's gravitational field, the observed response can be assumed to represent chiefly horizontal motion at the end of the bridge. On the abutment itself, alongside the anchor bolts, under the (L.L.) loading one set of measurements showed horizontal abutment movement of only 16% of the motion measured on the bottom chord at this point, indicating that the bridge was sliding on the base plate. It was previously mentioned that the motion on the floor of the abutment structure, about 13" above the bridge bearing, was 0.0035 times the penthouse floor motion. Several possibilities can be advanced to explain the fact that the motion on the floor of the abutment structure relative to penthouse floor motion was measured to be only 70% of the relative motion measured next to the anchor bolts on the abutment. Relative motion within the abutment structure between the two points, rotation of the abutment, and the difference in shaking machine force level for the two cases, resulting in different ratios of sliding force at the abutment to penthouse floor motion, are possibilities. Probably the variation results at least in part from the fact that the measurements were made several days apart, and the sliding resistance of the bridge was different on the two days.

If the structure vibrates at a sufficiently small amplitude, bridge sliding should not occur and the fundamental mode shape should be the one predicted in row d of Table 2.6. Measurements of bridge sliding, relative deflections of the centerlines of the bridge spans, and computed longitudinal force are shown in Table 2.8 for three loading conditions. Under the (L.L.) loading the observed relative motions at T_2 and at the tower anchorages of the bridge are roughly double the values which would

Load	Penthouse Floor Ampl. in. x 10^{-4}	Sliding Across B_1-B_2 in. x 10^{-4}	Sliding at Tower in. x 10^{-4}	Relative Ampl. ℄ B_1	Relative Ampl. ℄ B_2	Computed Force Across B_1-B_2 #
(L.L)	22.6	0.8	0.2	1.00	1.46	223
(0-1)	173	13.1	3.2	1.09	1.33	1710
(0-2)	230	26.9	6.5	1.11	1.34	2470
Computed Bridge Ampl. with no bridge sliding				1.37	1.57	

All measurements made at 2.113 cps. (Resonance for (L.L) at 2.16 cps.)

TABLE 2·8

BRIDGE MOTIONS AT DIFFERENT EXCITATION LEVELS

be expected if there were no sliding, but only rotations of the bridge bearings about points on the assumed surfaces of sliding. Because of the uncertainty of the locations of the axes of rotation it cannot be stated positively that sliding occurred under (L.L.) except that at the abutment, as mentioned previously, the evidence indicated that sliding did occur. Sliding under (L.L.) indicates that the coefficient of friction of steel on steel was at least as low as 0.009. From the (0 - 1) loading case in Table 2.8 it can be concluded that the coefficient of friction at the tower and at T_2 was at least as low as 0.068. The nominal bearing pressures for the bridge reactions are 90 psi for steel on steel and 360 psi for steel on Lubrite and Lubrite on micarta.

The expected increase in relative deflection on the centerline of B_1, the measurements of which showed a spread from 0.96 to 1.10, did not occur when the (L.L.) loading was substituted for the (0 - 1) loading, nor did it occur under manual forcing, when the relative motion was observed to be 1.06 times penthouse floor motion. The evidence suggests that under (L.L.) loading sliding of B_2 decreased in proportion to the other structural motions, but that the sliding of B_1 increased proportionally.

Vibrations of the Entire Structure - Linearity of Response

Away from the peaks, the response in Figures 2.20 and 2.24, Appendix V, is seen to be very closely proportional to the amount of eccentric weight in the buckets of the shaking machine. In the report of the test of the old Encino intake tower,[2] it was noted that the response away from resonance did not increase in proportion to the machine loading. The apparent stiffening property of the spring in that case was not so

great as was reported, however, as a result of errors in the reported force levels. Recomputing the force levels shows that for the (2-2) loading condition, relative force level 4.06, the response was 3.36 times the response under the (0-2) loading conditions, relative force level 1.0, and was 1.87 times the response under the (1-1) loading condition, relative force level 2.03. The 2.03 force level produced 1.84 times the response of the 1.0 force level. Moving farther away from the peak showed much better linearity between the resonance curves of the two lowest force levels, so it is possible that the nonlinearity reported above was the result of measuring the response too close to the peak on the resonance curve. Unfortunately, the resonance curve of the 4.06 force level was not carried out farther in that test.

The proportionality between the machine loading level and the amplitude of response away from the peaks and the invariance of the fundamental frequency at different loading levels are indications of the linearity of the concrete and of the structural framework for small deflections in the first mode shape. Aside from these two observations, however, the general impression of the structure is one of nonlinearity.

First to be noted is the significant increase in damping with amplitude at the fundamental frequency. Undoubtedly, increased sliding of the bridge at higher force levels is at least partially responsible for the increased damping, although in the test of the old Encino tower, which had no bridge, damping was found to increase with amplitude. In the records themselves there were many examples of nonlinear behavior, all apparently due to structural nonlinearity of the bridge and its connections. Under lateral excitation at the frequency 1.76 cps, motion

in the direction of the length of the bridge at twice the frequency of excitation was measured on the penthouse floor. This longitudinal motion had an amplitude of roughly 0.0023 times the amplitude of lateral motion of the penthouse floor, which was approximately 0.03". Assuming the bridge mode shape at this frequency, Figure 2.25, consists of two sinusoidal loops, the calculated shortening of the centerline of the bridge due to lateral deflection is only 1.6×10^{-5} inches, whereas the observed longitudinal motion was approximately four times this amount. Inasmuch as the frequency of the longitudinal motion was 3.52 cps, not far from the frequency f_{B2} at 3.70 cps, it is apparent that dynamic amplification was taking place in the longitudinal direction.

At the tower anchorage of the bridge during this lateral vibration at 1.76 cps, it was observed that the anchorage of one truss acted as a hinge for the lateral bridge motion, but at the other anchorage the end of the truss moved back and forth longitudinally as the truss alternately compressed and extended. This type of action, if present at the other anchorages of the spans would force the tower in the longitudinal direction of the bridge at the same frequency as the frequency of lateral motion, not at twice the frequency. The actions at the other anchorages were not observed, however. An attempt to measure torsion in the tower at 1.76 cps revealed nothing of significance.

At the frequency f_1 with the force applied in the direction of the length of the bridge, an accelerometer oriented in the transverse direction on the centerline of B_1 recorded a motion at three times the forcing frequency, in magnitude approximately 0.018 times the longitudinal motion on the penthouse floor. Qualitatively this motion can be explained on the basis of unequal resistances to sliding of the two trusses of

B_1. At low amplitudes both trusses resist equally the longitudinal force, and there is no lateral deflection, but at higher amplitudes one truss offers more resistance than the other, and lateral deflection results. A first approximation to the expression relating lateral deflection and longitudinal force would thus contain a cubic term, resulting in the possibility of the third harmonic.[27]

At 1.56 cps, the frequency of a lateral mode of the bridge shown in Figure 2.25, sixth harmonic was noted in the lateral acceleration on top of T_2 and fourth harmonic in the lateral acceleration on the centerline of B_1. This record is shown in Figure 2.27 (b), Appendix V, in which the top trace is from the centerline of B_1, the center trace from the top of T_2, and the lower trace from the penthouse floor, all measuring acceleration in the lateral direction. Figure 2.27 (a), Appendix V, shows response of the same points at 1.43 cps. Figure 2.27 (c) shows nonlinear acceleration records at several frequencies. The top trace is lateral acceleration on the centerline of B_1, the center trace is lateral acceleration on the centerline of B_2, and the bottom trace is acceleration of the penthouse floor in the direction of the length of the bridge, the same direction as the applied force. Atkinson[28] has demonstrated with an electronic analog the existence of superharmonics of even order in the displacement of a one-degree of freedom system containing a cubic term in the restoring function. As mentioned previously, the relationship between lateral deflection of the bridge and longitudinal force might well contain a cubic term. It should be pointed out that the records here are of acceleration, not displacement, and in at least some of the cases illustrated the displacements would appear as very close to sinusoidal and at the frequency of the

forcing function.

Vibrations of the Entire Structure - Accuracy of the Computations and the Measurements

The accuracy of the computer's solution of the set of simultaneous equations representing the equilibrium and continuity conditions in the structure was checked by manually verifying that all the equations were satisfied in the modal shears, moments, rotations, etc. which were printed out, and by having the computer substitute the values it gave for the unknowns into the original equations and compare the thus determined right hand sides with the original right hand sides. All of the 21 equations were found to be satisfied as closely as could reasonably be desired, except that M_F, the moment at the top of T_{1b}, was sometimes not zero, but a few percent of the moment existing 12 inches below the top of the tower. This condition could be easily corrected by strengthening the criterion for convergence, but doing so made no noticeable change in the frequency or the mode shape.

The accuracy of the fundamental set of equations, 2.1 through 2.6, used in getting the transfer functions has been checked, as mentioned previously, by testing uniform cantilever beams for which solutions are known. The correctness of the set of equations in Figure 2.11, Appendix V, and the correctness of the values used for the properties of the tower and the bridge, however, cannot be verified by any means other than rechecking the properties against the plans of the structure and rewriting the equations. These steps have been carried out and no significant mistakes have been found, but there is no proof that the same mistake has not been made twice.

The absolute accuracy of the observations cannot be stated with

certainty, but the consistency of the observations and consideration of the dynamic properties of the instrumentation suggests that measured accelerations were in general within 10% of the absolute values. The static 2 g calibrations at the end of each day's testing never varied by more than 2% from the calibrations made at the start of each day. In contrast, the resistance calibrations, used throughout the day, varied some days as much as 5%, and the variations did not seem to be related in size or in sense to the variations noted in the 2 g calibrations. Although the calibrating resistors were rated as being quite insensitive to temperature in the range encountered, perhaps up to 180°F, no laboratory tests were conducted on their behavior under high temperature. The relays in the Miller C-3 amplifier which closed when the resistance calibration was carried out are suspected as being partly responsible for the variations in resistance calibration. In the first analyses of the data the observations were corrected for the changes noted in the resistance calibrations, and the consistency of the data seemed to be improved by the procedure. Later, however, the resistance calibrations were ignored.

The consistency of the different channels is illustrated in Figure 2.22 where the two sets of data were taken simultaneously with two accelerometers 8" to 10" apart on the penthouse floor. The maximum spread of the data is seen to be roughly 3% of the amplitudes. Both accelerometers here were mounted on the portable steel blocks which were resting on the floor, one thickness of plastic electrician's tape on the bottom of the blocks being used to increase the coefficient of friction. No comparison was made between this type of mounting and positive attachment of the accelerometers to the floor. The maximum

horizontal acceleration experienced by this type of mounting was 0.014g.

The consistency of the data from day to day is indicated in Figure 2.20, Appendix V, in which different symbols on one curve represent data taken on different days. Away from the peaks the data generally agrees within $\pm$ 5% of the average, whereas many readings over a period of three months on the peak at f_1 under the (0 - 1) loading showed a spread of $\pm$ 11% about the average. The acceleration records showed that forced vibrations of constant amplitude did not continue indefinitely at a given speed control setting near the fundamental resonance. In one instance, holding the speed count between 2.113 and 2.117 cps for thirty minutes or so showed acceleration amplitudes varying by $\pm$ 2% of the average. The "walking" of the bridge described earlier probably influenced the unsteadiness of the response.

At the very low acceleration levels at the bottom of the tower and on the abutment, errors in measuring the small record amplitudes affected accuracy, as described in connection with vibrations of the free-standing tower. Crosstalk among the channels, an effect on one channel resulting from a signal on another channel, was investigated at the high gains used for these measurements by deliberately inducing large signals on adjacent channels and noting the effect on the channel at high gain setting, the accelerometer for this channel, of course, being in a very quiet place. Crosstalk noted in one instance was eliminated by rearranging the individual amplifiers in the cabinet.

In measuring the trace amplitudes on the oscillogram, a horizontal line was drawn through the top and bottom peaks of several cycles, and this peak-to-peak amplitude was measured with a scale divided into 50 divisions to the inch, tenths of divisions being estimated. Where the

noise level was high compared to trace amplitude and where harmonics distorted the trace from a sinusoid the cycles were sketched in by eye for measuring. It is estimated that errors in these instances might be as high as 20%.

F. Summary and Conclusions

A careful experimental investigation has been conducted to determine the dynamic properties of a reservoir outlet structure consisting of a reinforced concrete tower 149 feet in height and a steel truss bridge 339 feet long, connected near the top of the tower. Five natural frequencies and mode shapes as well as foundation movements and sliding of the bridge on its supports have been measured. A detailed theoretical analysis of the structure has been carried out using an extension of the Holzer or Myklestad-Prohl technique, and proof has been presented that the technique is applicable for finding the natural frequencies for small vibrations of any linear structure composed of interconnected elements. The theoretical analysis showed good agreement with the observations for the lowest mode and fair agreement for the higher modes, the error in frequency of the fifth mode amounting to 6%. A number of specific conclusions and recommendations are presented below.

1. The analytical technique applied to this structure is of general application and appears promising as a tool for investigating vibrations of rigid frames and of trusses. Additional work is needed to indicate the efficiency and the accuracy of the technique on structures composed of a large number of members and to develop approximations to be used when exact application of the technique is uneconomical.

2. The substitution of a solid flexural member of equivalent I and A for a trussed member can be significantly in error, even for static loads. A further study of this substitution, which affords great simplification in dynamics problems, would be of practical value to engineers.

3. The most important unknown in carrying out the analytical work was the modulus of elasticity of the concrete. The average sonic value determined from three cores near the base of the tower was apparently 8% higher than the effective value at the vibration levels experienced in the field. More comparisons between sonic E and effective E as well as more experiments relating sonic E to specimen size and condition are necessary.

4. Foundation rocking had more effect on the structure than either horizontal or vertical translation of the foundation. Computations showed that foundation movements decreased the fundamental frequency by 0.08 cps, 4%, and decreased the second frequency of the tower by approximately 7%. Foundation rotation accounted for 9% of the deflection at the top of the tower in the first mode. In this case, where the foundation was sunk into the surface of the rock, better agreement between computed and observed translations was obtained by relating base translation to base moment than by relating base translation to base shear. Where the foundation rests on top of the rock the dependence of translation on moment is increased. The center of rotation for the lower end of the tower barrel in this case was

approximately two feet below the top of the 10' thick foundation pad. A careful experimental investigation of a free standing concrete tower with a simple exposed foundation resting on rock of known elastic properties would provide valuable data for calculating foundation compliance. The problem of an elastic disc embedded in an elastic medium, the disc supporting a rigid concentric shaft, needs to be solved for the cases of static moment and shear applied to the shaft.

5. The general behavior of the structure at higher frequencies is essentially that of a collection of elements which vibrate at their individual natural frequencies, only slightly modified by the motions of the rest of the structure.

6. The coefficient of friction determined as a result of the bridge sliding on its supports is as low as 0.009 for steel on steel at a nominal normal pressure of 90 psi. The motion of the bridge under steady excitation of the tower was not steady, but instead the spans gradually moved together and then moved apart while vibrating at fairly constant amplitudes. The frequencies of two modes of the bridge were observed to increase between measurements made three months apart. The increase is assumed to be chiefly the result of increased sliding resistance.

7. Equivalent viscous damping of the tower without the bridge attached was as low as 0.7% critical at the lowest amplitudes. With the bridge attached the damping of the structure

varied from 1.18% at the lowest amplitudes to 3.6% at an acceleration of 0.013 g at the top of the tower. The fundamental frequency at the lowest amplitude of free vibration was 3% higher than the fundamental frequency of forced vibration at testing amplitudes, but over a range of testing amplitudes the fundamental frequency did not change.

8. A relationship between the base rotation of a cantilever beam and the decrease in the fundamental frequency caused by the base rotation has been suggested on the basis of two examples. A relationship between the foundation compliance constant and the decrease in fundamental frequency resulting from the foundation compliance would be a valuable contribution to engineering knowledge.

9. Second, third, fourth, and sixth harmonics of the forcing frequency appeared clearly in the records of lateral accelerations on the bridge and on the top of the steel pier. These harmonics are possibly the result of a bilinear relationship between longitudinal force and lateral deflection, caused by unequal resistances to sliding on opposite sides of the bridge.

10. The frequency at which the acceleration lagged the force by 90° was approximately 0.01 cps below the frequency at which the amplitude was maximum in the first mode. The phase lag at the frequency of maximum amplitude was approximately 110°. No explanation is advanced for this phenomenon.

III. FORCED VIBRATIONS OF AN EARTH DAM

Introduction

Because of their great destructive potential dams have received much attention in the literature of engineering seismology. Over forty entries pertaining to dams appear in the 1958 edition of the Bibliography of Engineering Seismology.[29] In the Proceedings of the 1960 World Conference on Earthquake Engineering seven papers are devoted entirely to dams. In contrast to the large number of theoretical studies of the dynamic behavior of dams, experimental studies of actual dams have been few, due, of course, to the difficult problem of exciting dams into oscillations large enough to measure. In California in 1934 and 1935, two dams of concrete blocks were excited with mechanical vibrators.[30], [31] Heiland, in 1938, conducted model studies of an earth dam in conjunction with field vibration testing of the material to be used in the dam.[32] In Japan in recent years several full size concrete dams, both gravity and arch type, have been forcibly excited.[33], [34], [35] Model studies of vibrations of dams have been conducted by Japanese investigators in connection with the above mentioned tests of concrete dams. Clough and Pirtz, in 1956, studied the vibrations of models of rock-fill dams.[36] However, no experimental work appears to have been done on full scale earth dams. In this chapter a forced vibration test of an earth dam is described, and the results are related to recent theoretical work.

Background of the Test

In the earthquake of July 21, 1952 centered near Bakersfield, California, Dry Canyon Dam, an earth dam five miles north of Saugus,

California, suffered some damage and the owner, the Los Angeles Department of Water and Power, decided to strengthen the dam with a thick cap of compacted earth on the crest and on the downstream face. Figure 3.1, Appendix V, shows the major details of the original construction and the subsequent strengthening. More recently, especially in view of the increasing population downstream, the question of the earthquake resistance of the dam was reviewed. Forced vibration tests of concrete dams suggested that the structural vibration exciters recently developed at the California Institute of Technology might be suitable for exciting the earth dam into vibrations large enough to be detected. A test was therefore decided upon with the hope of learning something indicative of the structural condition of the dam. The Department of Water and Power furnished transportation, mounting facilities, and power for the shaking machines, and the California Institute of Technology furnished the shaking machines, instrumentation, and operating personnel. The University of California at Los Angeles and the Seismological Field Survey of the U. S. Coast and Geodetic Survey also participated in the test, furnishing personnel and instruments.

Exciting Equipment and Instrumentation

Two of the structural vibration exciters recently developed at the California Institute of Technology for the California Division of Architecture were used to excite the dam.[12], [13] These eccentric weight machines, which can be operated synchronously, are each capable of producing a maximum of 5000 pounds sinusoidal uniaxial force above $2\frac{1}{2}$ cps, so that a total of 10,000 pounds was applied on the crest, perpendicular to the length of the dam. Figure 3.2, Appendix V, shows the

exciters mounted on a concrete slab 8' x 12' x 16" thick cast into the compacted earth on the crest. The amplidyne control units for the machines are in the right foreground. Electric power for the machines was furnished by a gasoline engine-driven generator located on the bench on the downstream face of the dam.

The question of resonances between the earth and the slab on which the machines were mounted is worthy of consideration here. Such resonances between circular slabs and an elastic half space have been clearly shown by Arnold, Bycroft, and Warburton.[20] More recently Thomson, Kobori, and Reiter[37] have reported on the response of the infinitely rigid rectangular slab on an elastic half space. The mounting conditions on Dry Canyon Dam are not well represented by this theoretical treatment, but some idea of the interaction between the slab and the soil can be gained by assuming that the slab is rigid and the soil is a perfectly elastic, homogeneous, isotropic solid with a Poisson ratio of 0.25.

Thomson, Kobori, and Reiter state that the rotational response, ϕ, of the rigid slab subjected to a rocking moment $M_R e^{i\omega t}$ is given by

$$\phi = M_R \frac{b}{c^4 \mu} (f_1 + if_2) e^{i\omega t},$$

where c is one half the slab width in the direction parallel to the plane of M_R, b is one half the slab width perpendicular to c, μ is Lame's constant for the half space, and f_1 and f_2 are functions of the slab dimensions, the forcing frequency and the shear wave velocity in the half space. If a minimum shear wave velocity of 600 feet per second is assumed in the compacted material on the crest, the values of f_1 and f_2 for frequencies below 5 cps are seen from page 8 of Reference 37 to

be almost constant, indicating that the force applied to the dam in the frequency range 0-5 cps was not significantly influenced by any rocking resonant effects between the slab and the earth. Any local rotation of the earth would have only a small influence on the measured response of the dam inasmuch as the measured motion of the crest was translational, not rotational. Thomson, Kobori and Reiter have not computed the case of the slab forced parallel to the surface of the half space.

Resonances between the shaking machines and the slab have not been thoroughly investigated. At maximum force output the maximum observed amplitudes of the tops of the machines have been less than 1/16", which is approximately 0.5% of the radius arm of the eccentric weights. It is doubtful if in this test any resonant motion of the machines on their bases could have been responsible for more than a few per cent of the force applied to the dam.

The level of excitation required for a vibration test of a structure is determined by the sensitivity of the instrumentation and the level of background noise in the structure. Unless statistical methods are used on the data or a demodulator is a part of the instrumentation, such that only the frequency of excitation is passed, the minimum required excitation is the larger of either that which can excite the structure above the background, or that which can produce a response above the minimum which the instrumentation can record. At some distance from the vibration exciters and the engine-driven generator, the lower limit of response of Dry Canyon Dam was determined by the sensitivity of the instrumentation, but close to the exciters high frequency vibrations masked the response of the dam. It is recommended for future

tests that line power be provided for the machines, or if that is not possible, generators be mechanically isolated and be situated at as great a distance as possible from the points of measurement. Transducers of lower natural frequency would be better suited to tests of dams than the 100 cps instruments used here.

The instrumentation used for the Dry Canyon Dam test was the same as that used on the Encino Reservoir tower, Part II. This consisted of the William Miller Company C-3 carrier amplifier, the Statham A5-2-350 accelerometer, and the Consolidated Electrodynamics 5-124 oscillograph. Both the accelerometers and the recording galvanometers had natural frequencies of 100 cps. A galvanometer of $18\frac{1}{2}$ cps natural frequency was used later in the test to filter out 60 cps hum caused by a malfunction of an amplifier tube. The overall sensitivity of the system was such that 0.001g acceleration produced a galvanometer deflection of approximately three inches.

The amplifiers with the oscillograph resting on top are shown in Figure 3.3, Appendix V. The shield over the front of the oscillograph prevented the record from being destroyed by exposure to sunlight. In the foreground, an accelerometer is bolted to a protractor table for calibration.

Other instrumentation at the site were the Kanai Microtremor apparatus, manufactured by the Hosaka Shindo Keiki Company of Tokyo, and two Sprengnether Blast Recorders. The Kanai instrument, a displacement divice with a maximum magnification of 140,000, was operated by Mr. David Leeds of the College of Engineering, U.C.L.A. The Sprengnether instruments, three-component displacement meters of approximately 400 magnification, were operated by Mr. W. K. Cloud and Mr. C. Knudson of

the U. S. Coast and Geodetic Survey.

Experimental Procedure

Initially, "rundown" tests were performed, in which one of the machines was brought up to its maximum speed, 10 cps if unloaded, and then allowed to coast to rest as a record was made of the response. This technique, which was a necessity in the days before good speed controls were available, produces a rapid scanning of the frequency range, but it does not locate the resonant frequencies with nearly the accuracy of steady state excitation if the resonances are closely spaced. An example of the complicated nature of response to rundown excitation was shown in Figure 2.16, Appendix V. The major testing effort was devoted to steady state excitation, with a very close scanning of the frequency range, at approximately 0.02 cps intervals. It was found that measurements of the response at a point on the dam could be duplicated to within a few percent on succeeding days, giving credence to the whole testing procedure.

Experimental Results

The chief results of the testing are summarized in the three resonance curves shown in Figure 3.4, Appendix V. The locations of the points whose response is represented by the curves are shown on the sketch in Figure 3.4. The curves represent displacement per unit force, and were obtained by dividing the measured accelerations by a suitable constant times the fourth power of the frequency, the assumptions being that the motion was sinusoidal and that the structure responded linearly to a change in force level. Inasmuch as the oscillograms were of acceleration and were sinusoidal in appearance the first assumption is

reasonably justified, and several checks of linearity of response with force level justified the second. The data plotted on each curve were obtained over several days of testing, in general with more than one accelerometer and with more than one eccentric weight combination in the shaking machines.

Phase lags of displacement relative to the force, noted on the curves in Figure 3.4, were scaled from the oscillograms, the accuracy at the higher frequencies probably not better than $\pm$ 20°. Phase lag was monitored continuously from the low end to the high end of the frequency range, resulting in values greater than 360° in curve B. Although it is possible that some multiple of 360° should be added to all the phase lags, it is believed that the values shown are the absolute values.

The striking features of Figure 3.4 are the close spacing of the resonances, the sharpness of the peaks, and the high level of the "base" compared to the peaks, especially in the case of curve A. Had not a good speed control been available, the fine scanning of the frequency range necessary to define the resonances would not have been possible. The scatter noted on the low frequency end of curve A is probably the result of the small amplitude of the records at these frequencies, as low as 0.09" peak to peak. The steady state amplitudes were found to be not perfectly steady, perhaps due to poor generator control, and most of the plotted points are the average of five or so individually measured amplitudes. Such a data reduction procedure is very tedious, but the results by this procedure showed less scatter.

Vibrations of the Truncated Shear Wedge

Vibrations of earth dams, considered as shear wedges of finite length, have been treated by Ambraseys.[38], [39] Briefly, the relationships of the truncated wedge are developed here, using the nomenclature of Ambraseys.

Consider the elastic wedge shown in Figure 3.5, fixed against movement at the ends and at the bottom, and possessing only shearing resistance to deformation. Using the coordinates shown, the equation relating the inertial force and deformation of the undamped structure is:

$$-\rho ya\frac{\partial^2 u}{\partial t^2} + Gya\frac{\partial^2 u}{\partial x^2} + Gya\frac{\partial^2 u}{\partial y^2} + Ga\frac{\partial u}{\partial y} = 0, \qquad (3.1)$$

where ρ is the mass density of the material, G is the modulus of rigidity, and $\underline{a}$ expresses the relationship between the thickness and the distance from the vertex, b = ah'. If now the function u is assumed to have the form

$$u = \sum_{r = 1, 2,} u_r \sin\frac{r\pi x}{L} \sin\omega t,$$

then for each u_r equation 3.1 takes the form

$$y^2 u_r'' + y u_r' + \left[\omega^2/S^2 - (\frac{r\pi}{L})^2\right] y^2 u_r = 0, \qquad (3.2)$$

where $S = \sqrt{G/\rho}$, the velocity of shear waves in the material, and (') indicates differentiation with respect to y.

Equation 3.2 is recognized as Bessel's equation of order zero, with the solution

$$u_r = AJ_o(\beta y) + BY_o(\beta y),$$

where

$$\beta = \left[\omega^2/S^2 - (\frac{r\pi}{L})^2\right]^{\frac{1}{2}}.$$

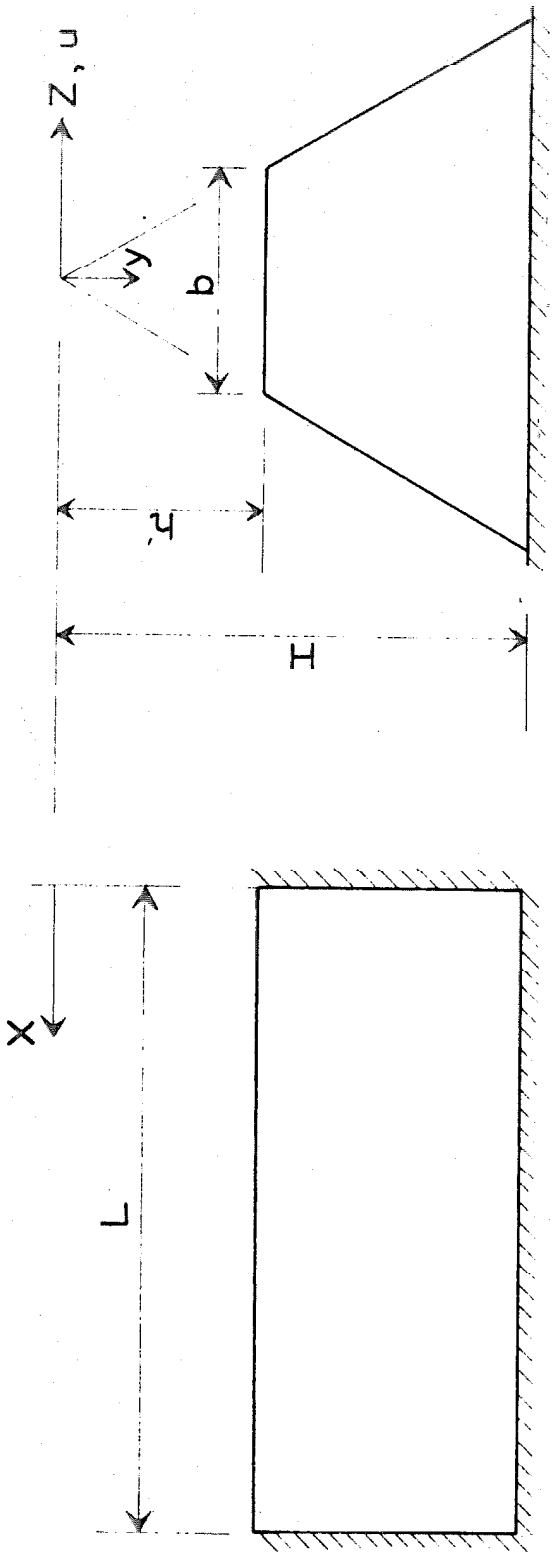

FIGURE 3.5
TRUNCATED WEDGE

When consideration is given to the boundary conditions

$$u_r(o,y) = u_r\,(L,\ y) = u_r\,(x,\ H) = \frac{\partial u_r(x,h')}{\partial y} = 0,$$

there results the characteristic equation

$$J_1(\beta_n h')\ Y_o(\beta_n H) - J_o(\beta_n H) Y_1(\beta_n h') = 0, \tag{3.3}$$

or in the more convenient form of Ambraseys,

$$J_1(k'a_n)Y_o(a_n) - J_o(a_n)Y_1(k'a_n) = 0, \tag{3.3}'$$

where $a_n = \beta_n H$ and $k' = h'/H$.

From equation 3.3 the natural frequencies are determined, and the equation of the nrth mode is given by

$$u_{nr} = \left[J_o(a_n\ y/H) - \frac{J_o(a_n)}{Y_o(a_n)} \cdot Y_o\ (a_n\ y/H)\right] \sin\left(\frac{r\pi x}{L}\right) \sin \omega_{nr} t,$$

where

$$\omega_{nr} = \frac{S}{H}\left[a_n^2 + \left(\frac{r\pi H}{L}\right)^2\right]^{\frac{1}{2}}, \tag{3.4}$$

and a_n is a root of equation 3.3'. The mode shapes of the wedge are thus seen to be sine waves in the longitudinal direction and curves defined by Bessel functions in the vertical direction.

To prove the orthogonality of the modes consider two modes, u_{mr} and u_{nr}, in equation 3.2:

$$y\ u_{mr}'' + u_{mr}' - \left[\frac{\omega_{mr}^2}{S^2} - \left(\frac{r\pi}{L}\right)^2\right] y\ u_{mr} = 0$$

and

$$y\ u_{nr}'' + u_{nr}' - \left[\frac{\omega_{nr}^2}{S^2} - \left(\frac{r\pi}{L}\right)^2\right] y\ u_{nr} = 0.$$

Multiplying the first of these equations by u_{nr} and the second by u_{mr} and subtracting, there results

$$\frac{1}{S^2}\left[\omega_{nr}^2 - \omega_{mr}^2\right] y\ u_{mr}\ u_{nr} + u_{nr}\,(y\ u_{mr}'' + u_{mr}') - u_{mr}(y\ u_{nr}'' + u_{nr}') = 0,$$

or

$$\frac{1}{S^2}\left[\omega_{nr}^2 - \omega_{mr}^2\right] y\, u_{mr}\, u_{nr} + u_{nr}\,(y\, u'_{mr})' - u_{mr}\,(y\, u'_{nr})' = 0. \quad (3.5)$$

The last two terms of equation 3.5 are the derivative of

$$y\,(u'_{mr}\, u_{nr} - u'_{nr}\, u_{mr}),$$

so upon integration over the range of y, equation 3.5 becomes

$$\frac{1}{S^2}\left[\omega_{nr}^2 - \omega_{mr}^2\right]\int_{h'}^{H} y\, u_{mr}\, u_{nr}\, dy = \left[y\,(u'_{mr}\, u_{nr} - u'_{nr}\, u_{mr})\right]_{h'}^{H} = 0.$$

Thus, if $n \neq m$, $\int_{h'}^{H} y\, u_{mr}\, u_{nr}\, dy = 0$.

The Fourier expansion of u along the length of the wedge guarantees orthogonality in the x - direction, therefore

$$\int_{h'}^{H}\int_{o}^{L} y\, u_{mr}\, u_{ns}\, dx dy = 0 \text{ for } u \neq m \text{ or } r \neq s.$$

The response of the wedge to any force may be found by first expanding the force in a double infinite series of the characteristic functions

$$F(x,y,t) = \sum_n \sum_r y\, A_{nr}(t) u_{nr},$$

where

$$A_{nr}(t) = \frac{\int_{h'}^{H}\int_{o}^{L} F\, u_{nr}\, dx dy}{\int_{h'}^{H}\int_{o}^{L} y\, u_{nr}^2\, dx dy}.$$

Then proceeding in the usual manner for characteristic value problems the response of any mode, $\xi_{nr}(t)$, is given by

$$\xi_{nr}(t) = \frac{\int_{o}^{t} A_{nr}(\tau)\, e^{-\zeta_{nr}\omega_{nr}(t-\tau)} \sin\left[\omega_{nr}\sqrt{1-\zeta_{nr}^2}\,(t-\tau)\right] d\tau}{\rho a\, \omega_{nr}\sqrt{1-\zeta_{nr}^2}},$$

where ζ_{nr} is the fraction of critical viscous damping in the mode. The response of a point b on the wedge to a sinusoidal force concentrated at point a is given by

$$u(b) = \sum_n \sum_r \frac{u_{nr}(b)\, Fu_{nr}(a) \sin(\omega_{nr} t - \phi_{nr})}{\int_{h'}^{H}\int_{o}^{L} \rho\, a u_{nr}^2 \omega_{nr}^2 y \sqrt{\left[1-(\omega/\omega_{nr}^2)\right]^2 + (2\zeta_{nr}\omega/\omega_{nr})^2}\, dx dy}, \quad (3.6)$$

where

$$\phi_{nr} = \tan^{-1} \frac{2\zeta_{nr}\,\omega/\omega_{nr}}{1 - (\omega/\omega_{nr})^2}$$

Application of Theory to Dry Canyon Dam

An attempt was made to apply this theory of the shear wedge to the observed behavior of Dry Canyon Dam under the sinusoidal excitation, although it is recognized that the dam differs from the wedge in the following respects:

1. The dam is made of several imperfectly elastic materials, the relative proportions of which, through the thickness, vary along the height of the dam.
2. The thickness of the dam does not taper uniformly along the height, and the thickness increases near the abutments.
3. The foundations and the abutments are not perfectly rigid, and are not smooth planes, horizontal and vertical respectively.

From the Figure 3.1, Appendix V, the height, H, to the apex of the wedge was taken as 65', h' as 5', and the length, L, as 485'. From Reference 38 in which Ambraseys has tabulated values of a_n for various values of the truncation coefficient ($k' = h'/H$), the first two roots of equation 3.4, the frequency equation, are $a_1 = 2.43$ and $a_2 = 5.66$. If an average shear wave velocity is assumed as 302 feet per second, the first ten calculated natural frequencies are those tabulated in Table 3.1 alongside the observed frequencies of curve A, Figure 3.4. Parentheses around an observed frequency means a resonance is suspected, but no peak was observed. The agreement of the frequencies in Table 3.1 is rather striking in view of the obvious differences between the dam and the elastic wedge. It will be noted that the differences between

Observed Frequency cps	Computed Frequency cps	Position Factor	Estimated Damping Fraction of Critical
1.82	1.81	0.92	0.10
	1.89	0.27	0.10
2.01	2.03	0.46	0.040
2.23	2.19	0.80	0.048
(2.45)	2.38	0.04	0.035
2.60	2.59	0.99	0.035
(2.80)	2.82	0.12	0.030
3.04	3.07	0.65	0.024
3.34	3.33	0.62	0.019
(3.65)	3.59	0.14	0.030

TABLE 3.1

NATURAL FREQUENCIES, POSITION FACTORS, AND DAMPING

two adjacent observed frequencies do not increase monotonically with frequency as indicated by equation 3.4, the resonances at 2.23 cps and 2.45 cps departing from the pattern predicted by theory.

The fact that several observed resonant frequencies appear only weakly in curve A, Figure 3.4 can be explained by a small value for the product $u_{nr}(b) \cdot u_{nr}(a)$ in equation 3.6. Relative values of this product for curve A are listed in Table 3.1 under the heading "Position Factor." It is seen that in general the weak resonances are associated with small values of the position factor.

The computed frequencies and the position factors of Table 3.1 are dependent upon the values assumed for H, h', L, and S and upon the positions of the effective ends of the dam with respect to the location of the vibration exciter. The position factors in the higher modes are especially sensitive to changes in the locations of the ends of the dam. From the longitudinal cross section of the dam, Figure 3.1, Appendix V, it is obvious that the values of all these dimensions might reasonably be varied to some extent. The values used are the result of scanning the variables with a digital computer and comparing the results with the values of the observed frequencies and the strengths of the resonances. For the position factors shown in Table 3.1, the ends of the dam were assumed at stations 0 + 90 and 5 + 75, whereas the shaking machines were located at station 3 + 75.

It will be noted from the frequency equation that for higher values of r the difference, Δf, between adjacent frequencies was approximately S/2L. This observed difference in Table 3.1 is approximately 0.30 cps, suggesting that $S \approx 0.6L$ feet per second. Velocities of P - waves, S_p, produced by striking a sledge hammer blow against the surface of the

dam were reported by Mr. David Leeds of UCLA as between 1325 and 2500 feet per second. Using the relationship

$$S_v = S_p \sqrt{\frac{1 - 2\nu}{2\,(1-\nu)}} \quad ,$$

Poisson's ratio, ν, must have the value 0.472 to correlate the minimum S_p value with the computed value of S_v of 302 feet per second. Unfortunately, representative values of ν do not seem to be available among the more common texts on soil mechanics.*

Determination of Damping

From the previously mentioned assumed values of the length, height, etc. of the dam, the lowest frequency associated with the second mode in the vertical direction, f_{21}, is calculated to be 4.18 cps. Referring to curve A, Figure 3.4, Appendix V, the resonance at 4.12 cps, assumed to be f_{21}, does not appear to have any significant influence which varies with frequency on the response of the dam at frequencies below 3.7 cps, so it was assumed that below 3.6 cps the resonance curve was the result solely of the first ten modes whose frequencies, f_{11} to $f_{1,10}$, are tabulated in Table 3.1, plus a "base" of constant response in phase with the force. The base represents the response of all the modes with frequencies above $f_{1,10}$.

Using the first ten modes and estimating damping, u(b) of equation 3.6 was then evaluated on a digital computer at intervals of 0.02 cps over the frequency range 1.7 cps to 3.8 cps, and to the result was added the base representing the response of all the higher modes. The base was, of course, estimated, the criterion being the appearance of the

---

* According to Professor G. W. Housner, wave velocity measurements in the mud under San Francisco Bay gave a value of Poisson's ratio of 0.495.

resulting resonance curve. On curve A the base tends to increase ordinates at the lower frequencies and to decrease ordinates at the higher frequencies. On curve B the effect is more complicated. The base used for curve A was 0.235 times the in-phase component of the response of the first ten modes at 1.7 cps, and of opposite sign to the in-phase component, suggesting that the base is composed chiefly of response of the second mode in the vertical direction. The base used for curve B was 1.0 times the in-phase component of the response of the first ten modes at 1.84 cps, and was of the same sign as the in-phase component. Only relative response was calculated, no attempt being made to obtain an absolute value of the double integral in the denominator of equation 3.6.

Figures 3.6 and 3.7 show the computed resonance curves corresponding to curves A and B in Figure 3.4. Damping constants for the first ten modes, listed in Table 3.1, were adjusted until the computed curve A appeared to agree best with the observed curve A. The relationship between the position factors and the damping coefficients is very obvious now. Curve B, Figure 3.7, was then computed using the same damping factors determined for curve A, but with the base adjusted by trial and error for best agreement with the observations.

It is seen that the agreement between the curves A is fairly good in view of the simplifying assumptions made in the calculations. Computed curve B, however, has only a few features in common with observed curve B. It seems probable that by readjusting the locations of the effective ends of the dam and by readjusting the damping that computed curve B could be made to show much better agreement with the observed curve B. Such readjustments however would very probably result in

FIGURE 3.6
COMPUTED RESONANCE CURVE FOR POINT A

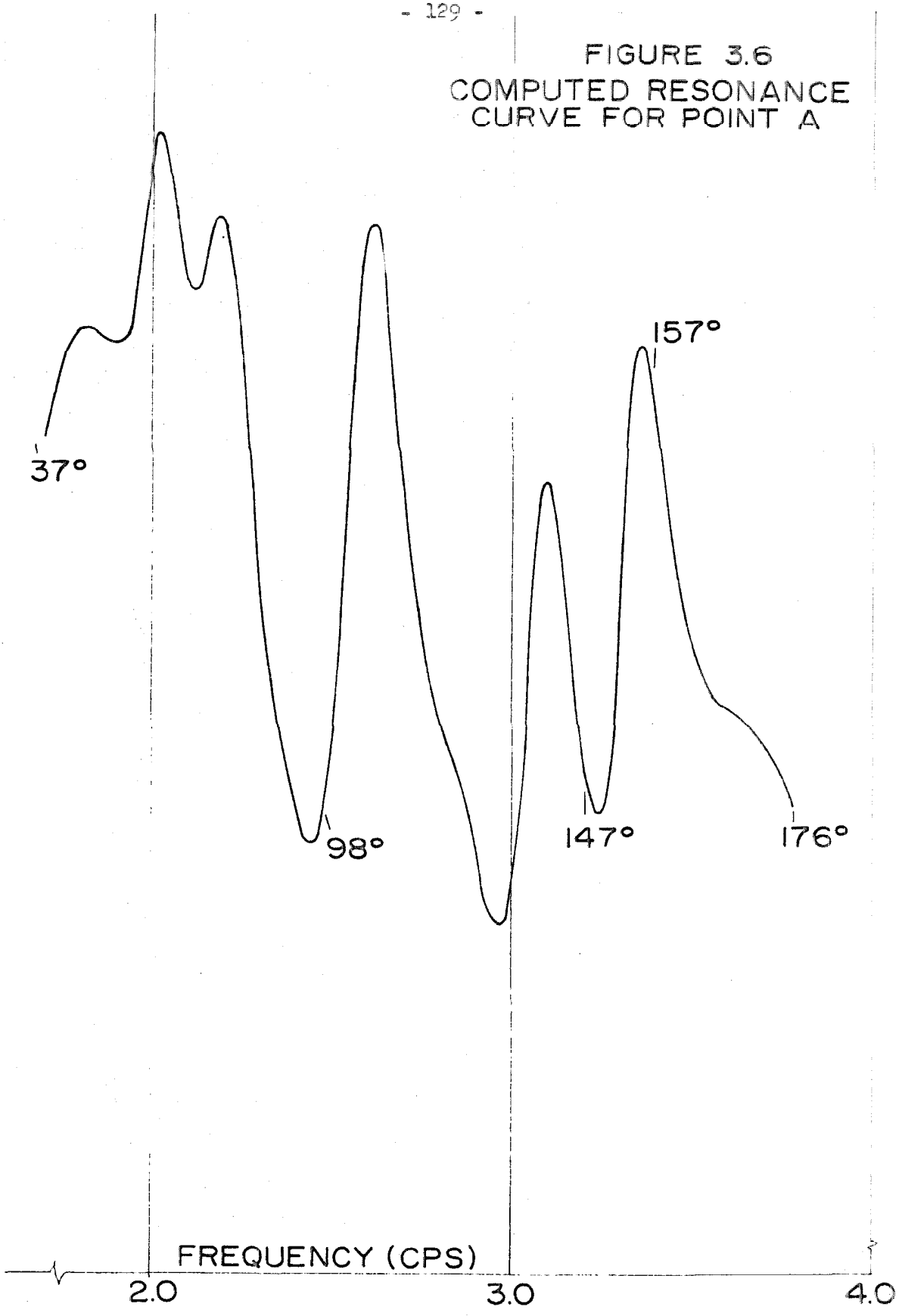

FIGURE 3.7
COMPUTED RESONANCE
CURVE FOR POINT B

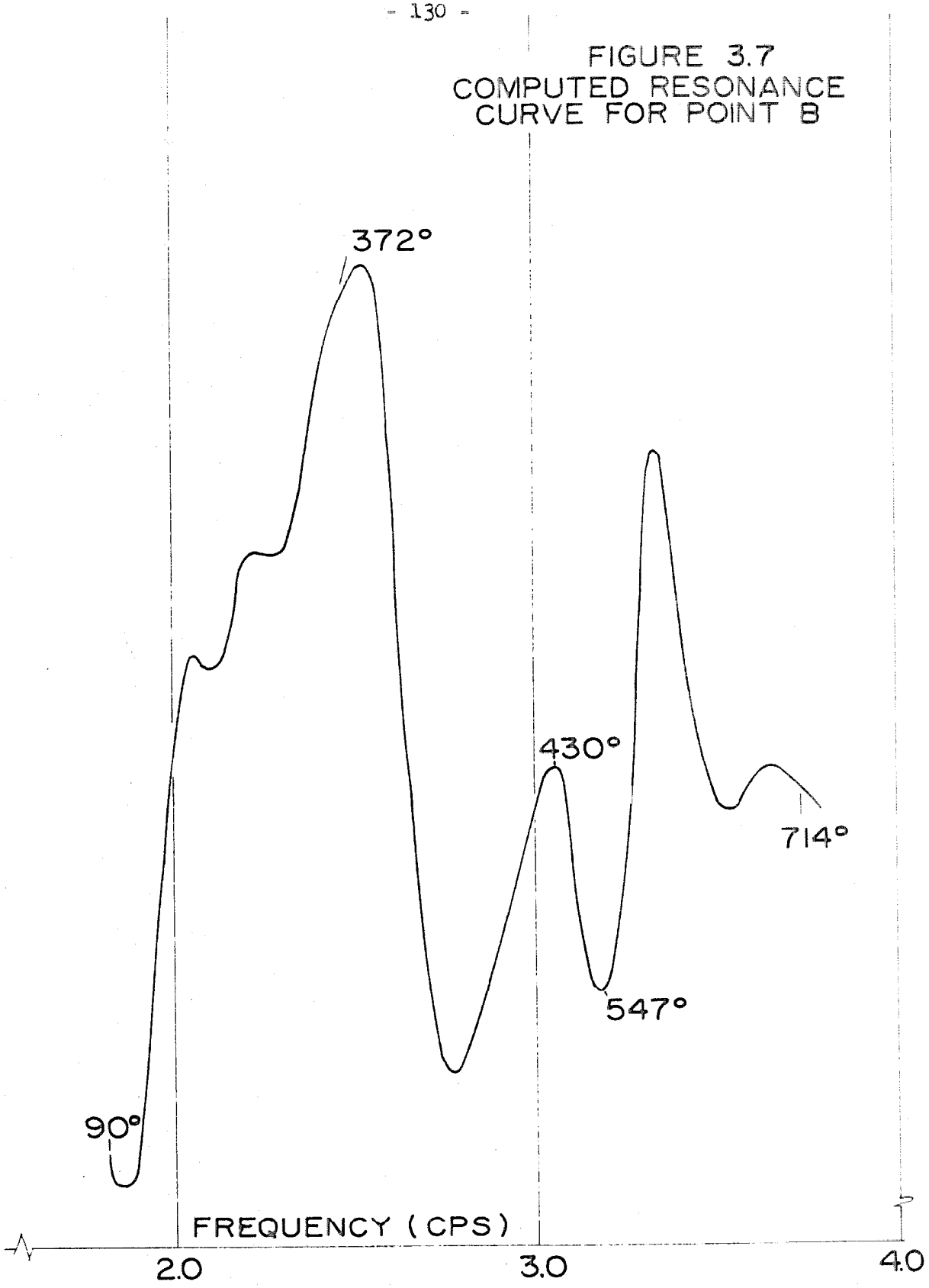

poorer agreement between the curves A. The damping factors in Table 3.1 are seen to vary from 0.019 in the ninth mode to 0.10 in the two lowest modes. Whether it is reasonable for damping to decrease in the higher modes is subject to question. It is very likely that the damping is more complex than the modal damping assumed here.

The order of magnitude of the shear stress in the dam resulting from the forced vibrations can be estimated by assuming all the response at 1.8 cps results from the first mode only. The force at 1.8 cps was 5300 pounds and the resulting deflection of the center of the dam at the level on which curve A was measured was then approximately 1.65×10^{-4} inch, resulting in a deflected shape in the horizontal plane given by $u = 1.65 \times 10^{-4}$ inch $\cdot \sin(\pi x/L)$. The shear strain at the abutment is then $\pi/L \cdot u(L/2)$, and if G is taken as 2150 psi to correspond with a shear wave velocity of 300 feet per second and an estimated density of 110 pounds per cubic foot, the computed shear stress is 1.9×10^{-4} pounds per square inch.

A Proposed Digital Technique for Finding the Frequencies of Dams of Irregular Outline.

The application of the theory of the vibrating shear wedge to Dry Canyon Dam, quite irregular in outline and with a foundation and abutments which are not perfectly rigid, suggests that a digital computer technique should be developed to compute the natural frequencies and mode shapes of actual dams. The method presented here is an extension of the Holzer or Myklestad-Prohl method, which has been successfully applied to flexural members, and to a flexural framework in Part II.

Consider the shear dam of Figure 3.8 (a) to be vibrating at a

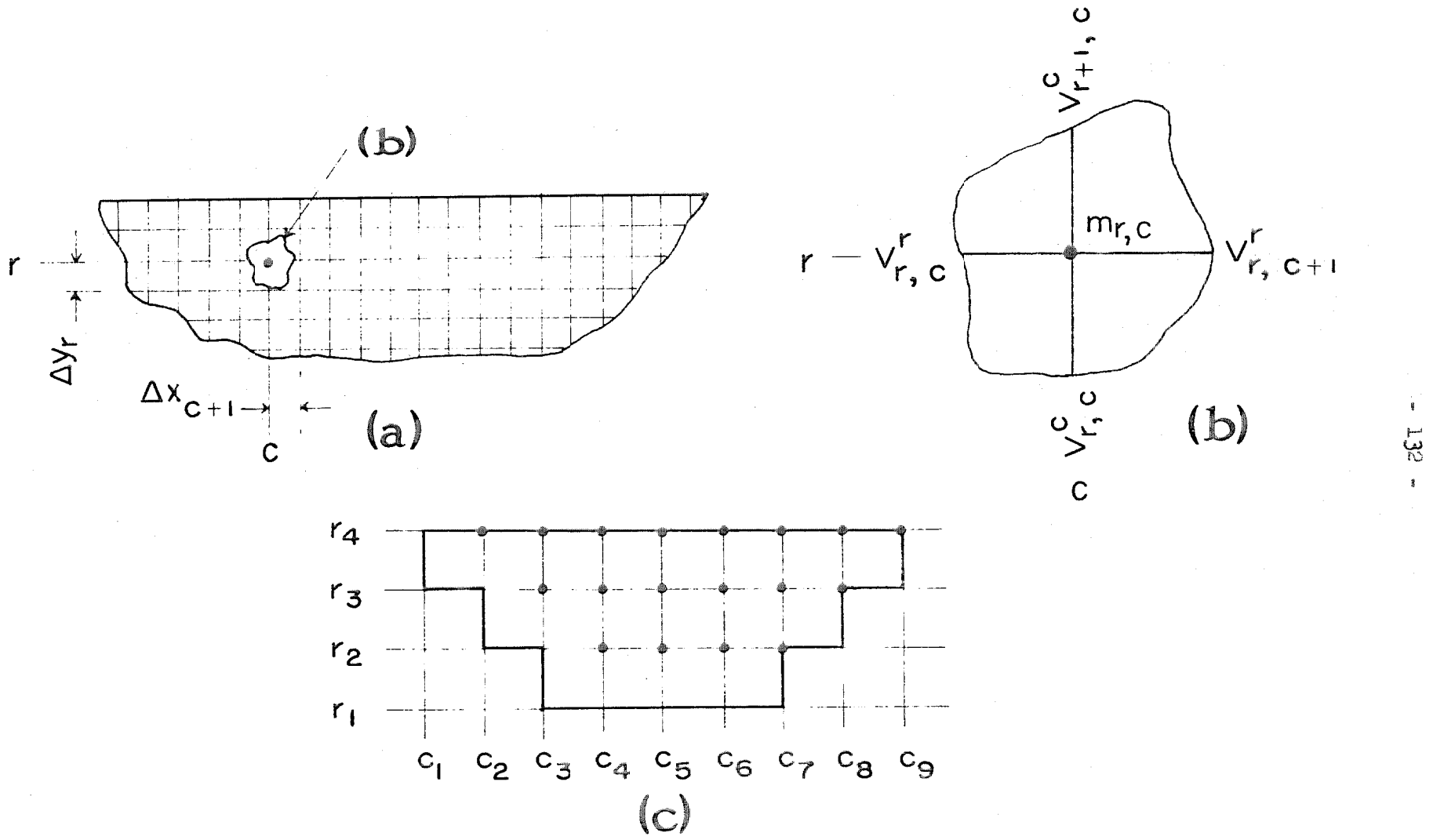

FIGURE 3.8
DISCRETE APPROXIMATION OF A SHEAR DAM

circular frequency ω. Let the dam be divided by a grid with nodes identified by row and column (r,c), numbered from the left and the bottom, and let the masses between the nodes be concentrated at the nodes. Acting on each mass m_{rc}, in addition to the inertia force will be four transverse forces dependent on the deflections of the adjacent masses relative to m_{rc} and on the shearing resistance of the material between the adjacent masses and m_{rc}. Figure 3.8 (b) illustrates the nomenclature. Using the sign convention that a shearing force is positive if it acts up from the paper at the left of or below a mass in Figure 3.8 (b), and negative if it acts into the paper at the right of or above, and letting u_{rc}, the transverse deflection of m_{rc}, be positive when directed into the paper in Figure 3.8 (a), the following equations may be written:

$$V^r_{r,c+1} = V^r_{r,c} + V^c_{r,c} - V^c_{r+1,c} - \omega^2 m_{r,c} u_{r,c} \tag{3.7}$$

$$V^c_{r+1,c} = V^r_{r,c} + V^c_{r,c} - V^r_{r,c+1} - \omega^2 m_{r,c} u_{r,c} \tag{3.8}$$

$$u_{r,c+1} = u_{r,c} + \frac{K V^r_{r,c+1} \Delta x_{c+1}}{G A^r_{r,c+1}} \tag{3.9}$$

$$u_{r,c+1} = u_{r-1,c+1} + \frac{K V^c_{r,c+1} \Delta y_r}{G A^c_{r,c+1}} , \tag{3.10}$$

where K is a constant, V is the transverse shear in the section between the concentrated masses, G is the modulus of rigidity, A is the transverse cross sectional area of the section between the concentrated masses, and Δx and Δy are the distances between node points, horizontal and vertical respectively.

Thus, if a sufficient number of shears and node deflections are

known, it is obvious that application of equations of the type 3.7 through 3.10 would permit step-by step determination of all the other shears and deflections in the dam. It can be demonstrated that if the shears in the three horizontal strings on the left side of the net in Figure 3.8 (a) are known, then all the other shears and deflections may be computed, the deflections at the left abutment and at the bottom being assumed zero for the time being.

For illustration, the dam has been divided into a coarser net in Figure 3.8 (c). Assume that the shear $V^r_{3,3}$ in Figure 3.8 (c) has the value $V^r_{3,3}$, and the shears $V^r_{4,2}$ and $V^r_{2,4}$ are zero. If equations of the type 3.7 through 3.10 are applied successively through the net, it will be found that on the right side of the dam the deflections $u_{4,9}$, $u_{3,8}$, and $u_{2,7}$ will in general not be zero, but for the trial frequency ω, they will have values linearly dependent on $V^r_{3,3}$ and dependent on ω in a more complicated manner. Thus

$$u_{4,9} = C_1 V^r_{3,3}, \quad u_{3,8} = C_2 V^r_{3,3}, \quad u_{2,7} = C_3 V^r_{3,3}.$$

If now $V^r_{3,3}$ is set to zero and a value is assigned to $V^r_{4,2}$, repetition of the step-by-step procedure will produce a linear relationship between deflections at the right abutment and $V^r_{4,2}$. The procedure may be repeated similarly for $V^r_{2,4}$.

Thus, deflections at the right abutment are expressed by the equation

$$\begin{Bmatrix} u_{4,9} \\ u_{3,8} \\ u_{2,7} \end{Bmatrix} = \begin{bmatrix} C \end{bmatrix} \begin{Bmatrix} V^r_{3,3} \\ V^r_{4,2} \\ V^r_{2,4} \end{Bmatrix}$$

where C is the 3 x 3 matrix of C's derived above. Inasmuch as $\{u\}$ must be zero if the abutments are rigid, unless $\{V\}$ is zero, the determinant

of $[C]$ must be zero. It will be found that there are only discrete frequencies for which the determinant of $[C]$ is zero, the natural frequencies of the structure. These natural frequencies are found by trial, the criterion being the minimization of the determinant of $[C]$.

If the foundations and the abutments of the dam are not perfectly rigid, the method that has been described is still applicable if the compliance of the rock is assumed to be that of an elastic spring, so that the deflection of a node point on the rock is proportional to the shear force in the string connecting to that node point. In this case, neglecting the inertia of the rock, the effect of compliance of the rock is simply a lowering of the stiffness of the strings between the rock and interior node points.

Summary and Conclusions

An earth dam 60 feet high by 485 feet long by 450 feet thick at the base was excited into transverse vibrations by two synchronized vibration generators having a combined capability of 10,000 pounds. The response of the dam was sufficiently large in the upper portion so that it could be recorded with an instrumentation system of commercially available accelerometers, amplifiers, and light beam galvanometers having a frequency response flat to 60 cps. The measured resonance curves showed many closely spaced natural frequencies, which can be fairly well explained by the theory of a truncated wedge vibrating in shear. Application of the theory to the dam indicated a shear wave velocity of 300 feet per second and equivalent viscous damping of from 2% to 5% critical in the third through the tenth modes and approximately 10% critical in the

two lowest nodes. The maximum shear stress developed during the test was estimated to be of the order of 2×10^{-4} psi. A digital computer technique is proposed for finding the frequencies and mode shapes of shear dams with irregular dimensions and with foundations and abutments which are not perfectly rigid.

The results of the forced vibration test indicate that further shaking of earth dams can be profitably conducted with the vibration exciters and the instrumentation used for this test. It is recommended that tests be conducted on earth dams or fills which are of more uniform composition and have more regular outlines than the Dry Canyon Dam. The source of power for the shaking machines preferably should be a utility line, otherwise good vibration isolation should be provided for any generator used. The instrumentation which was used for the Dry Canyon test should be suitable for measurements in the upper portions of low dams with shear wave velocities greater than 300 feet per second. Inasmuch as the fundamental frequency of a long dam varies approximately inversely with the height, geometrical similarity retained, the measured acceleration in the fundamental, due to excitation from an eccentric weight vibrator, would be approximately inversely proportional to the cube of the height. Higher dams therefore would require more sensitive instrumentation such as displacement or velocity transducers, or more sensitive accelerometers. In conjunction with such vibration tests, soil investigations should be conducted to relate the properties en masse to those determined from small samples.

IV. A NEW METHOD FOR DETERMINING STRUCTURAL PARAMETERS FROM DYNAMIC MEASUREMENTS

Introduction

Techniques of computing the dynamic response of hypothetical structures with precisely defined masses and restoring functions are well known. The literature is replete with examples of the response of linear systems to various exciting forces. Many solutions of hypothetical nonlinear systems have also been reported. Examples of the determination of the response of nonlinear structures are given by the Response Analyzer Committee at the Second World Conference on Earthquake Engineering, Berg,[40] Caughey,[41] and Iwan.[42][43]

The more difficult inverse problem, that of determining the properties of a structure from measured response, has not received the same attention. Berg has presented the theory for determining the mass, spring, and damping matrices of linear lumped-mass structures from observations of pure mode shapes and their associated frequencies.[44] Kobayashi has described and given an example of an analog technique for determining the masses, springs, and dampers in a linear structure from simultaneous records taken at the base and on the roof of the structure subjected to earthquake motion.[45] O'Kelly has illustrated the determination of modal damping constants from experimental data obtained on an electrical analog of a linear system.[46] No work, theoretical or experimental, on the determination of the parameters of nonlinear structures appears to have been published, however.

Although it may be argued that from the known mass distribution of a structure, the observed natural frequencies and mode shapes, and from the decay of free vibrations or the widths of resonance peaks that an

equivalent linear system may sometimes be constructed to adequately represent a nonlinear system, real progress in nonlinear vibrations can be made only by recognizing and defining the nonlinear parameters. In the paragraphs which follow, the theory of a new method for linear and certain types of nonlinear lumped-mass structures is outlined, and experiments on a nonlinear single-mass system are described to illustrate the method and to indicate its practical limitations.

Preliminary Considerations

To obtain a picture of the problem, consider the system of n lumped masses shown in Figure 4.1 (a) to be subjected to a known dynamic force system $F(t)$ consisting of one or more forces $F_i(t)$ acting on the masses, m_i, in the plane of the paper. In this example, for small displacements, the geometry of the structure limits the masses to horizontal movements, a situation representative of many actual structures. In the most general case, the columns are attached to the masses by hinges with hysteretic moment-rotation characteristics which change with the history of strain. Examples of such characteristics are shown in References 40 and 47. The equation of dynamic equilibrium of the mass m_i is given by

$$F_i(t) = m_i\ddot{x}_i + G_i\left(\int_o^{x_1} dx_1, \int_o^{x_2} dx_2, \ldots, \int_o^{x_n} dx_n, \dot{x}_1, \dot{x}_2 \ldots, \dot{x}_n\right).$$

The function G_i at any instant, expressing the effect of the remainder of the structure on the mass m_i, depends upon the previous displacement history of every other mass in the structure. Velocity terms have been added here to agree with past practice, although it is believed by some authors that the use of viscous damping has been based more on mathematical convenience than on experimental evidence.[48] To derive such a general expression for G_i from experimental dynamic data appears much too difficult at the present time.

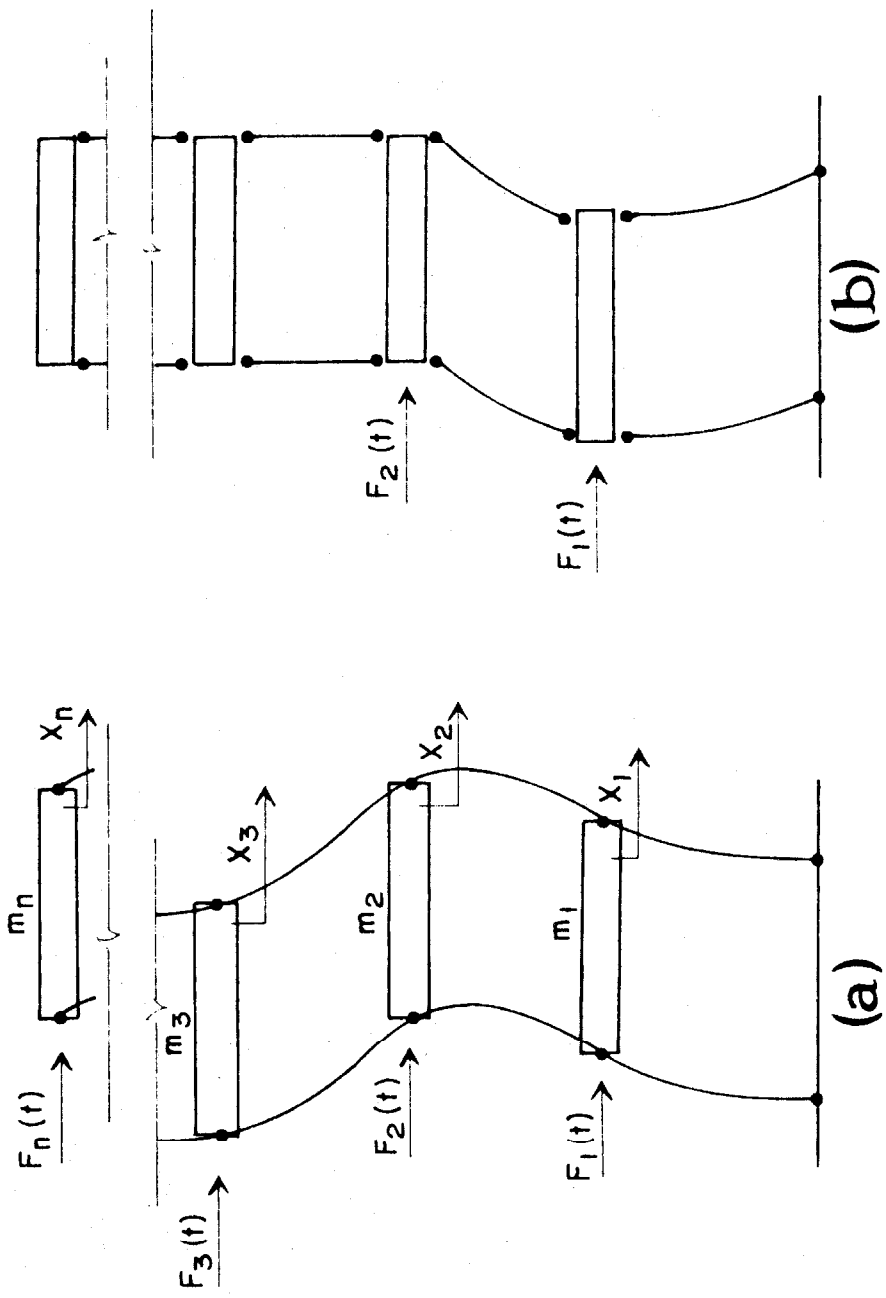

FIGURE 4.1
HYSTERETIC STRUCTURES

A much simpler structure is shown in Figure 4.1 (b). Here the columns are rigidly attached to the masses, which themselves are rigid, and hysteretic hinges can form between the masses, but it is only the relative deflections of the two adjacent masses which now affect the force on any mass. General expressions for the G functions for even this simple structure appear to be too complicated to be derived from dynamic experiments at the present time, but the method which will be described is applicable to defining the G functions over portions of the displacement paths actually followed in some dynamic process. In theory the same thing can be accomplished in the more difficult case considered first, but, practically, accurate results are much less likely.

If in Figure 4.1 (a) the moment-rotation characteristics of the hinges are nonlinear, but not hysteretic, then the force of the remainder of the structure on any mass at any instant is simply a function of the relative positions of the masses and the relative velocities at that instant, independent of the past history of motion, and the G functions are much more amenable to description. The method to be described is applicable to this class of structures as well as to linear structures.

The problem considered here can be very difficult. The view taken, however, is that when a lumped-mass structure responds to a dynamic force, a phenomenon involving a finite number of forces, masses, accelerations, velocities, and displacements takes place. If sufficiently accurate data of the phenomenon is gathered, reasonably accurate construction of the relationships among the variables should be possible.

Description of the Method

The method proposed for determining the masses and the G functions

of a structure consists of solving the equations of dynamic equilibrium of the masses, with observed simultaneous values of forces, accelerations, velocities, and displacements entered into each equation. The G functions can be expressed in terms of orthogonal polynomials of the variables involved, [49] or as an alternate choice a more simply formed expression for G can be assumed and the coefficients of powers of x and $\dot{x}$ can be determined by solving as many equations as there are unknown coefficients. If more data are available a least squares technique may be used to obtain a best fit. In theory if there are assumed terms in G which are not actually related to the phenomenon, the coefficients of these terms will turn out to be zero. What actually happens in this case is illustrated later.

The Linear Viscous Damped Structure

For the linear viscous damped structure of n masses, the G function for the ith mass has the form

$$G_i = K_{i1}(x_i - x_1) + K_{i2}(x_i - x_2) + \ldots + K_{in}(x_i - x_n) + K_{io}x_i +$$

$$C_{i1}(\dot{x}_i - \dot{x}_1) + C_{i2}(\dot{x}_i - \dot{x}_2) + \ldots + C_{in}(\dot{x}_i - \dot{x}_n) + C_{io}\dot{x}_i .$$

There are in the most general case $(n^2 + n)$ unknown coefficients in an n-mass structure.

To solve for the masses and the restoring and dissipative constants of a linear structure, the experimentally observed values of F, $\ddot{x}$, $\dot{x}$, and x must come from response to more than one frequency if the excitation is steady state sinusoidal. The reason for this is illustrated by the simple example of a single degree of freedom system. The response of the system to a steady sinusoidal force is

$$x(t) = \frac{F \sin(\omega t - \phi)}{K\sqrt{\left[1 - (\omega/\omega_n)^2\right]^2 + (2\zeta\omega/\omega_n)^2}}, \quad \phi = \tan^{-1}\frac{2\zeta\omega/\omega_n}{1 - (\omega/\omega_n)^2}$$

where $\zeta = \frac{C}{2\sqrt{KM}}$. The simultaneous records of force, acceleration, velocity, and displacement would look similar to those shown in Figure 4.2. Since there are three unknowns to be found, m, K, and C. The records are cut at a minimum of three places, a, b, c in Figure 4.2 to obtain simultaneous values of F, $\ddot{x}$, $\dot{x}$, and x for the following equations of dynamic equilibrium.

$$\begin{aligned} F_a &= m\ddot{x}_a + Kx_a + C\dot{x}_a \\ F_b &= m\ddot{x}_b + Kx_b + C\dot{x}_b \\ F_c &= m\ddot{x}_c + Kx_c + C\dot{x}_c \end{aligned} \tag{4.1}$$

Now the accelerations of a linear system under steady sinusoidal excitations are always equal to $(-\omega^2)$ times the displacements, and if a solution of equations 4.1 is attempted by Cramer's method of determinants it will be found that the determinant of the coefficients of the unknowns is zero. It can also be easily demonstrated that the determinant in the numerator of this solution is zero. If at least one of the equations 4.1 pertains to a different frequency, however, the determinants in Cramer's solution can still be zero by unfortunate combination of frequencies and the locations of the cuts, but they are not necessarily zero as in the previous case, so a solution is possible. Although no formal criterion is established here for locating the cuts, the solutions would logically be best defined from data taken throughout the entire range of the natural frequencies of a multiple-mass structure.

The Nonlinear Nonhysteretic Viscous Damped Structure

In this type of structure G_i is again independent of the sign of $\dot{x}$

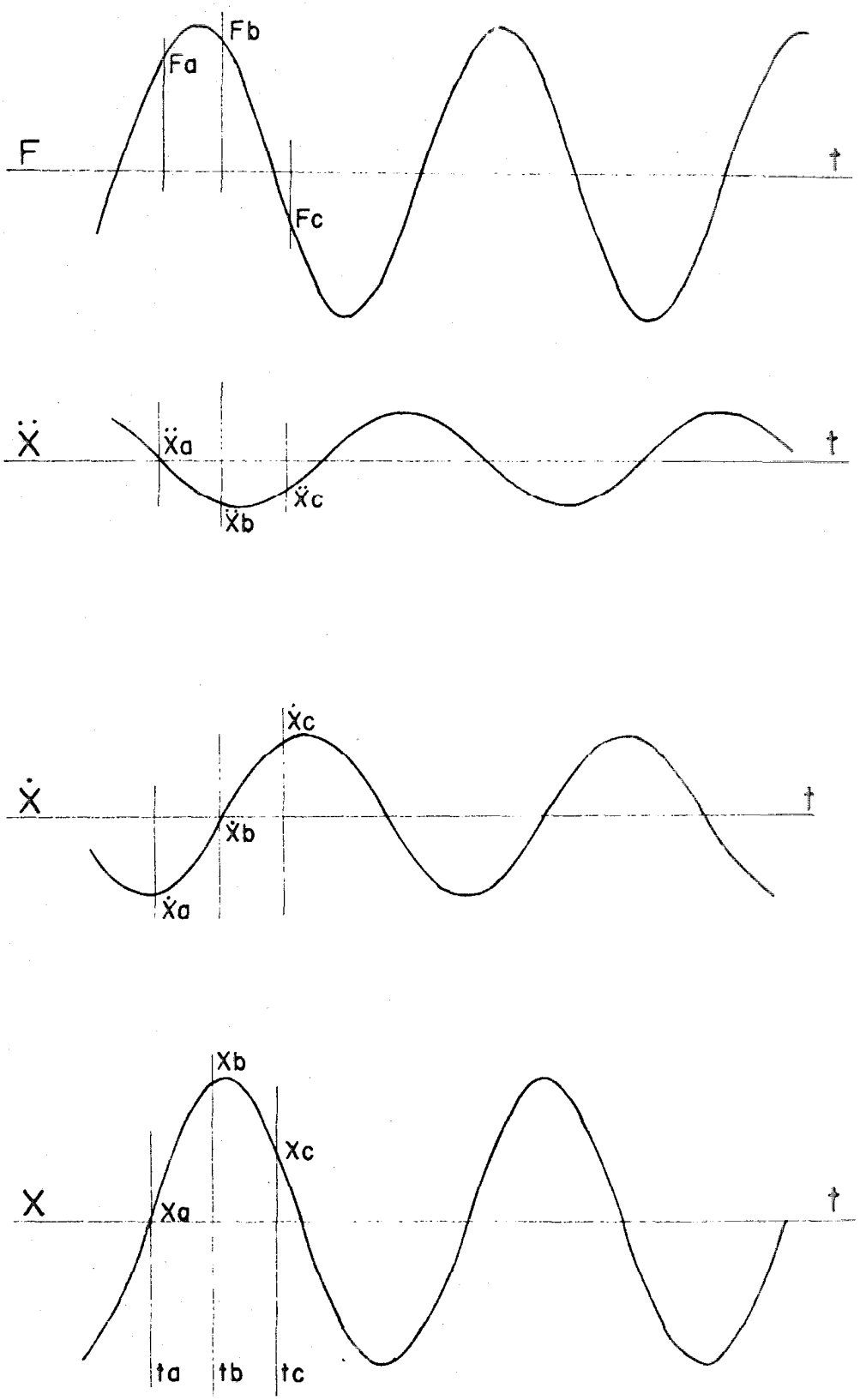

FIGURE 4.2
ILLUSTRATIVE RECORDS

as in the linear structure, but the expression for G_i is more complex:

$$G_i = \sum_s K_{i1}^{(s)} (x_i - x_1)^s + \sum_s K_{i2}^{(s)} (x_i - x_2)^s + \ldots + \sum_s K_{in}^{(s)} (x_i - x_n)^s +$$

$$+ \sum_s K_{io}^{(s)} (x_i)^s + \sum_{j=1}^{n} C_{ij} (\dot{x}_i - \dot{x}_j) + C_{io}\dot{x}_i .$$

The Nonlinear Hysteretic Viscous Damped Structure with Columns Rigidly Attached to the Masses

For this structure it is suggested that the data for defining the G functions should come from one continuous piece of record over the length of which neither of the relative velocities, $(\dot{x}_1 - \dot{x}_{i-1})$ and $(\dot{x}_i - \dot{x}_{i+1})$, undergoes a change in sign. The G functions so derived would, as in the cases of the two previously considered structures, pertain only to the actual paths represented by the record, but in this case each determination would pertain to only a short path, which would be dependent upon the previous history of the motions. The function G_i over this length of record could be expressed by

$$G_i = \sum_s K_{i,i-1}^{(s)} (x_i - x_{i-1})^s + \sum_s K_{i,i+1}^{(s)} (x_i - x_{i+1})^s +$$

$$+ \sum_{j=1}^{n} C_{ij} (\dot{x}_i - \dot{x}_j) + C_{io}\dot{x}_i .$$

If this same technique were to be applied to the more general case, in which the effects of the deflections of a mass are transmitted beyond the adjacent masses, the length of record in which none of the relative velocities changed sign might be very short. In theory the cuts in the record could be made very close together in such a case, but obviously this would result in equations of dynamics equilibrium being almost identical at adjacent cuts, and would require more refined instrumentation and more precise reading of the records.

Quality of Instrumentation

The method described is seen to require exceptionally good experimental data. Not only must the amplitudes of F, $\ddot{x}$, $\dot{x}$, and x be recorded accurately, but phase lags in all the records must be very small or be all the same. Reference to Appendix I indicates that if the response of the structure is measured with seismic-type acceleration, velocity, and displacement transducers, it is doubtful if the several records could be obtained with sufficient accuracy so that the proposed method could be applied. If, however, velocity and displacement were measured absolutely from a fixed reference platform adjacent to the structure, records of suitable quality would be more likely.

Reference platforms are generally not available for other than experimental structures, however, so it is proposed to measure only acceleration and to obtain velocity and displacement by integration of the acceleration records. In Appendix II a numerical integration technique is described and the accuracy on a steady sinusoidal record is illustrated. Unless acceleration is integrated continuously from rest, the absolute value of displacement cannot be determined from steady state acceleration records.

A Structure and Instrumentation for Testing the Method

Ideally the method should be tested with hypothetical data before experimental work is conducted, but the question of the adequacy of commercially available instruments to furnish accurate data was of such importance to practical application of the technique that experimental work was undertaken first to provide data for testing purposes.

The steel structure shown in Figures 4.3 and 4.4, Appendix V, was

built to test the method. It consists of two beams of 8" wide flange section at 17 pounds per foot by 42" long, held 12" apart by plates bolted to the top and bottom flanges. Pieces of 1" steel plate were placed in the pocket formed between the beams to add to the mass. Each column consists of a 3" channel at 4.1 pounds per foot, pinned at the base and connected to a beam with two 1/4" thick angles welded to the back of the channel, the web of the beam passing between the outstanding legs of the angles. Three 3/4" bolts connect a beam web to the angles on each column, the distance from the center bolt, at the middepth of the beam, to the pin at the base being 45½". The total concentrated weight, counting one-half the weight of the columns, is 469 pounds. The natural frequency of the structure for small oscillations is approximately 4 cps, and the equivalent viscous damping determined from the decay of small oscillations, is approximately 2% critical.

Two methods were used to apply dynamic forces to the structure. The Lazan mechanical oscillator, model LA-1, manufactured by the Baldwin Locomotive Works, is shown in Figure 4.3 mounted on top of the structure. This oscillator, which with its motor and mounting base weighed 145 pounds, is rated as producing a sinusoidal force, parallel to the beams in this case, of 3.14 pounds x $(\text{cps})^2$. The control used for the 1/4 horsepower D. C. motor was the General Electric Thy-Mo-Trol shown beneath the structure. This control held the force amplitude reasonably steady at amplitudes of motion up to 1/2" below the natural frequency of the structure, but above the natural frequency the force amplitude was modulated by lower frequencies.

The oscillator rested on ball bearings so that except for slight

frictional forces its entire horizontal output was transferred to the structure through a force gage, only a small portion of which can be seen above the leg of the buttress to the left of the oscillator in Figure 4.3. The measured force, of course, included the inertia force of everything supported on the ball bearings. To decrease the transmission of high frequency vibrations from the oscillator and to insure that the force transmitted to the structure was not sinusoidal, a short length of rubber hose was placed between the oscillator and the force gage. The entire assemblage thus became a two-mass system, but the measurements of force and acceleration pertained only to the structure proper.

The second method of applying a dynamic force consisted of striking the structure with the pendulum, the mass of which is shown at the left in Figure 4.3. In this case the oscillator was removed and the force gage was mounted on the opposite side of the buttress to receive the blow of the pendulum. A spring between the force gage and the pendulum prevented overloading the force gage.

Acceleration of the structure was measured with a Statham unbonded strain gage accelerometer, model A5A-200-220 of approximately 800 cps natural frequency, yielding 0.2 mv/g output at 10 volts excitation. The force gage, similar to the one pictured in Reference 50, p. 223, consisted of a cross of four equal arms of 1/2" width, meeting at right angles, cut from 3/16" steel plate. The outer ends of the arms were fixed in a rigid ring of $4\frac{1}{2}$" diameter, which was attached to the structure; the force from the oscillator was applied over a $1\frac{1}{2}$" diameter disc at the point of intersection of the arms. Four c-5 electric resistance strain

gages of the SR-4 variety on the arms of the cross were wired in a Wheatstone bridge circuit to give a voltage output proportional to the force transmitted by the gage. A Schaevitz L.V.D.T., type 1000 S-L was used to monitor displacement, but this instrument was found to be nonlinear in the region around zero displacement, so no quantitative readings were made with it. Static displacements were measured with a dial indicator acting against the stand shown at the right of the structure in Figure 4.3.

The accelerometer, the force gage, and the L.V.D.T. were all used with a Miller C-3 carrier amplifier, described in Appendix I and pictured in Figure 3.3, Appendix V. The three channels were recorded by galvanometers of 100 cps natural frequency in a Consolidated Electrodynamics oscillograph, model 5-124, described in Appendix I. The resistance damping circuits of the galvanometers were all identical, the resistances being those which produced 0.6 critical damping in one of the galvanometers. Actual damping in the other galvanometers was not checked experimentally.

The spacing of timing lines flashed on the oscillogram by a timing system in the oscillograph at approximately 0.0075 sec. intervals, was checked with a General Radio vacuum tube fork of 1000 cps frequency.

Digital Computer Treatment of the Data

Records were made of cyclic force and acceleration due to the mechanical oscillator. A typical record made with the bolts in the beam-column joints at low tension, 30 foot-pounds torque, is shown in Figure 4.5, Appendix V. The high frequency components of this record are possibly the result of the bolts moving against the sides of the

holes in the joint. At high bolt tensions, Figure 4.6, Appendix V, these high frequency components were not present. As indicated by the dots in Figure 4.5, 77 ordinates of force and of acceleration were read from the oscillogram at equal time intervals over one cycle of motion. In this instance, because of the high frequencies present, the interval selected was one-half the timing interval, which was 0.00791 seconds.

The data were then entered into the Burroughs 220 digital computer at the California Institute of Technology computing center. The force ordinates were scaled to pounds and the acceleration record was scaled and integrated twice in the manner described in Appendix II for cyclic records, the resulting displacement being arbitrarily centered so that its integral over one cycle was zero. The computer then put out a tape for later use, in which the corresponding values of F, $\ddot{x}$, $\dot{x}$, and x were sorted into two groups, depending on the sign of $\dot{x}$.

Next, the integrated data were entered back into the computer with a second program which calculated the mass and the coefficients in the G functions. This program was written to handle up to 70 sets of ordinates with $\dot{x}$ of one sign and to solve for as many as 14 coefficients in the G function. The method of solution is as follows.

$$F_a = m\ddot{x}_a + K_o + K_1x_a + K_2x_a^2 + \ldots + K_7x_a^7 + \\ + C_1\dot{x}_a + C_2\dot{x}_a^2 + \ldots + C_4\dot{x}_a^4 + P_1x_a\dot{x}_a + P_2x_a^2\dot{x}_a + P_3x_a\dot{x}_a^3. \qquad (4.2)$$

An equation of the type 4.2 was assumed by the operator. The letter subscripts here pertain to a particular cut, a, in the records. The program allowed equation 4.2 to be formulated with any or all of the terms shown, so the computer was instructed as to which terms were desired on the right side by a simple code from the operator at the

console. The operator also instructed the computer as to the number of equations to be formed and from what place in the stored data the values of F, $\ddot{x}$, $\dot{x}$, and x entering into the equations were to be taken. Thus, r equations of the type 4.2 were to be solved for s unknowns, which were the value of the mass and the values of the K's, C's and P's on the right side of equation 4.2

It is shown by Mirsky (51) that for the system of equations $Ax = b$, the solution

$$x = (A^TA)^{-1}A^Tb$$

is the one in which $\sum_{i=1}^{r} (Ax_i - b_i)^2$ is a minimum, and hence is a best solution in the least squares sense. This solution technique, using a 17 digit inversion procedure for A^TA, was used for the set of equations of the type 4.2. For an answer, the computer printed out the mass and the coefficients in the assumed G function, the values of F, $\ddot{x}$, $\dot{x}$, and x used in formulating the equations, the determinant of A^TA, the quantity $\sum_{i=1}^{r} (Ax_i - b_i)^2 = V^2$, and the values of the restoring and the dissipating functions, those associated with displacement and with velocity respectively, corresponding to the data points used in the equations.

Experimental Results

It was at first believed that the inclusion of all 14 terms in the G function of equation 4.2 would lead to the best answer, and the coefficients of those terms which did not relate to the phenomenon would be found to be very small. This was not the case in practice. When the value of the computed mass in the solution was compared with the known mass it was found that the inclusion of certain terms in G resulted in computed values of the mass very greatly in error, in fact sometimes even

of negative sign. The reasons for this unexpected behavior were not fully investigated, but two observations can be made. First the data contains systematic as well as random errors, and second, it is possible that the inclusion of some terms produced columns in the matrix A which were very close to linear combinations of other columns, in which case the determinant of A^TA should become very small. A check of the determinants in those cases of very erroneous computed mass did not reveal any apparent relationship between the value of the determinant and the accuracy of the computed mass.

Table 4.1 summarizes some computed results from steady state data with the connection bolts tightened to 70 foot-pounds torque. The amplitude of motion here was 0.29". The column headed "Det A^TA, F.P." is the determinant of A^TA in floating point notation. If the first two digits of the number in this column are subtracted from 50, the result is the number of zeros between the decimal point and the third digit. Thus 483 means 0.003. The column labelled "Quantities" lists those quantities whose coefficients were computed in equations of the type 4.2. The values listed under m, K_0, K_1, C_1, K_2, K_3 are the computed values of these quantities. A value for m of 1.216G means that on the left side of equation 4.2 there was entered $F - 1.216\ddot{x}$, the true mass being 1.216 pound-sec^2/in. In these cases the right side of equation 4.2 contained only the G function. The entry "0.4#f" means that 0.4 pounds friction was assumed transmitted from the oscillator through the bearing mount to the structure.

In row i of Table 4.1 it is seen that the inclusion of an $\dot{x}$ term in the solution yields a computed mass of only 0.65, whereas if $\dot{x}$ is

Row	Sign $\dot{x}$	No. Data Points	Det A^TA, F.P.	$\leq v^2$	Quantities	m #sec^2/in.	K_o #	K_1 #/in	C_1 #sec/in	K_2 #/in^2	K_3 #/in^3	
a	-	15	482	21	$(m\ x\ x^3)$	1.34	-13.8	869	-	168	412	
b	-	5	382	2×10^{-7}	$(m\ x\ x^3)$	-0.77	0.7	-33.8	-	-566	1475	
c	-	20	492	24	$(m\ x\ x^3)$	1.31	-14.0	858	-	168	359	
d	-	20	473	17	$(x\ \dot{x}\ x^3)$	1.216G	-3.11	820	1.68	55	334	
e	+	5	333	0.16	$(x\ \dot{x}\ x^3)$	1.216G	67.7	690	-0.31	-1525	4490	
f	-	5	334	2	$(x\ \dot{x}\ x^3)$	1.216G	372.0	886	64.9	-1501	-73	
g	+	20	474	19	$(x\ \dot{x}\ x^3)$	1.216G	13.5	807	4.17	-147	503	
h	+	20	491	19	$(m\ x\ x^3)$	1.25	13.9	818	0.36	-151	543	
i	-	20	489	7	$(m\ x\ x^3)$	0.65	22.4	589	5.38	-244	184	
j	+	20	484	19	$(m\ x\ x^3)$	1.31	16.2	842	-	-173	623	
k	-	21	365	13	$(m\ x\ x^3\ x^5)$	1.09	-12.0	774	-	17	-18	
l	+	20	484	20	$(m\ x\ x^3)$	1.29	16.3	836	-	-174	562	0.4#f
m	-	21	492	26	$(m\ x\ x^3)$	1.29	-14.1	853	-	167	327	0.4#f
n	-	21	471	27	$(x\ x^3)$	1.216G	-13.7	823	-	157	307	0.4#f
o	-	21	473	19	$(x\ \dot{x}\ x^3)$	1.216G	- 4.06	823	1.55	65	307	0.4#f
p	+	20	471	20	$(x\ x^3)$	1.216G	16.2	811	-	-172	472	0.4#f

TABLE 4.1

COMPUTER RESULTS FOR LABORATORY STRUCTURE

omitted, row (c), the computed mass is 1.31 for the data in which $\dot{x}$ is negative. Rows h and j, where $\dot{x}$ is positive, show that the inclusion of $\dot{x}$ in the G function yields a better value for the computed mass, 1.25 compared with 1.31. In other cases not tabulated the inclusion of $\dot{x}$ in the G function in general resulted in poorer values of the computed mass. The inclusion of products of x and $\dot{x}$ always resulted in less accurate values of the computed mass. The five data points used to compute the negative mass in row b included some very small forces and displacements, so such an erroneous result is not surprising.

Shifting the force data 9° backward with respect to $\ddot{x}$, $\dot{x}$, and x resulted in a computed mass of 10.2 and a forward shift of 9° resulted in a negative mass for the same G function which resulted in a mass of 1.31 when the force data was not shifted. This indicates that phase lag in the seismic type pickups should be kept very small, a difficult thing to do if much sensitivity is needed.

It became apparent, then, that the mass of the structure could not be reliably determined, but rather the known mass would have to be used as a criterion for the accuracy of the other terms in the answer. The assumption that if the computed mass is accurate, then the accuracy of the other terms in the answer is greatest is, of course, not true if systematic errors are present in the data. This is a matter which would best be investigated with hypothetical data.

Comparison of Dynamic and Static Hysteresis Loops

Data from steady cyclic motion of the structure were collected under three different conditions: 70 foot-pounds bolt torque and 30 foot-pounds bolt torque at 0.30" displacement amplitude, and 30 foot-pounds bolt torque at 0.565" displacement amplitude. Using the

technique described, the G functions were computed to yield the best computed values of the mass. Then the true values of the mass times acceleration were entered on the left side of the equations as described previously, and the G functions were recomputed. These G functions are plotted in Figures 4.7, 4.8, and 4.9, respectively. The computed masses associated with the form of the G functions shown in Figure 4.7 were 1.29 for $\dot{x}$ negative and 1.29 for $\dot{x}$ positive, in Figure 4.8 they were 1.05 and 1.05 respectively, and in Figure 4.9 they were 0.86 and 1.15 respectively. The measured data in both cases in which the bolt torque was 30 ft pounds provided a severe test of the method. The high frequency components noted in Figure 4.5, Appendix V, are of approximately 150 cps, above the natural frequency of the recording galvanometers. It should be noted that no velocity-dependent terms are included in any of the plotted G functions.

To see how these dynamically determined restoring functions compared with static restoring functions, the structure was forced through static loops by mounting the force gage on the opposite side of the buttress and attaching to it a long rod on which was threaded a collar seated in a yoke. The end of the rod and the frame on which the yoke was mounted are seen at the left of the structure in Figure 4.3, Appendix V. By turning the collar with a wrench the structure could be displaced in either direction, the force passing through the force gage. Deflections were measured with a dial indicator.

To obtain the static loop in Figure 4.7 the structure was simply forced to the desired displacement from its rest position and then one loop was obtained. Before the static loops in Figures 4.8 and 4.9 were recorded, the structure was forced through several cycles in an

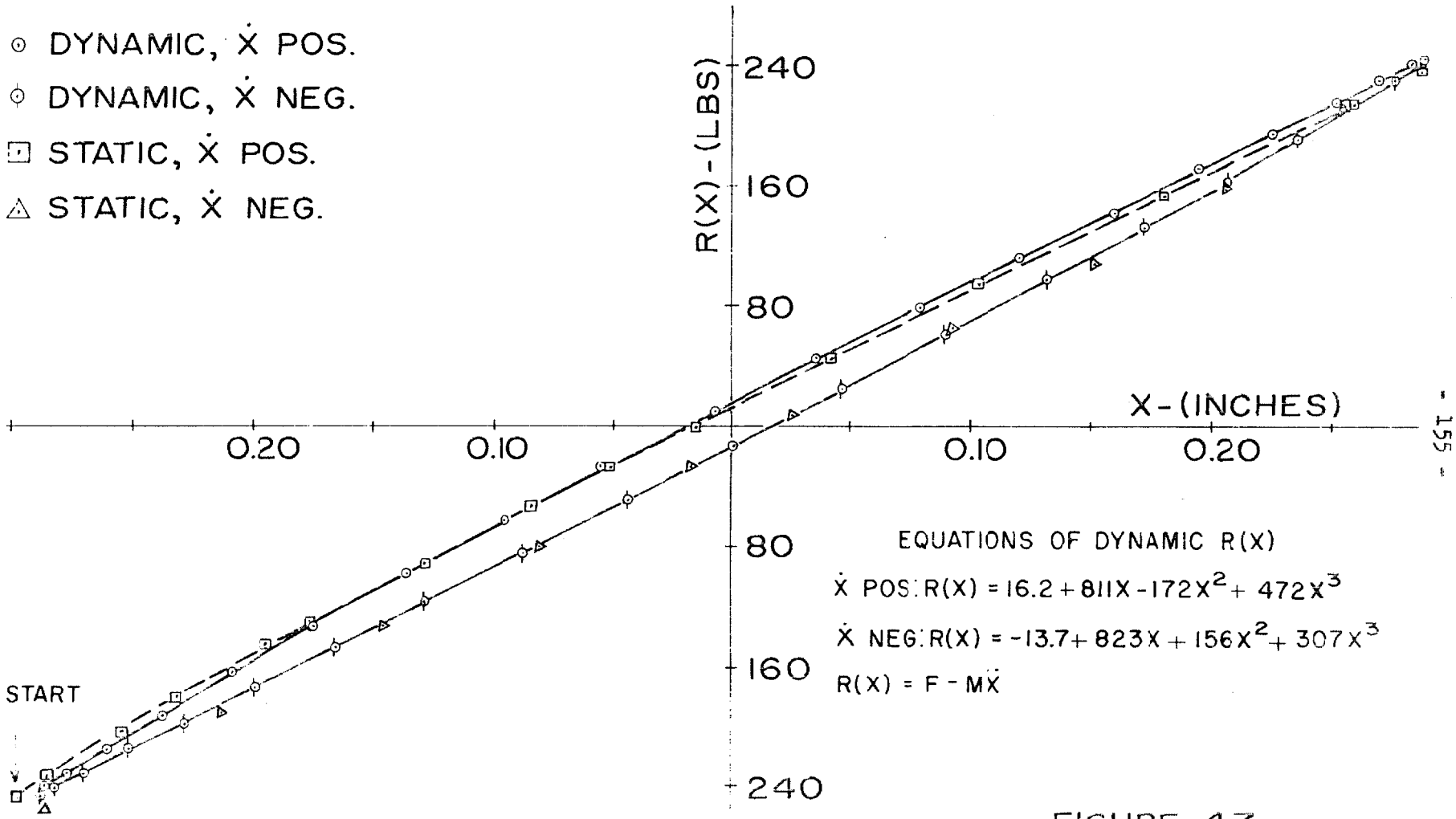

FIGURE 4.7
DYNAMIC AND STATIC
RESTORING FUNCTIONS

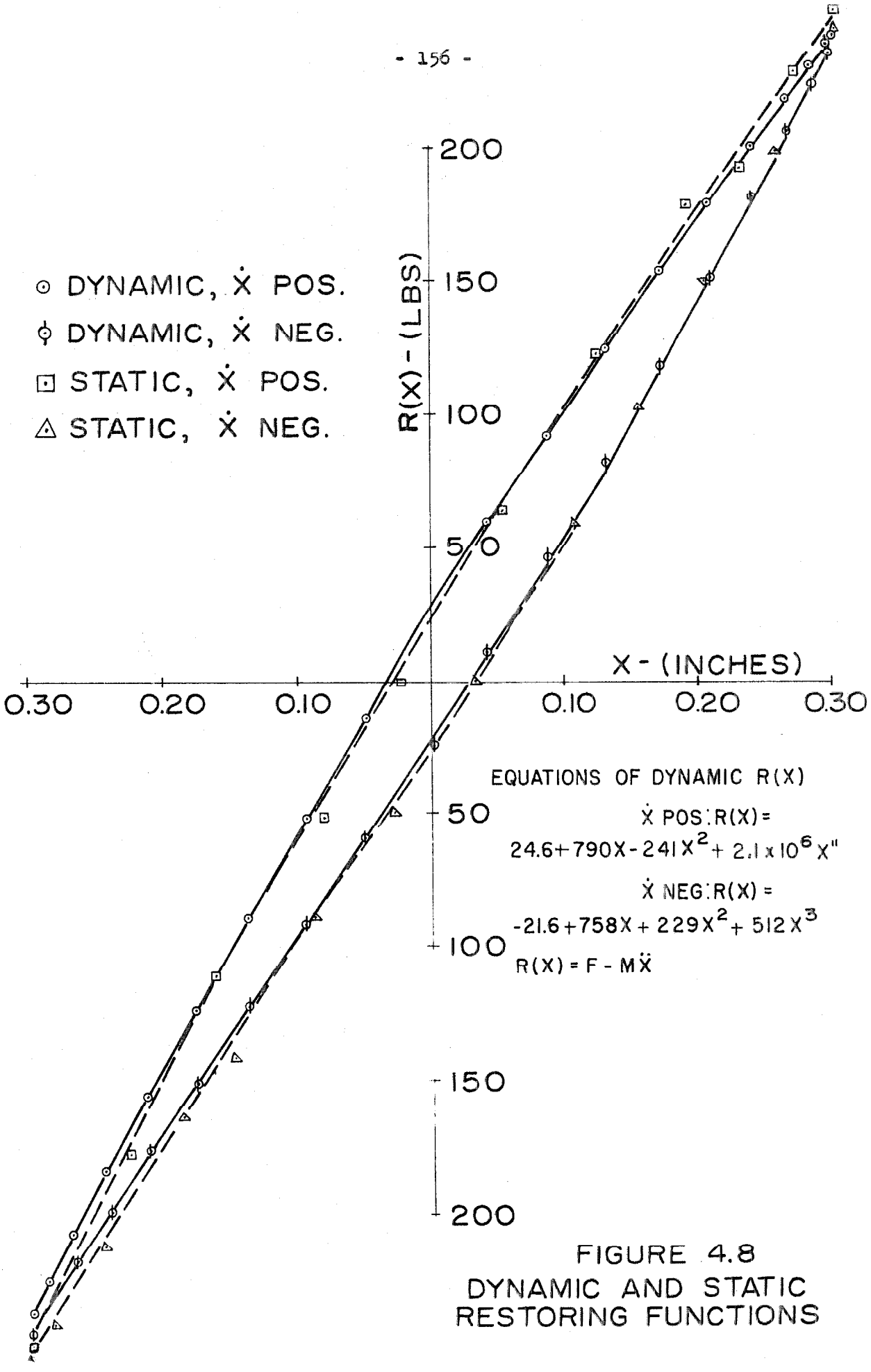

FIGURE 4.8
DYNAMIC AND STATIC
RESTORING FUNCTIONS

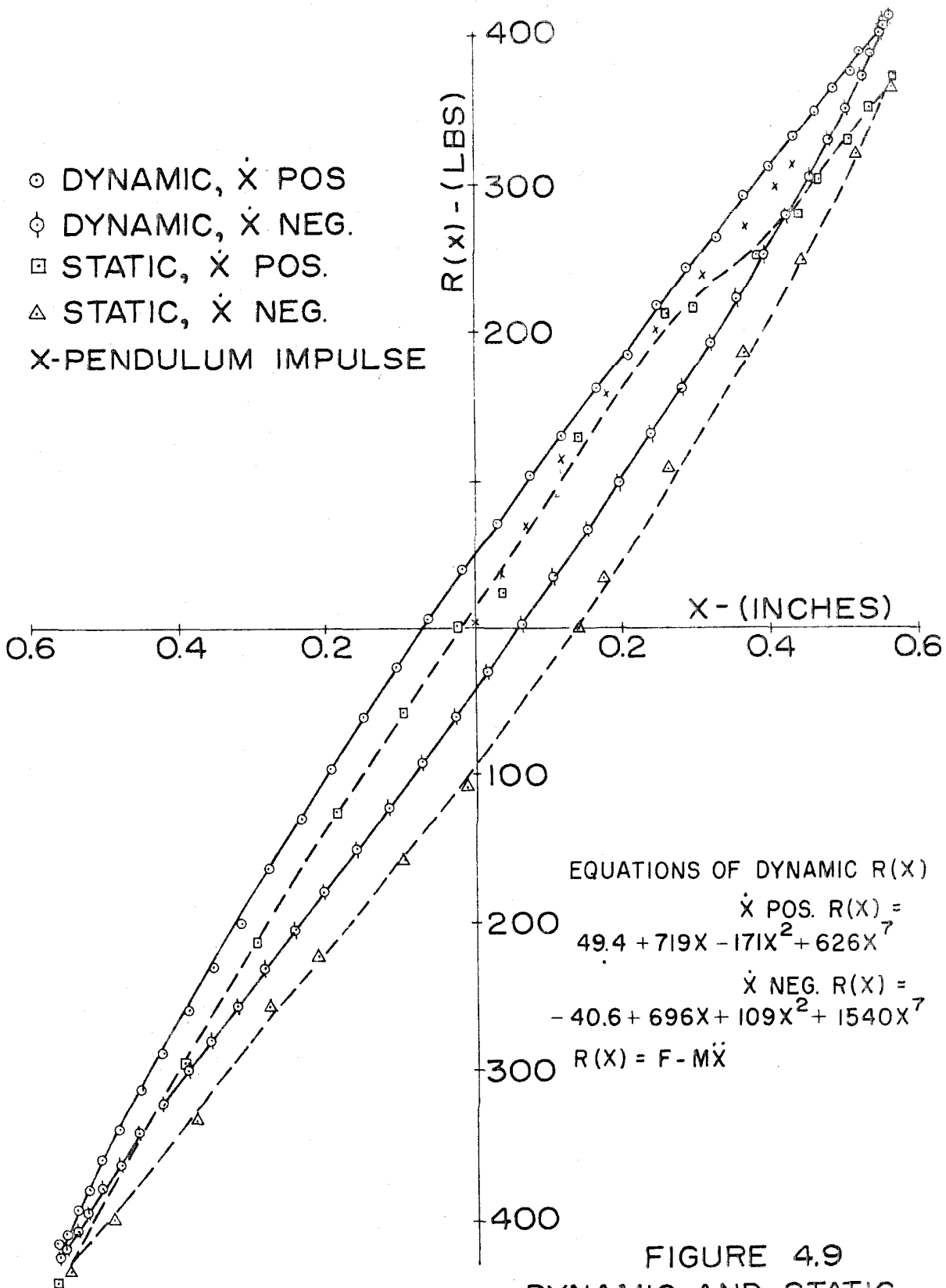

FIGURE 4.9
DYNAMIC AND STATIC
RESTORING FUNCTIONS

attempt to get a loop which would close. Unfortunately the L.V.D.T. was not monitored over the static loops, so it is not known if the static displacements represent the same absolute displacements experienced by the structure during the forced vibration. The extremes of dynamic displacements always appeared fairly well centered on the rest position of the structure.

The static forces transmitted by the force gage were much larger than the dynamic forces transmitted over a loop of the same amplitude. In Figure 4.9 for instance, the maximum static force was 440 pounds, but the maximum dynamic force measured by the force gage in the same loop was only 120 pounds. It was observed that after high static loads the trace of force would not return to zero under zero force. The quadrants of the static loops in Figures 4.8 and 4.9 were adjusted to allow for this, and hence the loops do not quite close at the tips.

Fair agreement between the static and dynamic loops is noted in all the cases. The lateral positioning of the dynamic loop was arbitrary, so the agreement in Figure 4.9 can be made better than appears at first glance. The downward displacement of the static loop suggests that this loop was not centered about the same point, in absolute coordinates, as the dynamic loop. Although the data are not spaced closely enough to accurately describe the phenomenon, several sudden jumps in the force took place during each cycle of static loading, particularly noticeable under increasing load. The jumps were signalled by an audible creak from the structure, followed by a small rapidly decaying vibration, after which the force level was found to have suddenly changed. The static curves are thus not smooth, but have a sawtooth appearance. No attempt was made to accurately locate the positions of the jumps in a cycle,

but some of them were noted to reappear on a second cycle at points close to their appearance in a previous cycle. Whether these jumps occurred in the dynamic case is not known. The high frequency components in the records made with bolt torque at 30 foot-pounds suggest the jumps took place, but at 70 foot-pounds torque at least two jumps were observed in the static loop, yet the acceleration record, Figure 4.6, is quite smooth.

Test with the Pendulum

Dynamic excitation of the structure with one pulse, provided by the pendulum, was intended to illustrate what could be learned on a larger structure excited by a measured rocket blast. Scruton and Harding applied such a blast to a tall chimney, exciting its first mode.(6)

A pulse record is shown in Figure 4.10, Appendix V. The bolt torque in this case was 30 foot-pounds and it will be noted that high frequency components are present in the acceleration. Velocity and displacement were determined by integrating the acceleration from rest. Using all the data from rest to very close to the point of reversal of velocity, at 0.43" displacement, the best computed value of the mass was 1.22 pound-sec^2/in., accompanied by the restoring function

$$G = 2.8 + 1037x - 948\,x^2 + 1.42 + 10^4x^7.$$

This function is plotted by crosses in Figure 4.9. It will be noted that K_1 is considerably higher than the value which was found from the steady state data. Whether this increase is the result of experimental error or if it actually occurs is not known. No static run was made from the same starting conditions.

Summary and Conclusions

A technique has been proposed for determining the masses and the restoring and dissipating functions of lumped-mass structures. The technique is based on the solution of many simultaneous equations of dynamic equilibrium of the masses, the form of the restoring and dissipating functions being assumed. Preliminary considerations suggest that the technique is applicable to linear structures, nonlinear non-hysteretic structures, and hysteretic structures of the shear type, in which a spring force is not transmitted beyond the masses contacting the spring. In the latter case the proposed technique does not find a general expression for the restoring function.

Experiments on a bolted joint single-mass structure with reasonably good instrumentation indicate that practically the method does not work as the theory indicates. If terms not related to the phenomenon are included in the assumed restoring function, the accuracy of the computed mass is decreased. It is suggested that the known value of the mass be used as a criterion for judging the form of the restoring function.

Experimentally measured static hysteresis loops showed fair agreement with loops determined from dynamic measurements by the method described. The static hysteresis loops of the bolted structure were found to be of a sawtooth form due to bolt slippage.

The work presented here points out the need for a study with hypothetical data to indicate the effects of systematic errors in the data, to indicate the precision necessary in the data if the method is applied to multiple-mass systems with far reaching coupling among the masses, and to develop a relationship between the required precision of data and the spacing of the record cuts.

It is hoped that in additon to presenting new possibilities for experimental analysis, the introduction of this method will result in more vigorous efforts toward improving the instruments used in structural dynamic work.

APPENDIX I

INSTRUMENTATION FOR STRUCTURAL VIBRATIONS

Introduction

The measurement of structural vibrations for the purpose of determining the dynamic characteristics of structures presents a challenging problem from the standpoint of instrumentation. An instrumentation system suitable for a wide range of structures should be capable of obtaining, from widely separated points on a structure, simultaneous time records of motions with amplitudes varying from below 0.0001 inch to above 0.50 inch, at frequencies ranging from below 0.5 cps to above 10 cps. In most cases these measurements must be made from the structure itself, without the aid of a stationary reference platform. In addition, any phase lag should be small or should be accurately known, and the system should be portable, rugged, and versatile in order to meet a wide range of field conditions. In aggregate, these requirements form a severe specification for the instrumentation components which are available today.

In the paragraphs which follow a specification is presented for an instrumentation system which would be ideal for recording any phenomenon. Then, using this specification as a guide, a specification is written for instrumentation to be used for recording vibrations of structures. Following this are the results of tests on a system composed of certain commercially available components, and the performance of the system is evaluated in the light of the specification. Finally, the characteristics of a number of other components are discussed.

It should be noted in connection with the discussion of particular instruments, that it is not implied that complete tests were made to establish the overall quality of the equipment. In some cases the instruments were used in a way different from that intended by the manufacturer, and the equipment was perhaps not always operating at its optimum level of performance. In a number of cases manufacturers not mentioned produce equipment of similar characteristics.

The prices given for the equipment represent the prices which were in effect in 1962, taken chiefly from manufacturers' catalogs. This information is presented not for the purpose of comparing one manufacturer's product against another, but rather as an aid in preparing preliminary cost estimates.

Properties of an Ideal Instrumentation System

In order to prepare a specification for an instrumentation system to record structural vibrations, it is worthwhile to consider the properties desirable in a system which would be ideal for recording any dynamic phenomenon. These properties will then serve as an outline for enumerating the specific properties desirable in the instrumentation system for structural vibrations.

An ideal system for measuring and recording any dynamic phenomenon should have the following properties:

1. The system should record instantaneously, at a suitable scale, the value of the measured quantity, with a constant ratio between the amplitude of the recording and the value of the measured quantity. This means that in the case of a sinusoidal variation there should be no phase lag in the record and that the calibration constant should be independent

of the frequency and the amplitude of the measured quantity.

2. The system should give exactly zero record for zero occurrence of the measured quantity; that is, there should be no noise, no drift, no stray pickup, no cross-axis sensitivity, and no crosstalk among the channels.

3. The system should permit easy and accurate calibration.

4. The system should provide accurate and closely spaced timing indications and should allow the simultaneous recording of several signals to fix the time relationships among them.

5. The system should maintain these characteristics over a wide range of environmental conditions, and the characteristics should not change with the age of the system.

6. The system should be sufficiently rugged to withstand the mechanical and electrical overloads encountered in service.

7. The system should produce a permanent record immediately visible, capable of being reproduced, and able to withstand the mechanical treatment and the environmental conditions encountered in reducing the data.

8. The system should be portable, versatile, easy to operate, and not excessively costly.

No instrumentation system, of course, can possess in full measure all the above properties. Compromises always must be made on the bases of cost, the range of the variable to be measured, the accuracy desired, operating conditions, and the existing state of instrumentation technology.

Specifications for an Instrumentation System for Structural Vibrations

Using the properties of the ideal instrumentation system as a guide, specifications for a system to measure and record structural vibrations

are now presented. The system is not all inclusive, but it is intended to be useful for a wide range of structures. The values given below specify the record quality desirable for conducting an analysis of the dynamic behavior of the structure, and they specify characteristics desirable for a practical instrumentation system to be used in the field. To some extent the specifications are based on the capabilities of present day instruments, although in most cases the performance required is considerably better than is commercially available today. As techniques in structural vibration work improve and as increasing knowledge of structural dynamic behavior requires more precise information, some of the requirements given below will undoubtedly be made more severe. It is assumed that the motion is sinusoidal and that the recording is a trace suitable for visual analysis.

1. (a) Phase lag over the range 0.5 - 10 cps should be known within 1°, and preferably should not exceed 1°. For comparison, this is the phase shift caused by a measuring error of 0.01 inch on the abscissa of a sine wave having a 3.6 inch period. A counter-rotating force producing machine, with ordinary installation efforts, should produce a sine wave within 2° of the presumed alignment.

(b) Over the frequency range 0.5 - 10 cps the system should produce a record magnifying displacement at least 500 times, or yield a trace amplitude of at least 3 inches per 0.001g acceleration, whichever requirement is more severe.

(c) For the worst combination of frequency in the range 0.5 - 10 cps, amplitude of motion in the range 0 - 0.5 inch, and scale of recording in the range 0 - 3 inch amplitude, a sinusoidal motion representing an acceleration in the 0 - 0.5g range should be recorded

with an error in instantaneous trace position of not more than 1% of the trace amplitude.

2. The portion of the record representing anything except the motion being measured should be not greater than 1% of the amplitude of the recording for record amplitudes greater than 1 inch.

3. The system should be able to be calibrated in the field with a calibration signal in the range of the signals being measured, and it should be repeatable to within 1%.

4. Timing indications should occur at rates up to 1000 per sec. with an error of not more than 1% of the interval. The record drive should provide speeds up to 60 inches per second and over any record length of 1/16 inch, the speed should vary from the set rate by not more than 1%. The system should be able to record simultaneous motions occurring at as many as 18 points, with as much as 1000 ft. between the most widely separated points.

5. Detectable changes in the performance of the system should not occur due to: air temperatures in the range 32°F - 110°F, humidity, strong sunlight, 60 mph wind (with reasonable precautions taken), altitude from 0 to 10,000 ft., $\frac{1}{2}$ g ambient acceleration at frequencies above 10 cps and 1/10 g ambient acceleration at any frequency, or location of 60 cps power lines carrying 30 amps within 3 feet of any portion of the system.

6. All components of the system should be able to withstand a 5 g step loading without damage. The equipment should operate properly on line voltages between 105 - 125v and not be damaged by voltages in the range 95 - 130 v.

7. The record should be visible as soon as it is made and should

not be reduced in quality by natural or artificial light, humidity, or age. The record should allow easy, economical reproduction.

8. (a) The units sensing the motion should be light and small in size so that they can be easily carried to and affixed to almost any place in a structure.

(b) The system should be capable of measuring separately rectilinear motions occuring in any direction, and angular motions occurring in any plane. With reasonable precautions underwater measurements should be possible.

(c) The system should require no special mechanical skills or extensive training on the part of the operator.

(d) The cost of the system should not exceed $2000 per channel for 6 or more channels.

The specification presented is seen to be severe. It is hoped, however, that these performance requirements will be accepted as a temporary goal toward which structural vibration instrumentation will proceed.

The Choice of Transducer

To obtain the most complete data for the determination of structural dynamic characteristics it is necessary to make simultaneous time records of the displacements, velocities, and accelerations of all the points of interest on a structure when it is under the influence of some known external forcing function of time, which may be zero. If only one of these quantities is measured, theoretically the other two can be derived from it, and the number of sensing and recording channels can be reduced by two-thirds. Characteristics of the different types of transducers and problems of treating the data determine which of the quantities is the

most suitably measured for a particular structural test.

If only displacement is measured, velocity and acceleration must be derived by differentiation, but in practice the resulting errors in the second derivative make the method impractical.[52] Where the motion is purely harmonic, double differentiation of the record need not be performed, but unless an apparently sinusoidal trace is accurately determined to be sinusoidal, the second derivative cannot be assumed as simply a multiple of the original trace. A good example of this is shown in Figure A1.1, in which the sinusoidal-appearing displacement is actually associated with square-wave acceleration. For a seismic-type displacement transducer to record with an amplitude error of less than 2%, its natural frequency must be not greater than approximately 40% of the frequency being measured, meaning an extremely delicate, if not impractical, instrument for sensing structural vibrations at 0.5 cps. In a list of 14 low frequency transducers, the lowest natural frequency appearing is 1 cps, indicating variable sensitivity around and below this frequency as well as large variations in phase lag.[53] These facts, in addition to the bulk and weight of displacement transducers, the difficulty of field calibration, and the inability of one transducer to measure both horizontal and vertical motions, make displacement measurement optimum only in those instances in which amplitudes and frequencies are so low that the large signal from the displacement transducer is a necessity.

If only velocity is measured, one differentiation of the velocity record might produce an acceleration record of acceptable accuracy. However, for a seismic-type velocity transducer to accurately measure velocity, the dynamic characteristics of the instrument must be the same

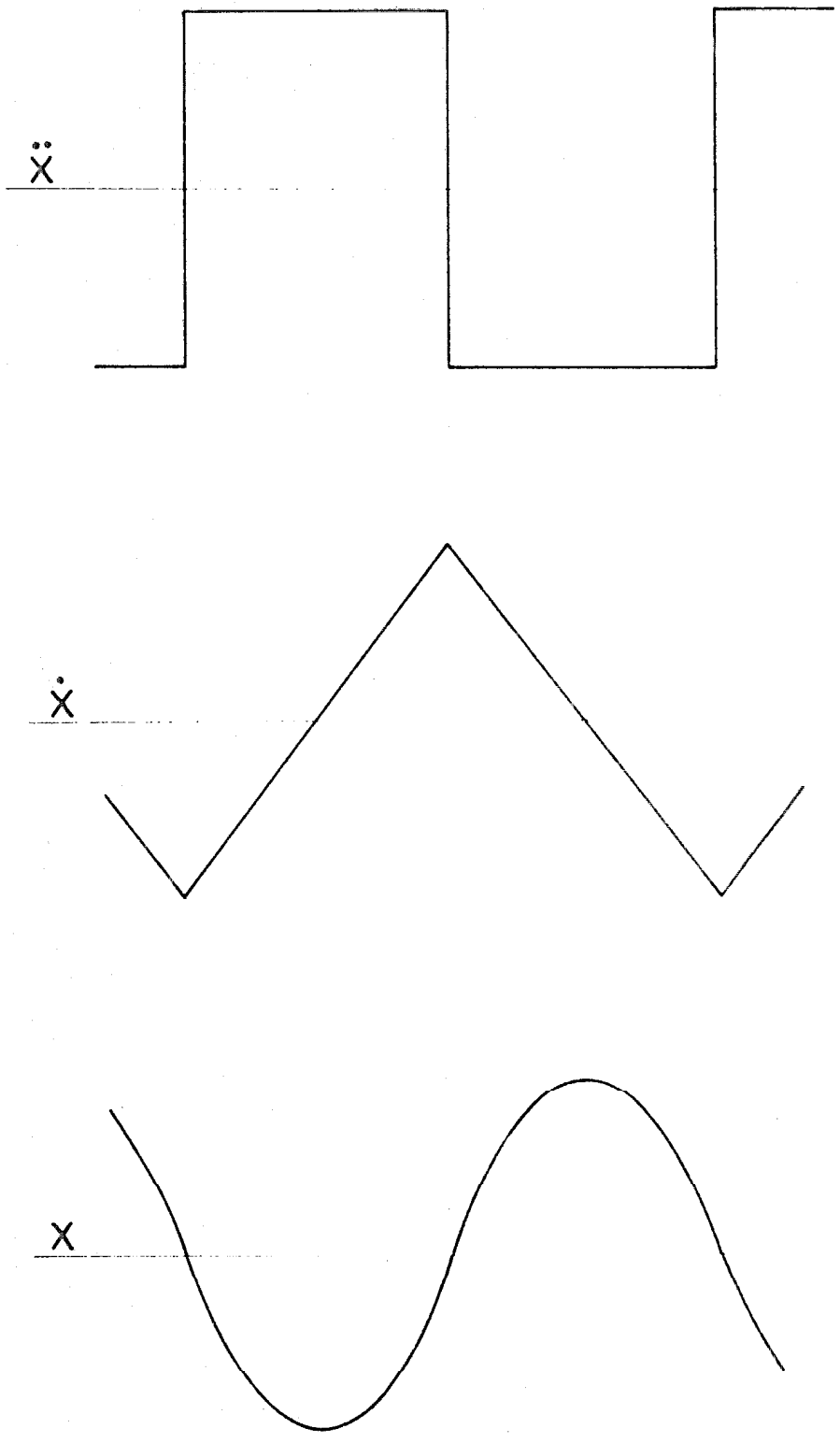

FIGURE A1.1
DOUBLE INTEGRATION OF A SQUARE WAVE

as those of a displacement transducer. Hence velocity measurement does not appear to be ideal for the frequencies and field conditions encountered in structural testing.

If only acceleration is measured, velocity and displacement must be obtained by integration, a process inherently more accurate than differentiation. It is shown in Appendix II that numerical double integration of a sinusoidal record can easily produce results accurate to within a fraction of 1% of the amplitude. Moreover, the acceleration transducer is a small, fairly rugged instrument that exhibits good linearity and small phase lag at frequencies well below its own, and, if it is of large enough range, it is easily field calibrated and one transducer can be used for both vertical and horizontal measurements. The chief disadvantage of the accelerometer is that the relative motion of its seismic mass to its case is small, meaning that extremely large amplification is required to actuate a recording device. Reasonably good electronic amplifiers as well as very sensitive and versatile recording devices are available, however, so that a very wide range of structural motions, from those caused by a gentle wind to those large enough to cause structural damage, can be successfully measured with one accelerometer.

Characteristics of an Instrumentation System

An instrumentation system for structural dynamic testing was put together from commercially available components and was subjected to laboratory and field tests. The tests were by no means exhaustive, and only one particular sample of each component was tested, and the results should be viewed with this fact in mind. The capabilities of this

system will be discussed according to the outline given previously, and following this, the characteristics of a number of other components will be presented.

The system tested consisted of the following:

1. Statham A5-2-350 accelerometer. This instrument consists essentially of a seismic mass supported within its case by wires forming a 4-arm unbonded Wheatstone bridge of 350 ohms bridge resistance. The manufacturer states the instrument has a natural frequency of 100 cps, 0.7 critical fluid damping at room temperature, yields 17 mv/g output at 9 volts bridge excitation, has transverse sensitivity of less than 2%, and weighs 4 oz. The price is $300 each.

2. Belden 8424 cable. This cable consists of 4 wires of AWG No. 20 and a shield in a neoprene jacket. Capacitance between wires is 55 mmf per ft., and capacitance between one wire and all the other wires tied to the shield is 95 mmf per ft. The price is approximately 10¢ per ft. The cable terminated in Cannon XLR-4 connectors, 4 pin connectors with a snap lock. The price per pair of connectors is approximately $4.00.

3. Brush RD 5612-11 carrier amplifier. This unit consists of a voltage source of approximately 3.6 volts r.m.s. at 2000 cps to excite the accelerometer's bridge, a graduated attenuator in steps from 1 to 1000 to limit the size of the incoming signal from the bridge, and an A.C. amplifier, a demodulator, and a D.C. amplifier in that order to produce a maximum output of 20 ma into a 1500 ohm load. The weight is 23 pounds and the price is $825 per channel.

4. Consolidated Electrodynamics model 5-124 direct writing oscillograph. The particular unit used was an engineering model, built before

production had started, but similar in major respects to the production model. The unit consists of a bank of miniature galvanometers holding mirrors which deflect a beam of ultraviolet light onto light-sensitive paper, producing a visible trace in a few seconds if ambient light conditions are proper. The oscillograph is capable of recording up to 18 traces simultaneously on 7-inch wide paper, with paper speeds up to 64 inches per second. The galvanometers used were Consolidated Electrodynamics number 7-341, with a natural frequency of 100 cps, sensitivity of 6.12 μ a/in. at 11 inch optical arm, terminal resistance of 47 ohms, 350 ohms damping resistance required. The oscillograph weighs 40 pounds and the price is approximately $3030 if provided with timing and grid lines flashed on the paper and a trace interrupter to aid in identifying traces. The 7-341 galvanometers are $180 each, and in general there is needed with each galvanometer a damping resistor mounting shell costing $8.25 each. The oscillograph paper, Du Pont Lino-Writ, Type W, costs approximately 10 cents/foot.

The capabilities of the system are now presented according to the outline given previously.

1. (a) Phase lag of the system at 10 cps can be known to within 4° by exciting the accelerometer on an electrodynamic shaking machine which produces a clean sinusoidal acceleration at this frequency, and comparing the trace with that produced by a very high frequency system subjected to the same excitation. Using as a standard an Endevco 2215 piezoelectric accelerometer driving a C.E.C. 7-005 galvanometer of 3400 cps natural frequency through an Endevco model 2702 amplifier, phase lag of the accelerometer-amplifier combination was checked at several

frequencies, the results appearing in Table A1.1. The high frequency capabilities of the Endevco system were presumed to result in zero phase lag, so the observed lag represents the true lag of the Statham-Brush system. The crystal accelerometer and the accelerometer under test were mounted with their cases almost touching each other on a 1-1/4 inch thick aluminum block held away from the magnetic field of the shaker by a yellow pine 4 x 4 post, 11 inches long. Acceleration amplitudes of approximately 1 g were used in order to get sufficient signal from the Endevco system.

The data show that in the 15 - 30 cps frequency range phase lags can be determined consistently to within 5°, but in this instance the accuracy is in doubt below 30 cps due to the poor waveform produced by the shaker, an MB model S3B. Below 30 cps the acceleration traces showed pointed peaks and were not perfectly symmetrical, the amount of distortion varying from test to test. This is a possible explanation for the erratic behavior of the amplitude ratios, although two of the crystal accelerometers which were used as standards, when tested side by side over the 15 - 100 cps frequency range, showed amplitude ratios differing by 5% from those shown by the manufacturer's calibrations.

Accurate phase lag determinations were made difficult by the erratic paper speed in the oscillograph. In the 1/4 inch peak-to-peak distances on the oscillogram of a signal from a Hewlett-Packard model 202 C oscillator, spacing variations up to 8% were noted. In obtaining the data for Table A1.1, typical linear measurements between the peaks on the oscillograms were 0.08 inch. To obtain consistent results it was necessary to average five or so measurements made on both the top and the bottom of the record with a scale divided into 50 parts per inch,

Temp.	cps	Observed Lag	Lag of Standard	Amplitude Ratio Brush ÷ Endevco		
80°F-83°F	15	31.4°	---	1.00		
" "		32.3°	---	"		System Tested
" "		31.6°	---	"		Statham A5-2-350 accelerometer
" "		32.1°	---	"		Brush RD5612-11 carrier amplifier
130°F		27.0°	---	"		C.E.C. 7-005 galvanometer
						Pen Compensation off.
80°F-83°F	20	41.0°	---	1.02		
" "		46.1°	---	0.97		Standard
" "		42.9°	---	0.92		Endevco 2215 accelerometer
" "		43.0°	---	0.97		Endevco 2202 amplifier
130°F		43.7°	---	0.99		C.E.C. 7-005 galvanometer
80°F-83°F	30	55.3°	---	0.96		
" "		53.1°	---	0.91		
" "		52.1°	---	0.92		
" "		56.6°	---	0.93		
130°F		49.6°	---	0.96		
76°F	15	22°	---	1.00	Pen Comp.	
	20	32°	---	0.97	off	System Tested
	30	40.5°	---	0.92		Statham A5A-200-220 accelerometer
	50	63°	---	0.75		Brush RD5612-11 carrier amplifier
						C.E.C. 7-005 galvanometer
	15	9°	---	1.00	Pen Comp.	
	20	17.5°	---	1.002	Against Left	Standard
	50	32°	---	0.943	Stop, But Not Off	Same as above

TABLE A1.1

PHASE LAGS OF MEASURING SYSTEMS

estimating to tenths of the scale divisions.

Electromagnetic damping in the C.E.C. 7-341 galvanometer was adjusted to 0.63 critical by measuring the overshoot due to a step function. A check of this value was made by measuring the phase lag of the galvanometer trace when it was excited, along with a 7-005 galvanometer, by an H.P. 202C oscillator. At 15 and 30 cps the measured values checked within 1/2° those calculated on the basis of 0.63 critical damping. The value of resistance used to obtain this damping would result in 0.79 critical damping according to the manufacturer's data, illustrating the necessity of determining phase lag of a system by actually conducting tests.

The pen compensation control on the Brush amplifier has a great effect on the phase lag and frequency response of the amplifier. When the control is switched off, the D.C. section of the amplifier is reasonably flat to at least 1000 cps, but the amplifier as a whole shows an amplitude droop of approximately 25% and a phase lag of almost 60° at 50 cps. This information was obtained by using a Statham A5A-200-220 accelerometer of approximately 1000 cps natural frequency as a transducer with the Brush amplifier, and recording both this trace and the trace from the crystal accelerometer on C.E.C. 7-005 galvanometers. The results of this test, shown in Table A1.1, indicate that viscous damping in the Statham A5-2-350 varies from approximately 0.45 critical at 30 cps to 0.65 critical at 15 cps. A change of 6° in either of the phase lag determinations at 30 cps would change the apparent damping to 0.61 critical.

The test also disclosed that the output from the Hewlett-Packard

2020 oscillator at a given frequency and output setting can vary by as much as 5%, depending on the settings of the decade knob and the graduated frequency dial. With the Brush pen control turned against its lower stop, but not off, the amplifier as a whole showed a 6% droop and a 32° phase lag at 50 cps. The load on the Brush amplifier for all the tests varied between 3K and 10K ohms resistance.

The effect of temperature on the damping ratio of fluid damped accelerometers has been reported by G.E. White.(54) The temperature sensitivity of the Statham A5-2-350 accelerometer was investigated by mounting a cardboard box over the head of the shaking machine and heating the enclosed space with a hair dryer. The changes in characteristics due to heating to 130°F, shown in Table A1.1, are seen to be small. At the elevated temperature the zero of the trace from the crystal accelerometer shifted rapidly, probably the result of temperature fluctuations, described in Reference 55.

(b) At 0.5 cps the system being tested multiplied displacement by 50 times, the magnification increasing as the square of the frequency above this frequency. An acceleration of 0.001 g was recorded with an amplitude of 2.0 inches with a rough cps noise level of 0.06 inch peak-to-peak. These sensitivities were obtained by boosting the level of the carrier voltage to 6.3 v by connecting to a different tap on the transformer at the oscillator output.

(c) Error in trace amplitude due to frequency response of the system can probably be made less than 1% of the amplitude in the 0.5 - 10 cps range. Dynamic measurements with the pen compensation control against its stop, but not off, showed no drop in amplitude between

15 and 30 cps. No dynamic measurements were made below 15 cps, nor were measurements relating static calibration to dynamic calibration made. Static tests of the linearity of the system were conducted with a protractor table and with a sine bar. The protractor table is illustrated in Figure 3.3, Appendix V. The sine bar consisted of a pair of knife edges held $62\frac{1}{2}$" apart by a piece of $1\frac{1}{4}$" pipe so that a 1/16" shim placed under one end produced a 0.001 g signal on an accelerometer attached to the bar with its sensitive axis horizontal. The protractor table was found to be faster and more convenient for laboratory tests than the sine bar. Some measurements made with the protractor table are shown in Table A1.2. These measurements were made by plumbing the accelerometer and then swinging the table about a horizontal axis, making readings at equal angular deflections on each side of the vertical. The errors shown in Table A1.2 include the effects of the graduation and setting of the protractor table, reading the record, drift due to temperature and other causes, and the linearity and freedom from hysteresis of the entire system. As mentioned in Appendix IV, the relatively large errors at small angle settings are probably in large part due to positioning errors. From this static test data it can be concluded that the reliability of low frequency amplitudes is not better than $\pm$ 4% for amplitudes above 0.001 g. The calibration equipment was not sufficiently sensitive to accurately calibrate the system at levels below 0.001 g.

2. The measurement of electrical noise in the system, that is response other than that due to mechanical oscillation of the transducer, is difficult at high gain settings due to the almost inevitable

	θ	1-cos θ	Galvo. Zero Offset	Gain Setting	Trace Defl (1/50")	% Error
(a)	90°	1.000	4"	X1000	105.3	Standard
	180°	2.000	"	X1000	204.0	-2%
	1°	0.000152	"	X5	3.4	+7%
	1°	0.000152	"	X5	3.1	-3%
	2°	0.000609	"	X5	13.5	+5%
	4°	0.00244	"	X5	53.4	+4%
	7°	0.00745	"	X5	159.1	+1%
	9°	0.0123	"	X5	252.0	-3%
	9°	0.0123	"	X10	130.9	+1%
	2°	0.000609	"	X2	33.9	+6%
(b)	90°	1.000	2-3/4"	X1000	103.0	Standard
	90°	1.000	"	X500	200.0	-3%
	45°	0.293	"	X500	60.1	-0.4%
	20°	0.0603	"	X100	61.7	-1%
	20°	0.0603	"	X50	122.4	-1%
	15°	0.0341	"	X20	172.2	-2%
	5°	0.00381	"	X2	202.6	+3%

Statham A5-2-350 accelerometer
Brush RD5612-11 amplifier
C.E.C. 5-124 oscillograph
C.E.C. 7-341 galvanometer

TABLE A1.2

RESPONSE OF A MEASURING SYSTEM TO STATIC ACCELERATIONS

presence of some mechanical excitation. The best method seems to be to replace the sensitive transducer by another which has the same electrical characteristics, but which is less sensitive mechanically. The noise level of 0.06 inch peak-to-peak reported in paragraph 1 (b) was measured at maximum gain, with the Statham A5A-200-220 mounted on a five pound steel block resting on foam rubber, replacing the Statham A5-2-350, the former having a bridge resistance of 220 ohms and thus not exactly duplicating the A5-2-350. In several tests for noise at different locations about the city, the noise level was found to depend on whether the accelerometer cable shield was floating or tied to ground or to one of the bridge terminals, whether the amplifier was grounded, or whether the amplifier ground was tied to the accelerometer case. No set of circumstances was consistently best. A necessary procedure to combat 60 cps noise seems to be to reduce it by trial and error at the time and place the record is to be made. A discussion of noise control is given in Reference 56. No output could be noted by rapidly manually flexing the accelerometer cable or by shouting close to the amplifier. At full gain, breathing on the accelerometer produced very large drift. When the amplifier was within a foot of the oscillograph, pickup from the timing system was noted.

To investigate cross-axis sensitivity, the accelerometer was bolted to the MB shaker so that its sensitive axis was at approximately 90° to the shaker motion, and then shims were placed under the edges of the accelerometer by trial and error until minimum response was found. The minimum that could be obtained was 4% of the axial motion, but the size of the transverse component of the shaker motion was not known. A

static investigation was conducted by plumbing the accelerometer case with a sensitive level and noting the difference in the trace deflection for equal angular deflections on each side of the plumb line. Two A5-2-350 accelerometers showed internal misalignments of 1/3° and 3/4°. The significance of this misalignment is illustrated by the problem of attempting to measure a vertical motion in the presence of a horizontal motion ten times as great. A misalignment of 1° results in an unwanted signal amounting to 17% of the signal being measured. A suggestion for the solution to this problem is shown in Appendix III.

3. The system allows easily repeatable field calibration by simply reversing the accelerometer about a horizontal axis. A small level guarantees good orientation. If an accelerometer of less than 1 g range is used, a sine bar or protractor of some sort must be used for field calibration. The alternative to this is to calibrate in a laboratory by rotating the accelerometer through an angle in the earth's field and then to obtain a reference signal at this amplifier gain by shunting a resistor across one leg of the bridge, the latter procedure then being repeated in the field to measure sensitivity. The uncertainties of field measurements are such that direct field calibration is always preferable.

4. Timing lines in the oscillograph occur at rates up to 100 per sec., the accuracy of the interval depending on the temperature of the circuitry. Using as a reference a General Radio Company vacuum-tube fork of 1000 cps frequency and rated after warmup at 0.05% accuracy, the timing intervals were found to be long by 1.1% after a six minute warmup and short by 3.3% after one hour warmup. Very slight variations

of the timing indications with respect to the 1000 cps signal were noticeable, 0.0002 sec. or so, possibly due to the fact that the paper speed is variable and the timing lines are not focused on the paper at the same point as the galvanometer traces. The oscillograph holds 18 galvanometers, but practical experience indicates that without a trace identifying feature, four is a reasonable maximum number of traces to record if amplitudes are two inches or so. The system balanced satisfactorily with 460 feet of accelerometer cable, sensitivity being reduced about 10%. Balancing with long cable runs was possible only when the wires carrying the bridge input and the bridge output were arranged symmetrically within the cable.

5. The performance of the system throughout the environmental range specified has not been tested. The effects of temperature on the accelerometer have been noted in paragraphs 1 (a) and 2. The galvanometer specifications indicate satisfactory performance under $\frac{1}{2}$ g ambient acceleration, but the effects of base accelerations on the amplifier are not known. Power cables carrying 10 amps have been touched to all components without noticeable effect. The XLR-4 connectors showed deterioration with use. Cannon WK-5-21C and WK-5-22C costing $5.65 per pair appear to be an improvement.

6. The accelerometer is rated by the manufacturer for 6 g maximum acceleration. Two A5-2-350 accelerometers, used for about 20 days of field testing of structures, were transported in an automobile about 75 miles each day and were moved about considerably in the structures without suffering damage. The oscillograph underwent the same service without damage. Shock resistance of the amplifier is not known. Tests

of the equipment on line voltages between 105V and 125V showed no changes in sensitivity. No tests were made with voltages outside these limits or with other than 60 cps line frequency. The output circuit used was such that the amplifier overloaded at approximately 6½ inches trace deflection and thus could not overdrive the galvanometers.

7. Oscillograph records made outdoors and shielded from direct sunlight by two layers of amber colored plastic were usually visible within five to ten seconds and were of satisfactory quality for examination. These records were examined indoors under fluorescent lighting for approximately an hour and were then stored in lightproof boxes for as long as 12 months with no appreciable deterioration in quality. Records made under these outdoor conditions photographed only moderately well and were poorly reproduced on a Xerox copying machine. The records could be fixed with Du Pont 71-D Direct Writing Paper Developer, but the fixing decreased the contrast. For good reproduction of records, better shielding is needed outdoors. Prolonged exposure to indoor lighting and very short exposure to sunlight will destroy records which have not been fixed.

8. (a) In field testing, the accelerometers could be easily mounted to any surface by bolting them to aluminum mounting blocks which were held to the mounting surface by Epoxylite Corporation No. 204 adhesive, an epoxy resin which hardens in 60 to 90 seconds at room temperature. Figure 2.14, Appendix V, shows a portable mounting block which was simply carried from place to place and set down on horizontal surfaces without adhesive, the motion being transferred by friction.

(b) Accelerometers of 2 g range allow measurement in any direction by simply orienting the mounting block properly. The measurement of angular motions is discussed in Appendix III. No underwater measurements were attempted, but they appear feasible if the accelerometer case is sealed with paraffin and underwater connections are eliminated.

(c) No special mechanical skills or extensive training are required to operate the system.

(d) The cost of the system exclusive of cable and tax is approximately $2000 per channel for six channels.

Characteristics of Other Components

The manufacturers' specifications for many other components were examined, and several of the components were subjected to laboratory tests to determine their suitability for structural dynamic work. Once again it is pointed out that the equipment was not always used as the manufacturer intended, and the tests were not exhaustive. Dynamic and electronic instruments have the interesting property that seemingly small modifications can produce large changes in characteristics, and very few modifications were attempted.

Four other accelerometers were tested, two of the variable reluctance type, one containing a linear variable differential transformer, and one operating on a servo principle. The variable reluctance units, the Consolidated Electrodynamics 4-260, $\pm$ 12 g range, no longer manufactured, which puts out 45 mv/g at 10 v, 2000 cps, excitation and the Daystrom-Wiancko Engineering Company type A1001, $\pm$ 5 g range, priced at $250 which puts out 320 mv/g at 16 volts, 3000 cps, excitation and

the L.V.D.T. unit, the Schevitz HG-30, ± 30 g range, priced at $180, which puts out 40 mv/g at 10 volts, 2000 cps, excitation had two undesirable characteristics in common. The bridge output of all three units contained higher harmonics of the carrier, and at high gain settings the output of the entire carrier amplifier system showed a higher noise-to-signal ratio than was the case with strain gage accelerometers. The harmonics of the carrier were observed on an oscilloscope when attempts were made to balance the bridge, the fifth harmonic being most noticeable. Whether the harmonics were initially present in the carrier or a result of non-linearities in the accelerometers is not known.

Odd harmonics pass through a demodulator, appearing as D. C. output at the recorder, and it was found to be impossible to keep the trace on the paper when attempting to balance at high gains. In obtaining a null in the balancing operation, the bridge was actually unbalanced for 2000 cps excitation in order to overide the output due to the odd harmonics. It is not known if the residual unbalance due to harmonics remains constant when the accelerometer is subjected up to 1/10 g or so. Balancing was always found to be poorer when the sensitive axis was vertical than when it was horizontal. In one test of the C.E.C. 4-260 and the Brush RD 5612-11, the null at balance was 15 mm pen deflection at X2 gain, with 0.8 ufd across the bridge output and the accelerometer horizontal. When the accelerometer was swung through angles varying from 1° to 90° on the protractor table, the maximum non-linearity noted in the output of the system was 4%.

The obvious remedy for this situation is the insertion of a filter ahead of the demodulator to reduce the higher harmonics. The Daystrom-

Wiancko series 3000 amplifiers and the C.E.C. System D amplifiers contain filters to remove the third harmonic of the carrier. In Table A1.3, in which output and balancing data are given for four accelerometers used with the Brush system, the effects of capacitance across the bridge output, acting as a low pass filter, are shown. The fact that the sensitivities shown in Table A1.3 do not agree with those specified by the accelerometer manufacturers is possibly due to the fact that all but the strain gage transducer shift the frequency of the carrier considerably, and since the Brush amplifier provides a reference signal at the demodulator only at either 0° or 90° to the bridge excitation, the bridge output at shifted frequency produces less signal from the demodulator.

The servo accelerometer, the Palomar Scientific Corporation model PAL-1S-5052, $\pm$ 2 g range, priced at $500, does not require carrier excitation, but is powered by dry cells, $\pm$ 15 v, and puts out a D.C. signal of 3.75 v/g (open circuit). The output impedance is 5000 ohms, so the unit can be used to drive C.E.C. 7-341 galvanometers without further amplification, only an attenuator being used ahead of the galvanometer. With Hewlett-Packard model 350 A, 500 ohm attenuator set at zero Db, the sensitivity of the combination is approximately 3/8 inch trace deflection per 0.001 g, but this is accompanied by an overriding high frequency noise, at times exceeding the signal from 0.005 g. The unit therefore does not appear to be suitable for the majority of structural testing.

The Kistler Instrument Corporation manufactures a servo accelerometer, model 302, priced at $1100, which has specifications indicating sensitivity of approximately $\frac{1}{2}$ inch per 0.001 g with the C.E.C. 7-341

	Schaevitz HG-30 f_n = 107 cps	C.E.C. 4-260 f_n = 100 cps	Wiancko A1001, 5g f_n = 77 cps	Statham A5-2-350 f_n = 100 cps
Sensitivity mm/g at Gain X1000	28 mm	26 mm 8 mm*	25 mm 10 mm+	14 mm
Balance offset at Null	20 mm at gain X20	19 mm at gain X20 22 mm at gain X2*	24 mm at gain X50 21 mm at gain X10+	16 mm at gain X1

* 0.4 μfd across bridge output.

+ 0.3 μfd across bridge output.

Carrier voltage approx. 4.6v.

TABLE A1.3

COMPARISON OF FOUR ACCELEROMETERS USED WITH THE BRUSH RD 5612-11 CARRIER AMPLIFIER AND BRUSH PEN RECORDER

galvanometer. As with the Palomar accelerometer, however, there exists the problem of cancelling out a static 1 g signal when vertical accelerations are to be measured. To allow 0.001 g measurements to be made with an accuracy of 10%, the 1 g signal from the accelerometer and the balancing signal would have to be stable to 0.01%. Specifications for the Microdot Incorporated PS-290 power supply, priced at $250, indicate that a stable balancing signal is possible.

Although some piezoelectric accelerometers and charge amplifiers, such as those manufactured by the Endevco, Kistler, and Statham corporations, possess low frequency response, none was found with specifications indicating sufficient sensitivity for measurements in the 0.001 g range.

Several other strain gage accelerometers appear promising for special situations in structural dynamic testing. The Statham A4-0.25-350, $\pm$ 0.25 g range, 15 cps natural frequency, priced at $300, producing 140 mv/g at 9 volts excitation should be very useful for measuring the response of dams and building foundations to shaking machine excitation and for measuring the response of buildings to wind excitation. The Statham A 301-0.5-350, $\pm$ 0.5 g range, 5 cps natural frequency, priced at $245, producing 40 mv/g at 9 volts excitation, should be useful for wind induced vibrations in the presence of unwanted high frequency vibrations caused by machinery. The Statham A5-5-350 accelerometer, $\pm$ 5 g range, 190 cps natural frequency, priced at $300, producing 10 mv/g at 11 volts excitation is a more rugged instrument exhibiting less phase lag than the A5-2-350.

Among the carrier amplifiers considered, the William Miller Company model C-3 appeared to be the best suited for structural dynamic testing.

The system provides 3000 cps bridge excitation adjustable up to 10 volts and puts out up to 10 ma into a 40 ohm load. Reluctance type accelerometers can be balanced very well by the system, indicating a very pure carrier and/or built-in filters to suppress carrier harmonics. No circuit diagram of the system was available, and unfortunately the company is no longer in business. The particular system tested, about ten years old, consisted of one package of six amplifiers and one containing a power supply, total weight 230 pounds. Under the same test conditions, the noise-to-signal ratio of the Miller C-3 is approximately one half that of the Brush RD 5612-11. In both systems the noise increases as the bridge is unbalanced, indicating that some noise is on the carrier. Phase lags of the C-3 system only at 15, 30, 45, and 100 cps were measured as 5°, 5°, 10°, 12° respectively, using the Statham A5-200-220 accelerometer as a transducer with the C-3 and using the Endevco accelerometer and amplifier as a standard as was done in Table A1.1. Once again it is pointed out that the wave forms were not perfectly symmetrical. Amplitude ratios of the C-3's response to the Endevco's response at the above frequencies were 1.00, 1.002, 1.16, and 1.17 respectively. These ratios are difficult to explain on any other basis than conditions of mounting the accelerometers to the shaker.

System D, manufactured by Consolidated Electrodynamics Corporation is designed for use with reluctance transducers. When the system was tested with the C.E.C. 4-260 accelerometer and the C.E.C. 7-341 galvanometer, the maximum sensitivity that could be obtained was approximately 0.32 inch trace deflection per 0.001 g; noise-to-signal ratio

was not measured. The system costs approximately $1500 for a 12-channel power supply and rack plus $550 per channel.

The Sanborn Instruments model 850-1100 A carrier preamplifier when used with the Statham A5-2-350 accelerometer and the C.E.C. 7-341 galvanometer, showed a noise-to-signal ratio approximately double that of the Brush RD 5612-11. This amplifier has graduated attenuation in steps from 1 to 200 only, meaning that if a 2 g calibration signal at maximum attenuation fills the paper, a 0.001 g signal at maximum gain will have only one fifth this amplitude. The price of the 850-1100A is $550 for an 8-channel power supply plus $365 per channel.

Specifications for the Minneapolis-Honeywell Company's Heiland 130-20C carrier amplifier indicate sensitivity on the order of that of the Brush amplifier, but the amount of noise is not known.

No D.C. amplifiers were tested. Specifications for the Brush RD 4215-20 very high gain D.C. preamplifier indicate amplification about 1/15 that of the Brush RD 5612-11 carrier system.

The Sanborn model 650 direct writing oscillograph and the Minneapolis-Honeywell model 1508 Visicorder will perform the same functions as the C.E.C. 5-124 oscillograph. These models, both of which record on 8 inch-wide paper, possess a few features not found on the C.E.C. 5-124 and are priced competitively with it. No tests were made on the paper drive and timing systems of these oscillographs. Mid Western Instruments Company's model 621 F direct writing oscillograph records on 6 inch-wide paper and is priced several hundred dollars cheaper.

Pen recorders of up to 8 channels, using ink, electric, or thermal

writing, are available from the Brush and Sanborn companies. They produce clean traces of up to 50 mm peak-to-peak at paper speeds from 1 to 250 mm/sec. in some cases. The penmotors have a natural frequency of about 50 cps and are damped chiefly electromagnetically, although undoubtedly there is some friction between the pen and the paper. A 2-channel Brush RD 232100 costs $725; and 8-channel Sanborn 358-100 costs $2700. The chief disadvantages of pen recorders are their bulk and weight, their limited recording amplitudes and paper speeds, their poor high frequency response, low sensitivity, and lack of versatility. The multitude of galvanometers available for the light beam recorders, ranging in natural frequency from 18.5 cps to 8000 cps, the great sensitivity and the ease with which damping can be adjusted in the electromagnetically damped types, plus the possibility of recording amplitudes up to 7 inches or so peak-to-peak and the high paper speeds possible make the direct writing light beam oscillographs much more versatile recording instruments. On the other hand, the records from the light beam oscillographs have less contrast and do not reproduce as well as the records from the pen recorders.

APPENDIX II

NUMERICAL INTEGRATION OF STEADY STATE ACCELERATION RECORDS

A program was written for the Burroughs 220 computer to numerically integrate data from acceleration records to yield velocities and displacements. The method requires only that the motion be steady state, so that the wave form repeats itself from cycle to cycle. In the case of non-symmetrical records the zero of the acceleration record need not be known, but can be established from the steady state conditions. The zero of velocity can be established similarly, but no absolute frame of reference for displacement can be determined without the aid of an absolute displacement measurement.

The method of integration, previously described by Benscoter and Gossard,[57] consists of finding the areas beneath segments of second degree parabolas fitted to three equally spaced ordinates on the curve to be integrated. The details are illustrated in Figure A2.1. The first integration of acceleration usually yields a velocity at the end of the cycle different from that at the start of the cycle. This difference is used as a criterion to adjust the zero of the acceleration data so that a second trial at integrating the acceleration yields no net change in velocity over the cycle. The same procedure is then followed to obtain displacements from velocities, the criterion of no net gain in displacement over the cycle being used to adjust the zero of velocity.

To illustrate the accuracy of the method on sinusoidal data, the acceleration data was taken as the ordinates of a sine wave at intervals of 18°, giving 21 data points for one cycle. The largest numerical error in the resulting displacement was 0.2% of the amplitude of the displacement record.

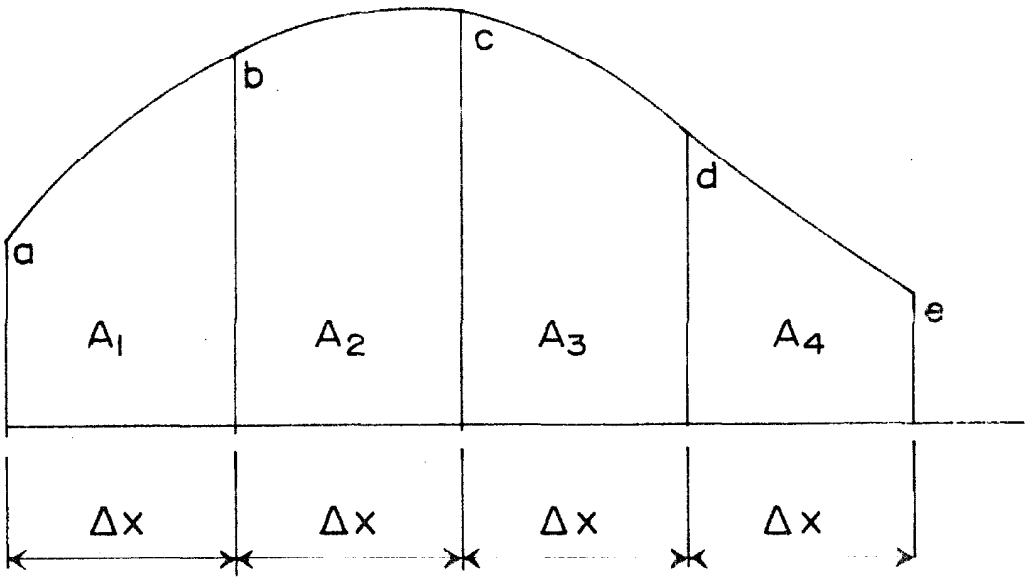

$$A_1 = \Delta x/12\,(5a + 8b - c)$$

$$A_2 = \Delta x/12\,(5b + 8c - d)$$

$$A_3 = \Delta x/12\,(5c + 8d - e)$$

$$A_4 = \Delta x/12\,(5e + 8d - c)$$

FIGURE A 2.1
NUMERICAL INTEGRATION
WITH A SECOND DEGREE CURVE

APPENDIX III

SEPARATION OF THE EFFECTS OF HORIZONTAL, VERTICAL AND ANGULAR ACCELERATIONS

Given two accelerometers mounted on a rigid surface, Figure A3.1, which undergoes rotation in the earth's gravitational field, $\alpha \sin \omega t$, and a reference point, o, on the surface experiences horizontal and vertical translations, h sin ωt and v sin ωt. The inclination of the equilibrium position of the plane to the horizontal, H, is shown as β. The angles α and β are assumed small so that their cosines are essentially unity, otherwise the motions of the accelerometers are not pure sinusoids of one frequency.

Transverse sensitivity of the accelerometers is assumed to be due solely to internal misalignment of their spring-mass systems to their cases. In Figure A3.1 the angles θ_1 and θ_2 designate the unknown misalignment of the axes of sensitivity, S, of the accelerometers to the plumb line, P. If the motions of the plane can be held steady or can be duplicated so that two measurements can be made, the effect of this transverse sensitivity can be eliminated by averaging the measurements made with the accelerometers mounted, first as shown by the solid arrows, and second, rotated 180° about the plumb line, as shown by the dashed arrows. If the axis of this rotation is not a plumb line, then sensitivity to horizontal motion has not been eliminated. Similarly, when the accelerometers are mounted to sense horizontal motion, rotation about the horizontal will eliminate the effects of vertical motion. If θ_1 and θ_2 are less than 8°, the loss of sensitivity in the direction of measurement is less than 1%.

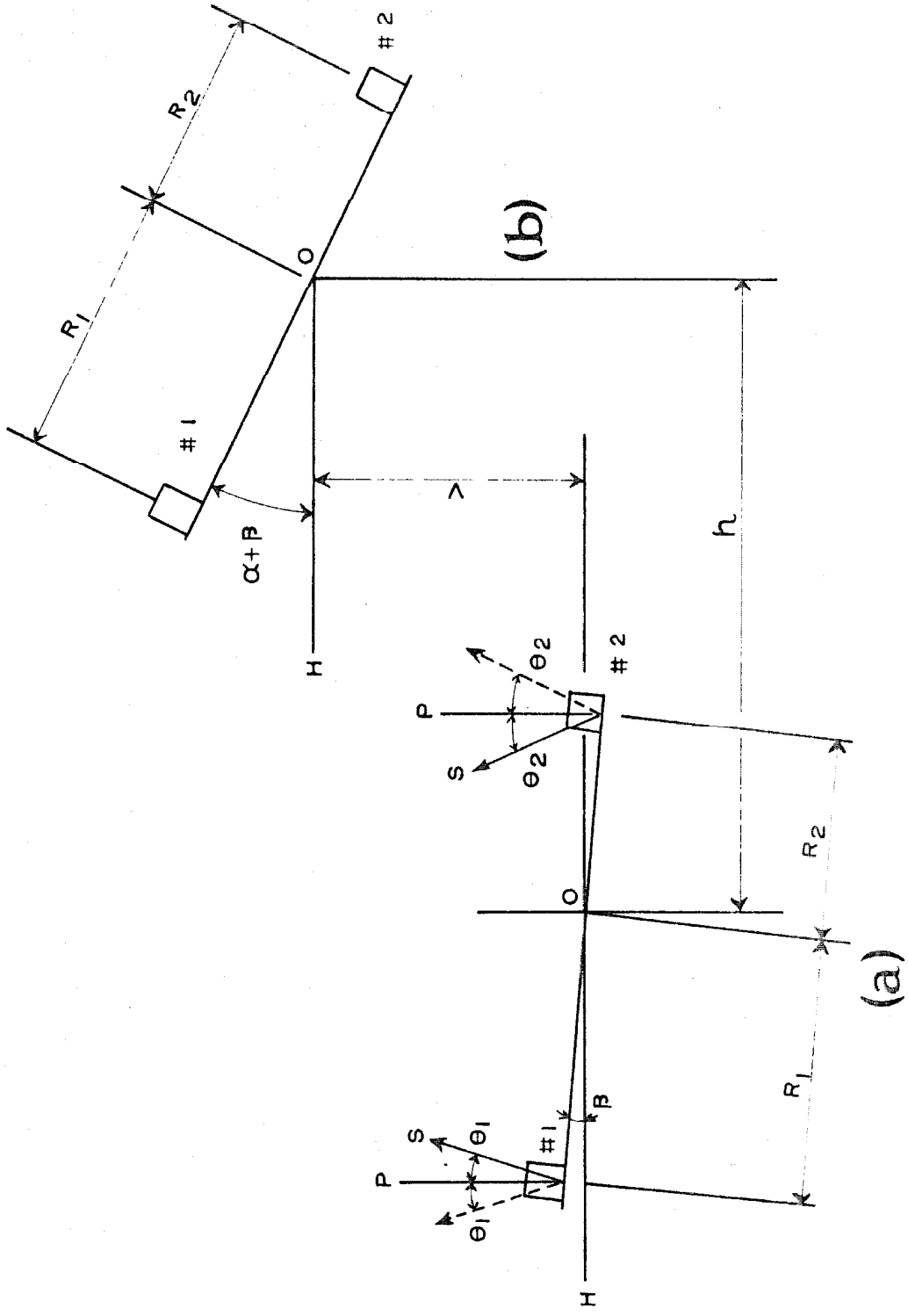

FIGURE A 3.1
PLANE MOTION OF ACCELEROMETERS

Assuming now that double measurements are made so that misalignment is not a factor, accelerometers #1 and #2 will record the following accelerations when the motion is at the extreme point of the cycle shown in Figure A3.1(b):

$$-\omega^2 h\alpha - \omega^2 v - \omega^2 R_1\alpha = a_{1v} \qquad \text{(A3.1)}$$

$$-\omega^2 h\alpha - \omega^2 v + \omega^2 R_2\alpha = a_{2v} \qquad \text{(A3.2)}$$

The first term in equations A3.1 and A3.2 results from the inclination of the sensitive axes, S, of the accelerometers to the horizontal acceleration when the mounting plane has undergone rotation, α . This term does not vary in time as $\sin \omega t$ as do the other terms, but as $\sin^2 \omega t$, meaning that the records contain a component at twice the forcing frequency. This presents no difficulty, however, since in practice amplitudes are usually determined by measuring the peak-to-peak distance of the trace, and this measurement automatically eliminates the effect of the first term. Subtracting equation A3.1 from A3.2:

$$\omega^2\alpha (R_1 + R_2) = a_{2v} - a_{1v}. \qquad \text{(A3.3)}$$

Thus, α can be determined.

Assuming now that a_{1v} and a_{2v} represent peak-to-peak measurements so that the first term does not appear, a solution for v, the amplitude of the vertical motion of point o, is now possible from either equation A3.1 or A3.2.

If now the accelerometers are rotated about a horizontal axis 90° to the right to sense horizontal accelerations, and once again double measurements are made to eliminate misalignment, the instruments will record the following accelerations at the extreme point of the cycle:

$$\alpha\omega^2(v + \alpha R_1) - \omega^2 h - \alpha g = a_{1h} \qquad \text{(A3.4)}$$

$$\alpha\omega^2(v - \alpha R_2) - \omega^2 h - \alpha g = a_{2h} \qquad \text{(A3.5)}$$

The first terms of equations A3.4 and A3.5 result from the inclination of the sensitive axes, S, to the horizontal at the extreme of the motion, and once again, if peak-to-peak measurements are made, these terms do not appear in equations A3.4 and A3.5. With α known from equation A3.3, h may now be determined, or if measurements of vertical accelerations are not made, the horizontal accelerometer may be rotated 180° about a vertical axis, and the average of this measurement and the initial measurement will not be influenced by α.

A numerical example is of interest to illustrate the importance of the terms in the equations above. A digital computer analysis of the new Encino Reservoir tower shows that at the fundamental frequency of 2.11 cps a 1-inch horizontal motion on the penthouse floor is accompanied by a rotation of 0.00108 radians and a vertical motion of 0.00036 inches measured at the center of the penthouse floor, which is 14'-8" in diameter. Then, if a_{1v} and a_{2v} are assumed to represent peak-to-peak measurements, equation A3.1 and A3.2 have the values shown in equations A3.1'and A3.2':

$$-(191)(0.00036) -(191)\ (88)(0.00108) = -18.22140 \qquad \text{(A3.1')}$$

$$-(191)(0.00036) +(191)(88)(0.00108) = 18.08388. \qquad \text{(A3.2')}$$

The difference between the right hand sides of equations A3.1' and A3.2' would be difficult to measure accurately on an oscillogram, indicating that vertical motion in this instance would have to be measured at the center of the tower, a measurement which would then include flexing of the floor.

Assume now that the accelerometers are not rotated about the plumb line to eliminate transverse sensitivity, and that total misalignment of each is $1\frac{1}{2}°$, a reasonable maximum, 1° of which is internal, and $\frac{1}{2}°$

external misalignment. Then the trace amplitudes in equations A3.1' and A3.2' will include the term (0.0262)(191)(1) resulting from horizontal acceleration. If the unknown alignment errors are in opposite directions the value of α calculated from equations A3.1' and A3.2' will be 0.000782, in error by 28%. If a vertical measurement were made at the center of the tower with an accelerometer having a $1\frac{1}{2}^{\circ}$ alignment error, the vertical signal would be hidden by a horizontal signal 73 times as great. Hence, the measurement of vertical motion at this point on the structure does not appear feasible.

The measurement of horizontal motions on the penthouse floor in the first mode does not require the refinement of rotating the accelerometer about the horizontal inasmuch as the vertical acceleration, even on the outside edge of the tower, would result in only 1/4 of 1% error for a $1\frac{1}{2}^{\circ}$ misalignment. Neglecting the term involving gravity in this instance would result in an error of 1/5 of 1%.

In the second mode of the structure, rotation is about $12\frac{1}{2}$ times as great as rotation in the first mode for the same horizontal deflection, but since the frequency is approximately four times as great, the importance of the (α g) term in equations A3.4 and A3.5 is not as great as before. The computer shows vertical motions in the second mode to be about 1/60 the horizontal motion on the penthouse floor. If a misalignment of only $\frac{1}{2}^{\circ}$ is assumed in measuring vertical motion at the center of the tower, the vertical signal will still be in error by 52%. The rotation of the floor in the second mode can be determined more accurately, the worst combination of $1\frac{1}{2}^{\circ}$ alignment errors causing errors in α of only 2%.

APPENDIX IV

STATIC CALIBRATION OF ACCELEROMETERS

Let it be assumed that an accelerometer is to be calibrated by mounting it with its sensitive axis vertical on a protractor table, and then rotating the table about a horizontal axis by equal amounts on either side of the vertical. In Figure A4.1(a), P represents the plumb line, P' represents the assumed plumb line, but in error by an amount θ_1, and S represents the sensitive axis of the accelerometer, which is assumed vertical, but due to internal misalignment makes an angle of θ_2 with P'. The calibration angle to be swept through is designated by α .

The acceleration, in g's, experienced by the accelerometer is $(-\cos \gamma)$, where γ is the total angle from the vertical. The signal which balances the effect of gravity when the accelerometer is assumed plumb is, in g's, $\cos (\theta_1 + \theta_2)$, assumed unchanged throughout the calibration. The net output, of the accelerometer then, is

$$N = \cos (\theta_1 + \theta_2) - \cos \gamma \ .$$

By reversing the accelerometer about P' the sign of θ_2 can be changed, and thus, by changing the direction of α, four values of γ and of N can be obtained.

$$N_1 = \cos (\theta_1 + \theta_2) - \cos (\alpha + \theta_1 + \theta_2)$$

$$N_2 = \cos (\theta_1 + \theta_2) - \cos (\alpha + \theta_1 - \theta_2)$$

$$N_3 = \cos (\theta_1 + \theta_2) - \cos (-\alpha + \theta_1 - \theta_2)$$

$$N_4 = \cos (\theta_1 + \theta_2) - \cos (-\alpha + \theta_1 + \theta_2)$$

By manipulating the various expressions for $N_{1,2,3,4}$ it becomes apparent that no simple combination of reversals can eliminate the

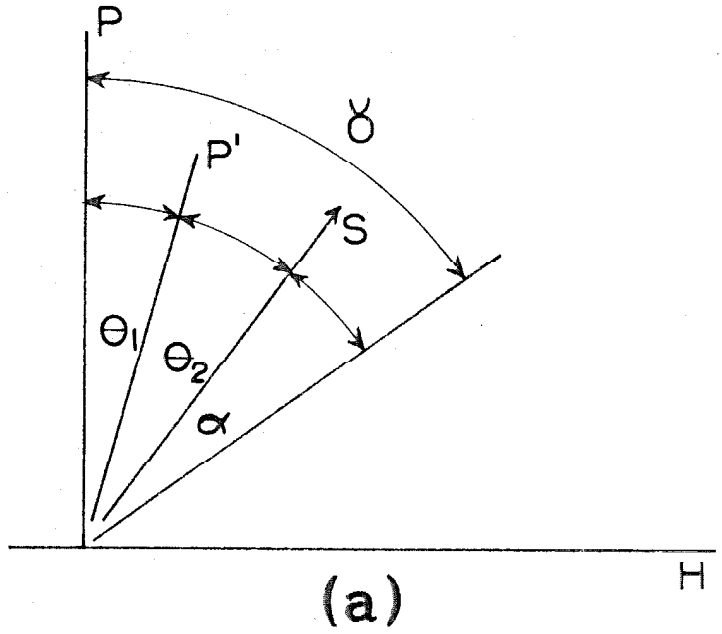

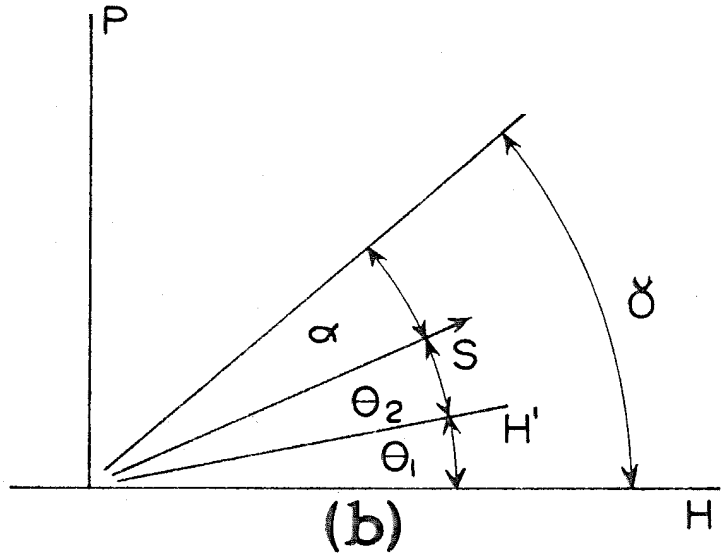

FIGURE A 4.1
STATIC CALIBRATION OF ACCELEROMETER

effects of θ_1, and θ_2. However, if the direction of α only is reversed, and the accelerometer itself is not reversed on its mounting, the result is:

$$N_1 + N_4 = 2 \cos (\theta_1 + \theta_2)(1 - \cos \alpha).$$

If $(\theta_1 + \theta_2)$ is less than 8°, the error in calibration, based on knowledge of α only, is less than 1%.

It is worth noting that for small values of α, the calibration signal varies as α^2, meaning that angular settings must be accurately made. When α is 1°, a setting error of three minutes of arc results in an error of 10% in the signal.

Let it be assumed now that the accelerometer is mounted with its sensitive axis horizontal as in Fig. A4.1 (b) where H represents the true horizontal, H' the assumed horizontal, and S the position of the sensitive axis for balancing. The net output in g's in this case is

$$N = \sin (\theta_1 + \theta_2) - \sin (\alpha + \theta_1 + \theta_2).$$

Here again four values of γ, and thus four values of N, are possible:

$$N_1 = \sin (\theta_1 + \theta_2) - \sin (\alpha + \theta_1 + \theta_2)$$

$$N_2 = \sin (\theta_1 + \theta_2) - \sin (\alpha + \theta_1 - \theta_2)$$

$$N_3 = \sin (\theta_1 + \theta_2) - \sin (-\alpha + \theta_1 - \theta_2)$$

$$N_4 = \sin (\theta_1 + \theta_2) - \sin (-\alpha + \theta_1 + \theta_2).$$

If the accelerometer is not reversed on its mounting, but α only is changed in direction,

$$N_1 - N_4 = -2 \sin \alpha \cos (\theta_1 + \theta_2),$$

and once again, if $(\theta_1 + \theta_2)$ is less than 8° the error in calibration is less than 1%. No other manipulation of the expressions appears to result in an expression with less dependence on θ_1 and θ_2.

REFERENCES

1. Okamoto, S., Kato, K., and Hakuno, M., "A New Method of Dynamic Model Test of Arch Dam," Trans. Japanese Society of Civil Engineers, No. 75, (July, 1961), pp. 47-58.

2. Keightley, W. O., Housner, G. W., and Hudson, D. E., Vibration Tests of the Encino Dam Intake Tower, Earthquake Engineering Research Laboratory, California Institute of Technology, Pasadena, Calif., (July, 1961).

3. Carder, D. S., "Vibration Observations," Earthquake Investigations in California, 1934-35, Special Publication No. 201, Coast and Geodetic Survey, U. S. Department of Commerce, Washington, D. C., (1936).

4. Hudson, D. E., "A Comparison of Theoretical and Experimental Determinations of Building Response to Earthquakes," Proceedings of the Second World Conference on Earthquake Engineering, Tokyo, Japan, (1960), pp. 1105-1119.

5. Okamoto, S. and Takahashi, T., "On Behaviors of an Arch Dam During Earthquakes," Proceedings of the Second World Conference on Earthquake Engineering, Tokyo, Japan, (1960), pp. 1401-1412.

6. Scruton, C. and Harding, D. A., "Measurement of the Structural Damping of a Reinforced Concrete Chimney Stack at Ferrybridge "B" Power Station," National Physical Laboratory, NPL/Aero/323/1957.

7. Hudson, D. E. and Housner, G. W., "Structural Vibrations Produced by Ground Motion," Trans. A.S.C.E., Vol. 122, (1957), pp. 705-721.

8. Bernhard, R. K., "Geophysical Study of Soil Dynamics," Tech. Publ. 834, American Institute of Mining and Metallurgical Engineers, (1938).

9. Earthquake Investigations in California, 1934-1935, Special Publication No. 201, Coast and Geodetic Survey, U. S. Dept. of Commerce, Washington, D. C., (1936).

10. Voigt, Herbert, "Recent Findings and Empirical Data Obtained in the Field of Ship Vibrations," David Taylor Model Basin Translation No. 268, (Feb., 1958).

11. Hatano, T., Takahashi, T. and Tsutsumi, H., Dynamical Study of Tsukabaru Gravity Dam, Technical Laboratory Report C-5801, Central Research Institute of Electric Power Industry, Tokyo, Japan, (June, 1958).

12. Hudson, D. E., A New Vibration Exciter for Dynamic Test of Full-Scale Structures, Earthquake Engineering Research Laboratory, California Institute of Technology, Pasadena, Calif., (June, 1961).

13. Hudson, D. E., Synchronized Vibration Generators for Dynamic Tests of Full-Scale Structures, Earthquake Engineering Research Laboratory, California Institute of Technology, Pasadena, Calif., (Nov., 1962).

14. Mazet, R. "Quelques Aspects des Essais de Vibration au Sol et en Vol," Note Technique no. 34, Office National D'Etudes et de Recherches Aeronautiques, (1956).

15. Hudson, D. E., "Dynamic Tests of Buildings and Special Structures," Experimental Techniques in Shock and Vibration, Amer. Soc. of Mech. Engr., (Nov., 1962), pp. 81-91.

16. Housner, G. W. and Keightley, W. O., "Vibrations of Linearly Tapered Cantilever Beams," Journal of the Engr. Mech. Div., Proceedings of the A.S.C.E., (April, 1962), pp. 95-123.

17. Lehman, F. G., "Materials for Reinforced Concrete," Concrete Engineering Handbook, W. S. Lalonde, Jr. and M. F. Janes, editors, McGraw-Hill Book Co., Inc., New York, N. Y., (1961), p. 1-49.

18. Miner, D. F. and Seastone, J. B., Handbook of Engineering Materials, John Wiley and Sons, Inc., New York, N. Y., (1955), p. 2-541.

19. Jacobsen, L. S. and Ayre, R. S., Engineering Vibrations, McGraw-Hill Book Co., Inc., New York, N. Y., (1958), pp. 110-112, 501-505.

20. Arnold, R. N., Bycroft, G. N. and Warburton, G. B., "Forced Vibrations of a Body on an Infinite Elastic Solid," Journal of Applied Mechanics, (Sept., 1955), pp. 391-400.

21. Withey, M. O. and Washa, G. W., Materials of Construction, John Wiley and Sons, Inc., New York, N. Y., (1954), p. VII-21.

22. Sutherland, J. G. and Goodman, L. E., "Vibrations of Prismatic Bars Including Rotatory Inertia and Shear Corrections," a Technical Report for the Office of Naval Research, Project NR-064-183, contract N6 - ori-71, Urbana, Illinois, (April, 1951).

23. Stokey, W. F., "Vibration of Systems Having Distributed Mass and Elasticity," Shock and Vibration Handbook, C. M. Harris and C. E. Crede, editors, McGraw-Hill Book Co., Inc., New York, N. Y., (1961), p. 7-17.

24. Jacobsen, L. S. and Ayre, R. S., Engineering Vibrations, McGraw-Hill Book Co., Inc., New York, N. Y., (1958), pp. 501-502.

25. Timoshenko, S., Vibration Problems in Engineering, 2nd ed., D. Van Nostrand Co., Inc., New York, N. Y., (1937), p. 366.

26. Troxell, G. E. and Davis, H. E., Composition and Properties of Concrete, McGraw-Hill Book Co., Inc., New York, N. Y., (1956), p. 259.

27. Abramson, H. N., "Nonlinear Vibration," Shock and Vibration Handbook, C. M. Harris and C. E. Crede, editors, McGraw-Hill Book Co., Inc., New York, N. Y., (1961), p. 4-31.

28. Atkinson, C. P., "Superharmonic Oscillations as Solutions to Duffing's Equations as Solved by an Electronic Differential Analyzer," Journal of Applied Mechanics, (Dec., 1957), pp. 520-525.

29. Hollis, E. P. Bibliography of Engineering Seismology, Earthquake Engineering Research Institute, San Francisco, Calif., (1958).

30. "Preliminary Report of Forced Vibration Tests of Searsville Dam," Coast and Geodetic Survey, U. S. Department of Commerce, Washington, D. C., (1934).

31. "Preliminary Report of Forced Vibration Tests of Morris Dam," Coast and Geodetic Survey, U. S. Department of Commerce, Washington, D. C., (1935).

32. Heiland, C. A., "Geophysical Investigations Concerning the Seismic Resistance of Earth Dams," Tech. Publ. 1054, Amer. Institute of Mining and Metallurgical Engineers, (1939).

33. Hatano, T. and Takahashi, T., The Stability of an Arch Dam Against Earthquakes, Technical Report C-5607, Central Research Institute of Electric Power Industry, Tokyo, Japan, (Feb., 1957).

34. Hatano, T., Takahashi, T. and Tsutsumi, H., Dynamical Study of Tsukabaru Gravity Dam, Technical Report C-5801, Central Research Institute of Electric Power Industry, Tokyo, Japan (June, 1958).

35. Takahashi, T., Tsutsumi, H. and Mashuko, Y., Behaviors of Vibration of Arch Dam, Technical Report C-5905, Central Research Institute of Electric Power Industry, Tokyo, Japan, (Dec., 1959).

36. Clough, R. W. and Pirtz, D., "Earthquake Resistance of Rock-Fill Dams," Journal of Soil Mechanics and Foundations Division, Proceedings of the A.S.C.E., (April, 1956).

37. Thomson, W. T., Kobori, T., and Reiter, G., Dynamical Compliance for Rocking Motion of Rectangular Foundations on an Infinite Half-Space, Report No. 62-51, Department of Engineering, University of California, Los Angeles, Calif., (Oct., 1962).

38. Ambraseys, N. N., "On the Shear Response of a Two-Dimensional Truncated Wedge Subjected to an Arbitrary Disturbance," Bulletin of the Seismological Society of America, (Jan., 1960), pp. 45-56.

39. Ambraseys, N. N., "The Seismic Stability of Earth Dams," Proceedings of the Second World Conference on Earthquake Engineering, Tokyo, Japan, (1960), pp. 1345-1363.

40. Response Analyzer Committee, "Non-linear Response Analyzers and Application to Earthquake Resistant Design," Proceedings of the Second World Conference on Earthquake Engineering, Tokyo, Japan, (July, 1960), pp. 649-668.

41. Berg, G. V., The Analysis of Structural Response to Earthquake Forces, University of Michigan Industry Program of the College of Engineering, Ann Arbor, Mich., (May, 1958).

42. Caughey, T. K., "Sinusoidal Excitation of a System with Bilinear Hysteresis," Journal of Applied Mechanics, (Dec., 1960), pp. 640-643.

43. Iwan, W. D., The Dynamic Response of Bilinear Hysteretic Systems, Earthquake Engineering Research Laboratory, California Institute of Technology, Pasadena, Calif., (July, 1961).

44. Berg, G. V., "Finding System Properties from Experimentally Observed Modes of Vibration," Proceedings of the First Argentine Conference on Earthquake Engineering, San Juan, Argentina, (April, 1962).

45. Kobayashi, H., "Dynamic Properties of Building Decided by Measurement of Vibration During Earthquake," Proceedings of the Second World Conference on Earthquake Engineering, Tokyo, Japan, (July, 1960), pp. 1121-1136.

46. O'Kelly, M. E. J., Normal Modes in Damped Systems, Dynamics Laboratory, California Institute of Technology, Pasadena, Calif., (1961).

47. Jacobsen, L. S., "Damping in Composite Structures," Proceedings of the Second World Conference on Earthquake Engineering, Tokyo, Japan, (July, 1960), pp. 1029-1044.

48. Pisarenko, G. S., "Vibrations of Elastic Systems Taking Account of Energy Dissipation in the Material," translated from the Russian in Technical Documentary Report No. WADD TR 60-582, Office of Technical Services, U. S. Dept. of Commerce, Washington 25, D. C. (February, 1962), p. 20.

49. Seidman, E. "An N-Dimensional Surface - Fit Program for the Burroughs 220 Computer," Technical Bulletin 109A, Petrochemical Technology Series, Burroughs Corp., Pasadena, Calif., (Aug., 1960).

50. Perry, C. C. and Lissner, H. R., Strain Gage Primer, McGraw-Hill Book Co., Inc., New York, N. Y., (1955).

51. Mirsky, L. An Introduction to Linear Algebra, Oxford University Press, London, (1955), pp. 156-157.

52. Ormondroyd, J. et al, "Motion Measurements," Handbook of Experimental Stress Analysis, M. Hetenyi, editor, John Wiley and Sons, Inc., New York, N. Y., (1950), pp. 380-386.

53. Bouche, R. R., "Inductive-Type Pickups," Shock and Vibration Handbook, C. M. Harris and C. E. Crede, editors, McGraw-Hill Book Co., Inc. New York, N. Y., (1961), p. 15-19.

54. White, G. E., "Secondary Effects in Seismic System Instruments," Statham Instrument Notes, no. 23, Statham Instruments, Inc., Los Angeles 64, Calif., (1952).

55. Levy, S. and Bickford, R. H., "Calibration of Pickups," Shock and Vibration Handbook, C. M. Harris and C. E. Crede, editors, McGraw-Hill Book Co., Inc., New York, N. Y., (1961), p. 18-3.

56. Conrad, R. W., "Shock and Vibration Instrumentation," Shock and Vibration Handbook, C. M. Harris and C. E. Crede, editors, McGraw-Hill Book Co., Inc., New York, N. Y., (1961), pp. 19-6 to 19-10.

57. Benscoter, Stanley U. and Gossard, Myron L., "Matrix Methods for Calculating Cantilever-Beam Deflections," TN 1827, National Advisory Committee for Aeronautics, (1949).

APPENDIX V

PHOTOGRAPHIC MATERIAL

NEW ENCINO RESERVOIR OUTLET STRUCTURE

FIGURE 2.1

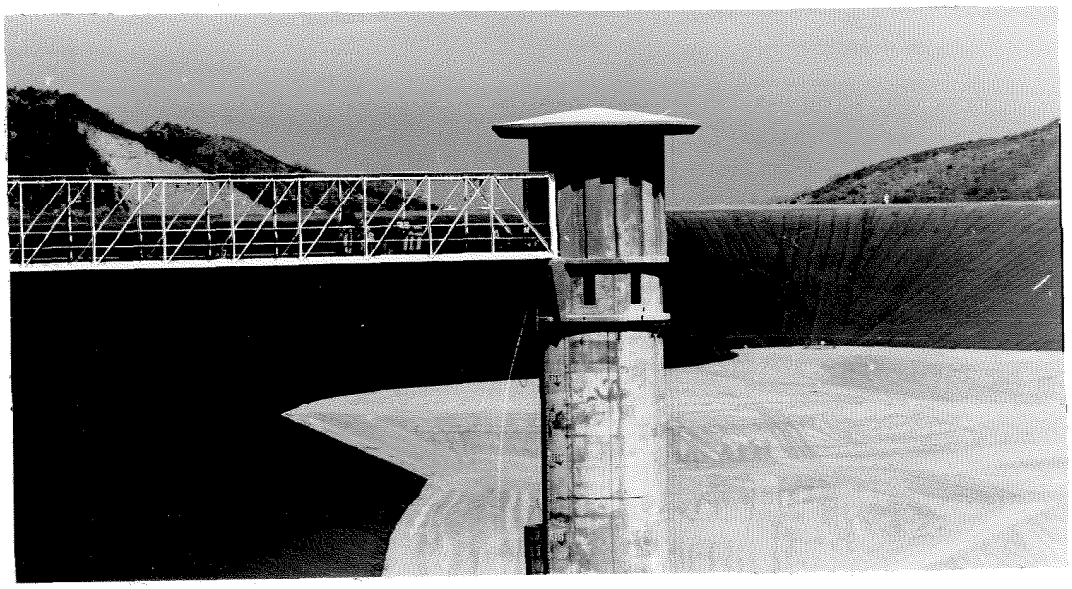

CLOSEUP OF PENTHOUSE

FIGURE 2.2

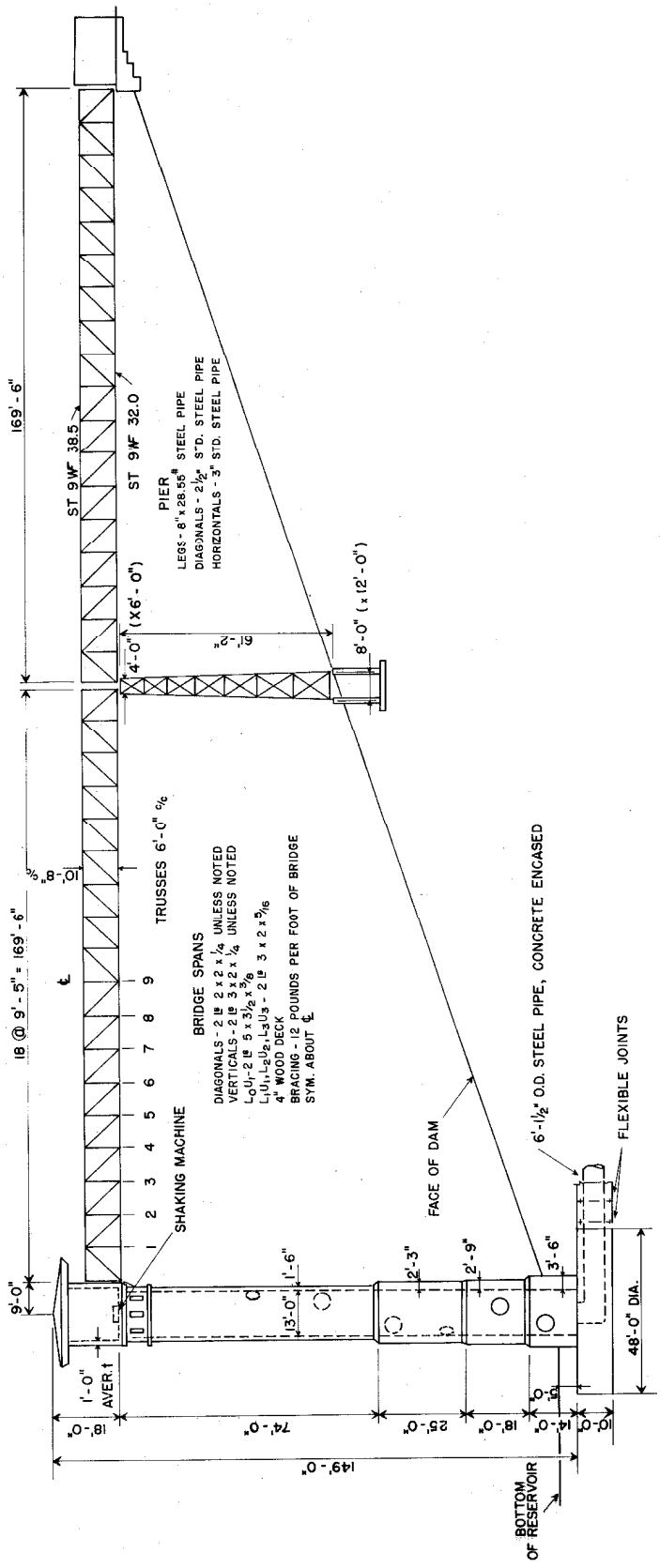

FIGURE 2.3
NEW ENCINO RESERVOIR TOWER

Col. / Row	1 M_B	2 F_B	3 V_D	4 M_D	5 Θ_D	6 Y_D	7 F_D	8 U_D	9 V_L	10 Θ_L	11 Y_L	12 F_L	13 U_L	14 V_A	15 M_A	16 F_A	17 V_M	18 Θ_M	19 Y_M	20 F_M	21 U_M		Equation
1	C_1^{12}		$-C_2^{51}$									C_2^{51}										$= -C_1^{11}$	$V_C + F_L - V_D = 0$
2	C_2^{12}			$-C_2^{51}$					C_1^{51}													$= -C_2^{11}$	$M_C - M_D + 9V_L = 0$
3	C_3^{12}				$-C_2^{51}$																	$= -C_3^{11}$	$\Theta_C - \Theta_D = 0$
4	C_4^{12}					$-C_2^{51}$																$= -C_4^{11}$	$Y_C - Y_D = 0$
5						C_2^{51}						K_{FL}	C_2^{51}									$= 0$	$U_L + Y_D + K_{FL}F_L = 0$
6		C_6^{15}						$-C_2^{51}$														$= 0$	$U_C - U_D = 0$
7					C_1^{51}			C_2^{51}			$-C_2^{51}$											$= 0$	$U_D - Y_L + 9\Theta_D = 0$
8		C_5^{15}					$-C_2^{51}$		$-C_2^{51}$													$= 0$	$F_C - F_D - V_L = 0$
9							C_5^{25}	C_5^{26}														$= 0$	$F_F = 0$
10			C_1^{21}	C_1^{22}	C_1^{23}	C_1^{24}																$= 0$	$V_F = 0$
11									C_2^{31}	C_2^{33}	C_2^{34}	C_2^{35}	C_2^{36}									$= 0$	$M_R = 0$
12									C_4^{31}	C_4^{33}	C_4^{34}	C_4^{35}		C_3^{41}	C_3^{42}	$-C_6^{45}$						$= 0$	$Y_R - U_T + 1.0\Theta_T = 0$
13										C_5^{33}		C_5^{35}	C_5^{36}	$-C_1^{41}$	$-C_1^{42}$					$-C_2^{51}$		$= 0$	$F_R - F_M - V_T = 0$
14														C_3^{41}	C_3^{42}	C_6^{45}			$-C_2^{51}$			$= 0$	$U_T + 1.0\Theta_T - Y_M = 0$
15														C_4^{41}	C_{16}^{42}					K_{FM}	C_2^{51}	$= 0$	$Y_T + U_M + K_{FM}F_M = 0$
16									C_1^{31}	C_1^{33}	C_1^{34}	C_1^{35}				C_5^{45}	$-C_2^{51}$					$= 0$	$V_R + F_T - V_M = 0$
17									C_1^{31}	C_1^{33}	C_1^{34}	C_1^{35}		C_2^{41}	C_2^{42}		C_2^{51}					$= 0$	$M_T + 1.0V_R + 1.0V_M$
18									a	b	c	d	e	C_4^{41}	C_4^{42}							$= 0$	$U_R + Y_T - K_{FR}F_R = 0$
19																	C_2^{31}	C_2^{33}	C_2^{34}	C_2^{35}	C_2^{36}	$= 0$	$M_N = 0$
20																	e	f	g	h		$= 0$	$Y_N - K_{VN}V_N = 0$
21																	i	j	k	l	m	$= 0$	$U_N - K_{FN}F_N = 0$
			C_2^{21}	C_2^{22}	C_2^{23}	C_2^{24}																$= 0$	$M_F = 0$

a: $C_6^{31} - K_{FR}C_5^{31}$

b: $C_6^{33} - K_{FR}C_5^{33}$

c: $C_6^{34} - K_{FR}C_5^{34}$

d: $C_6^{36} - K_{FR}C_5^{36}$

e: $C_4^{31} - K_{VN}C_1^{31}$

f: $C_4^{33} - K_{VN}C_1^{33}$

Check Equation

g: $C_4^{34} - K_{VN}C_1^{34}$

h: $C_4^{35} - K_{VN}C_1^{35}$

i: $C_6^{31} - K_{FN}C_5^{31}$

j: $C_6^{33} - K_{FN}C_5^{33}$

k: $C_6^{34} - K_{FN}C_5^{34}$

l: $C_6^{35} - K_{FN}C_5^{35}$

m: $C_6^{36} - K_{FN}C_5^{36}$

$C_2^{51} = 1$

$C_1^{51} = 9$

FIGURE 2.11

MATRIX EQUATION FOR STRUCTURE

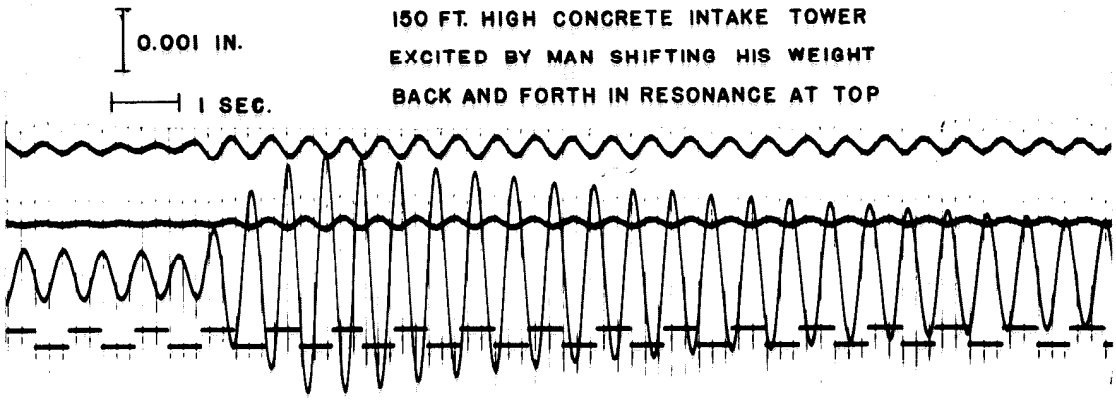

RECORD OF MANUALLY EXCITED VIBRATION

FIGURE 2.12

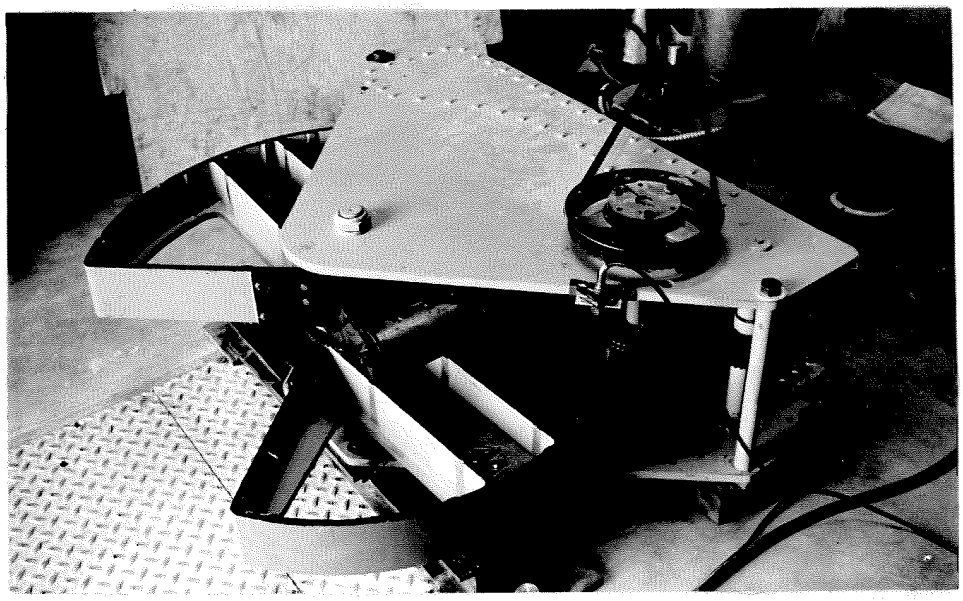

STRUCTURAL VIBRATION EXCITER

FIGURE 2.13

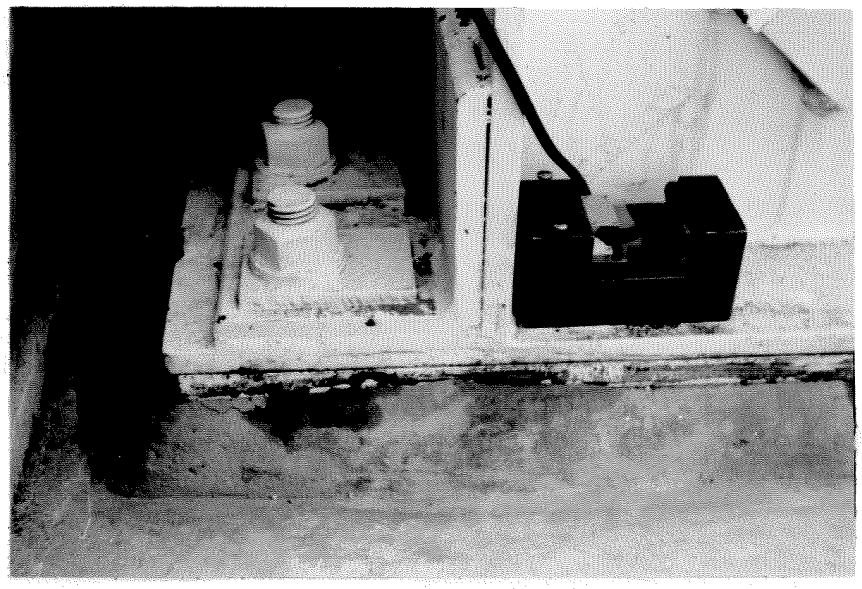

ACCELEROMETER ON PORTABLE STEEL BLOCK

FIGURE 2.14

VIEW OF BRIDGE, LOOKING TOWARDS DAM

FIGURE 2.15

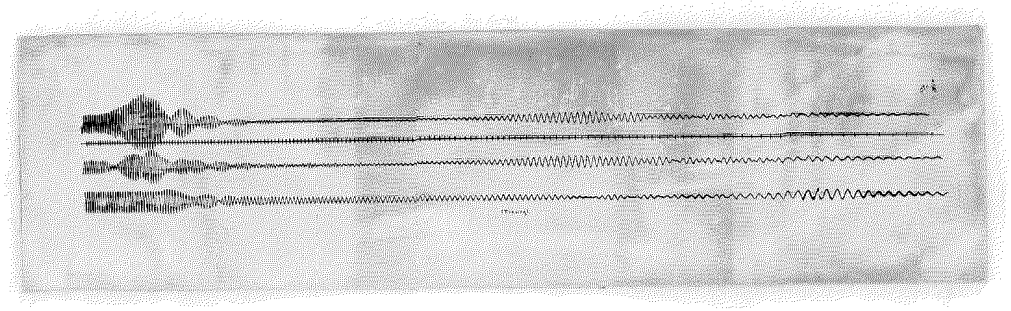

RUNDOWN RECORDS OF ACCELERATION ON THE BRIDGE AND ON THE TOWER

FIGURE 2.16

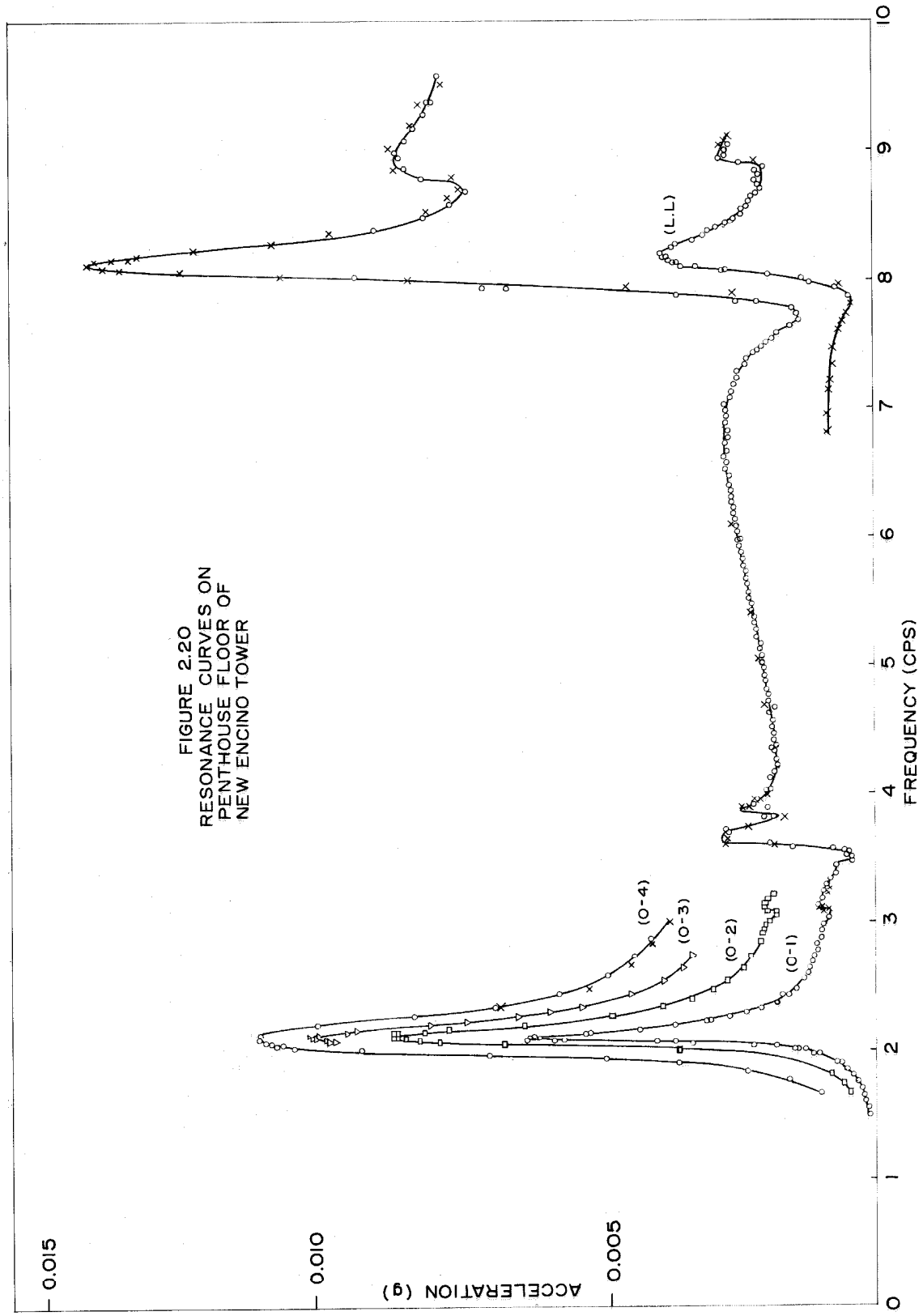

FIGURE 2.20
RESONANCE CURVES ON
PENTHOUSE FLOOR OF
NEW ENCINO TOWER

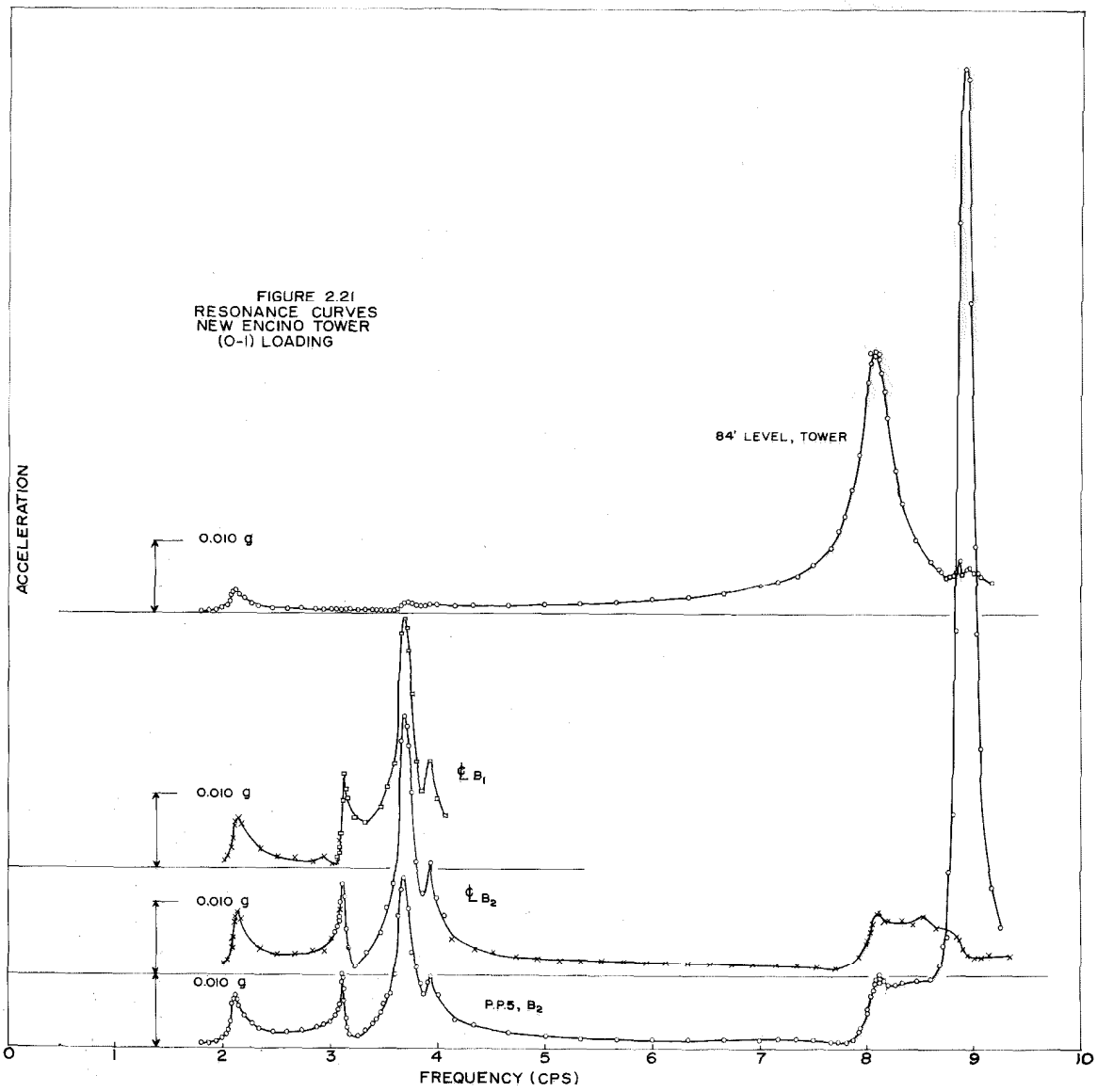
FIGURE 2.21
RESONANCE CURVES
NEW ENCINO TOWER
(O-1) LOADING
84' LEVEL, TOWER
0.010 g
ACCELERATION
℄ B1
0.010 g
℄ B2
0.010 g
P.P.5, B2
0.010 g
0
1
2
3
4
5
6
7
8
9
10
FREQUENCY (CPS)

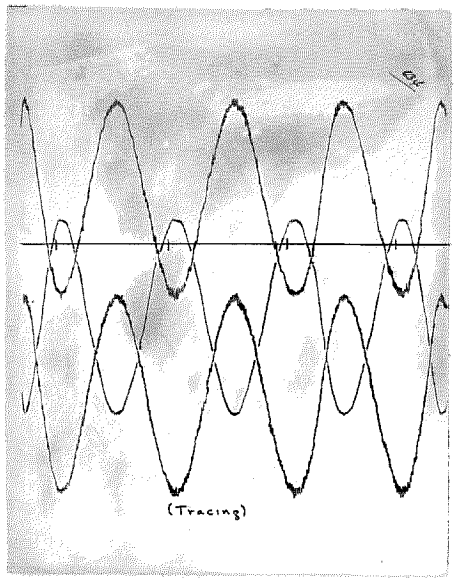

(a)

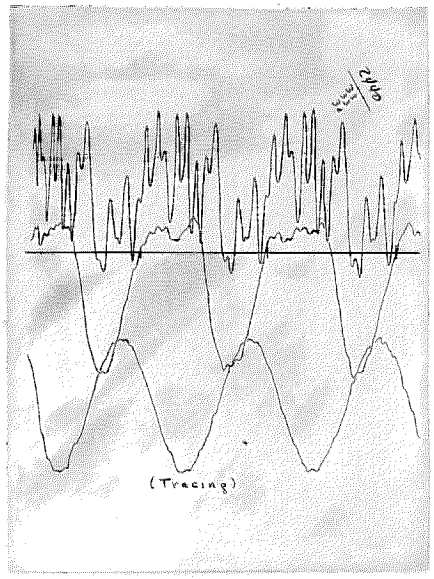

(b)

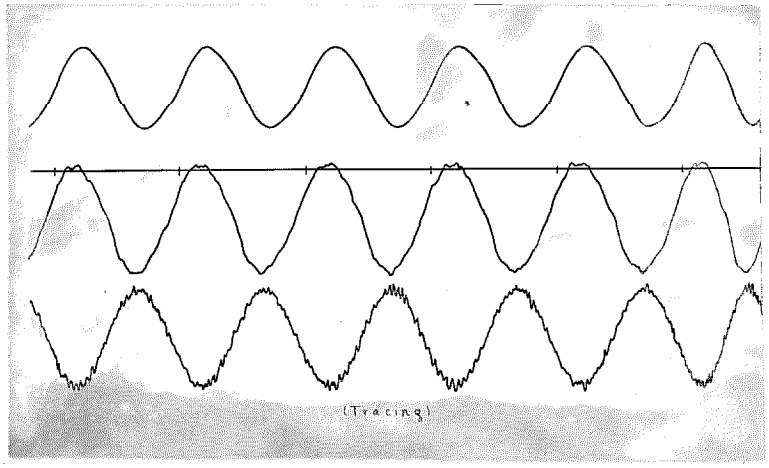

(c)

ACCELERATION RECORDS

FIGURE 2.23

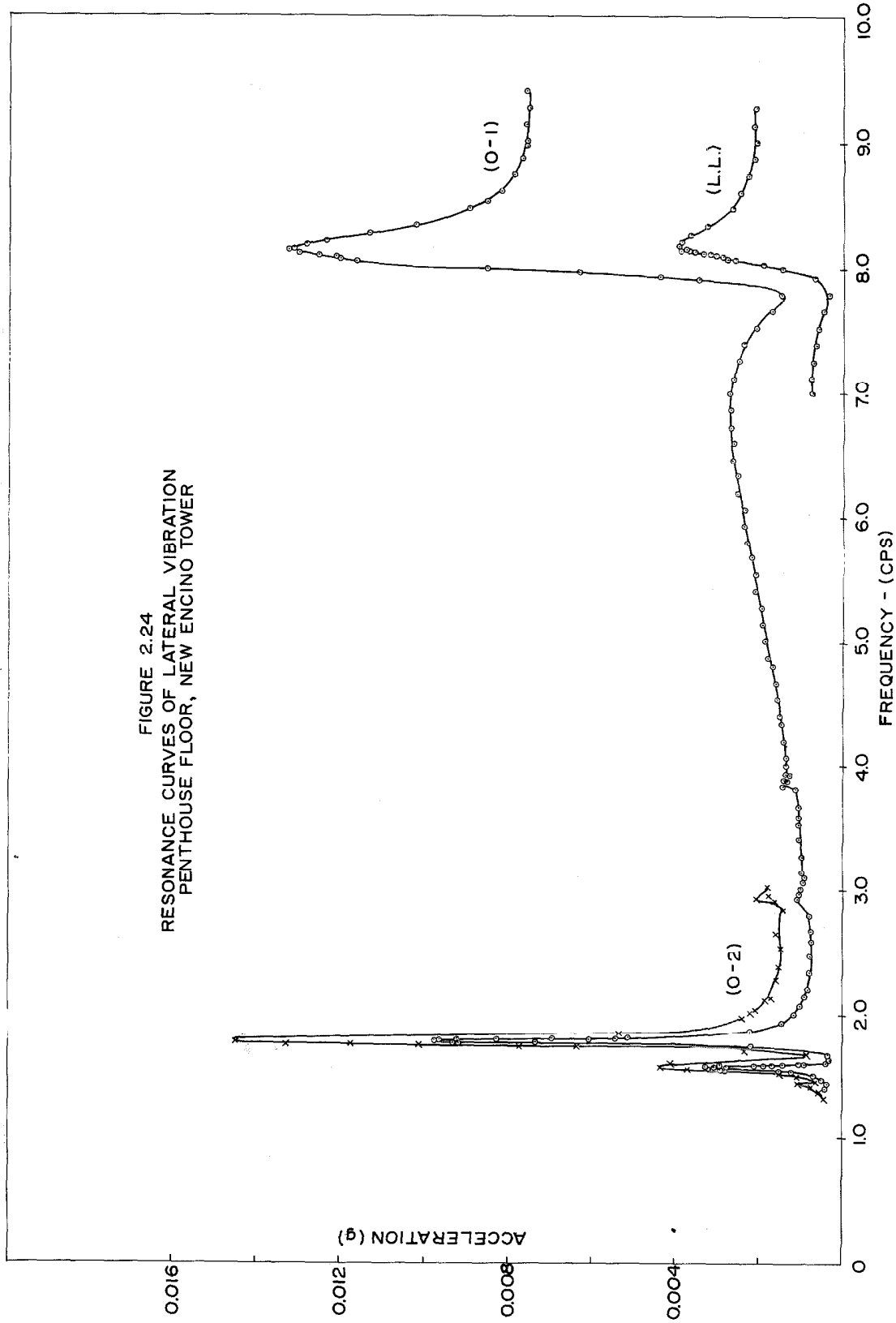

FIGURE 2.24
RESONANCE CURVES OF LATERAL VIBRATION
PENTHOUSE FLOOR, NEW ENCINO TOWER

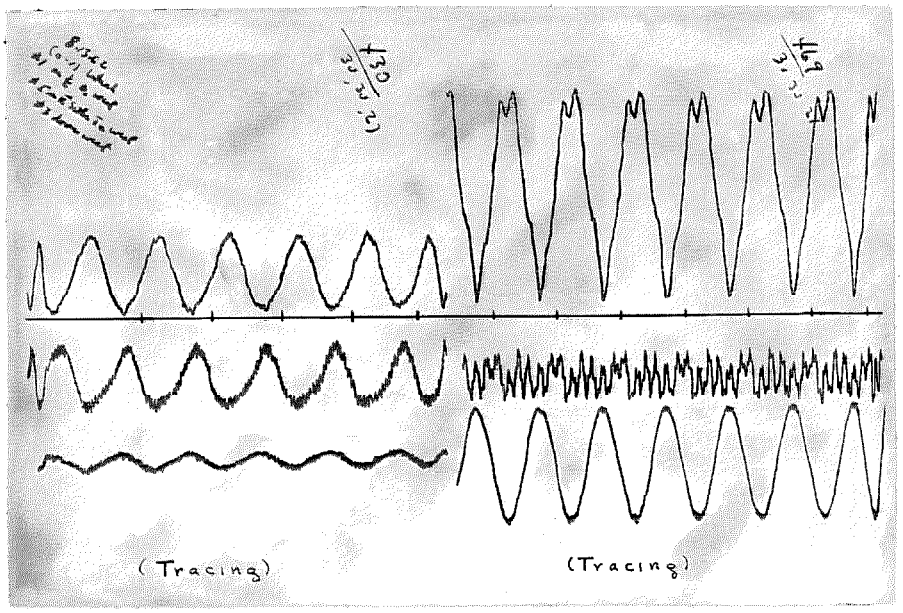

(a) (b)

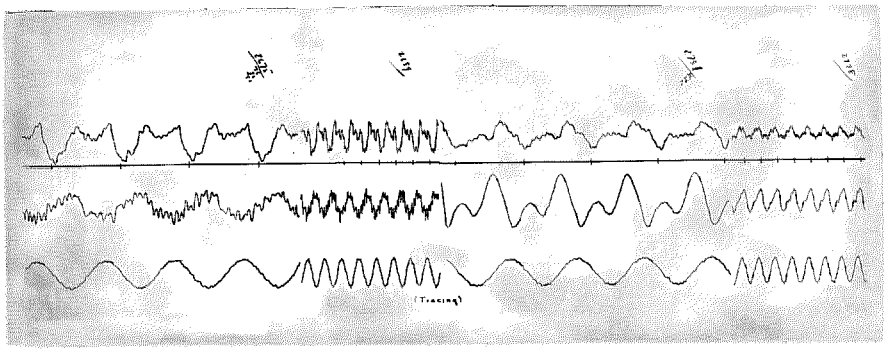

(c)

NONLINEAR ACCELERATION RECORDS

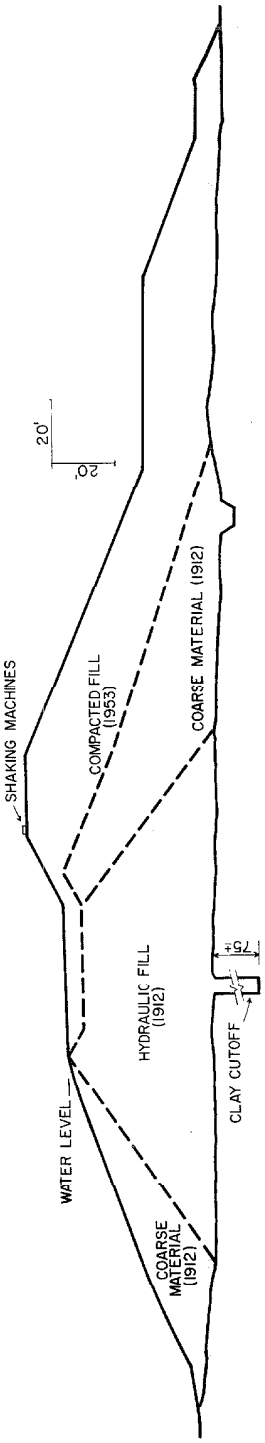

TRANSVERSE CROSS SECTION

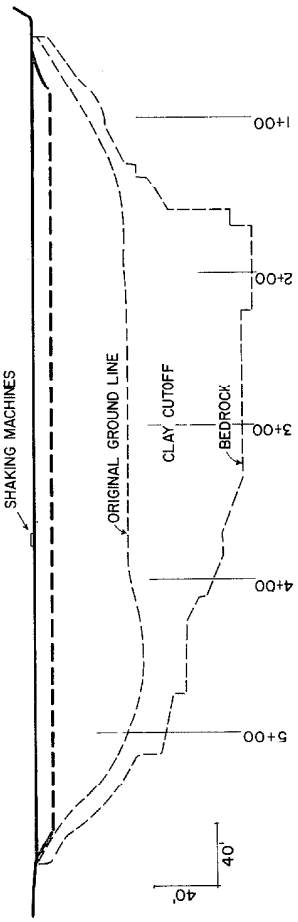

SECTION LOOKING UPSTREAM

FIGURE 3.1
SECTIONS OF DRY CANYON DAM

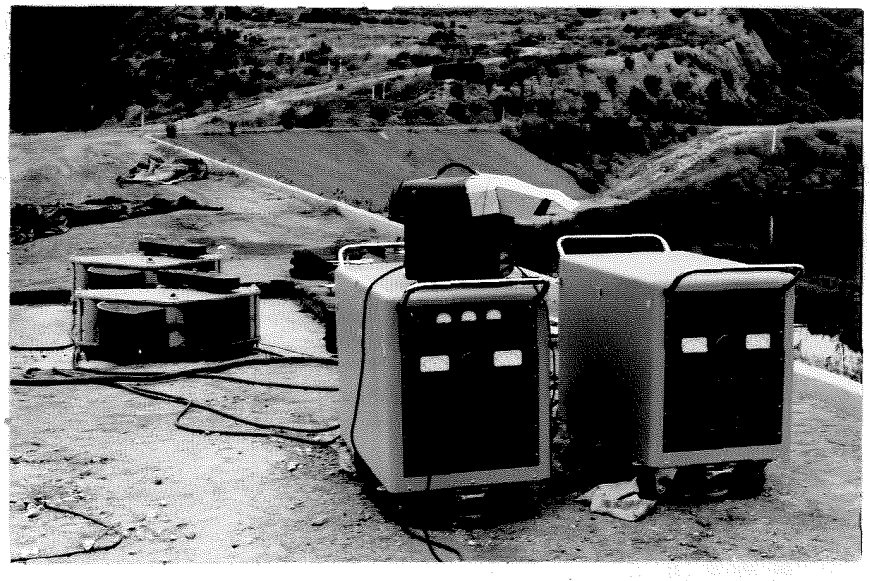

STRUCTURAL EXCITERS ON DRY CANYON DAM

FIGURE 3.2

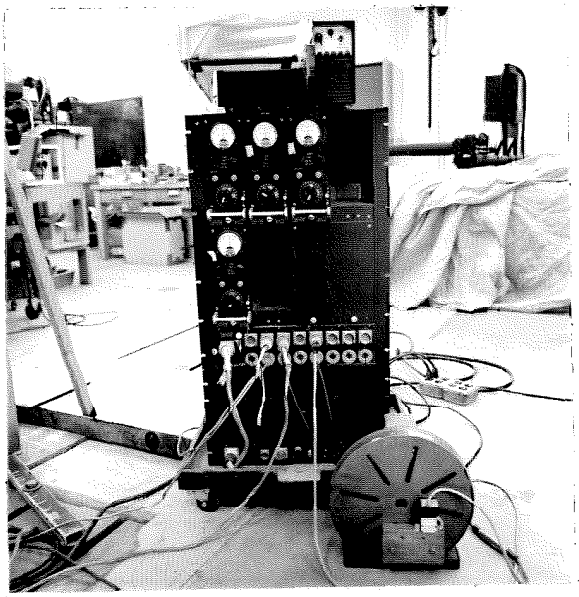

INSTRUMENTATION

FIGURE 3.3

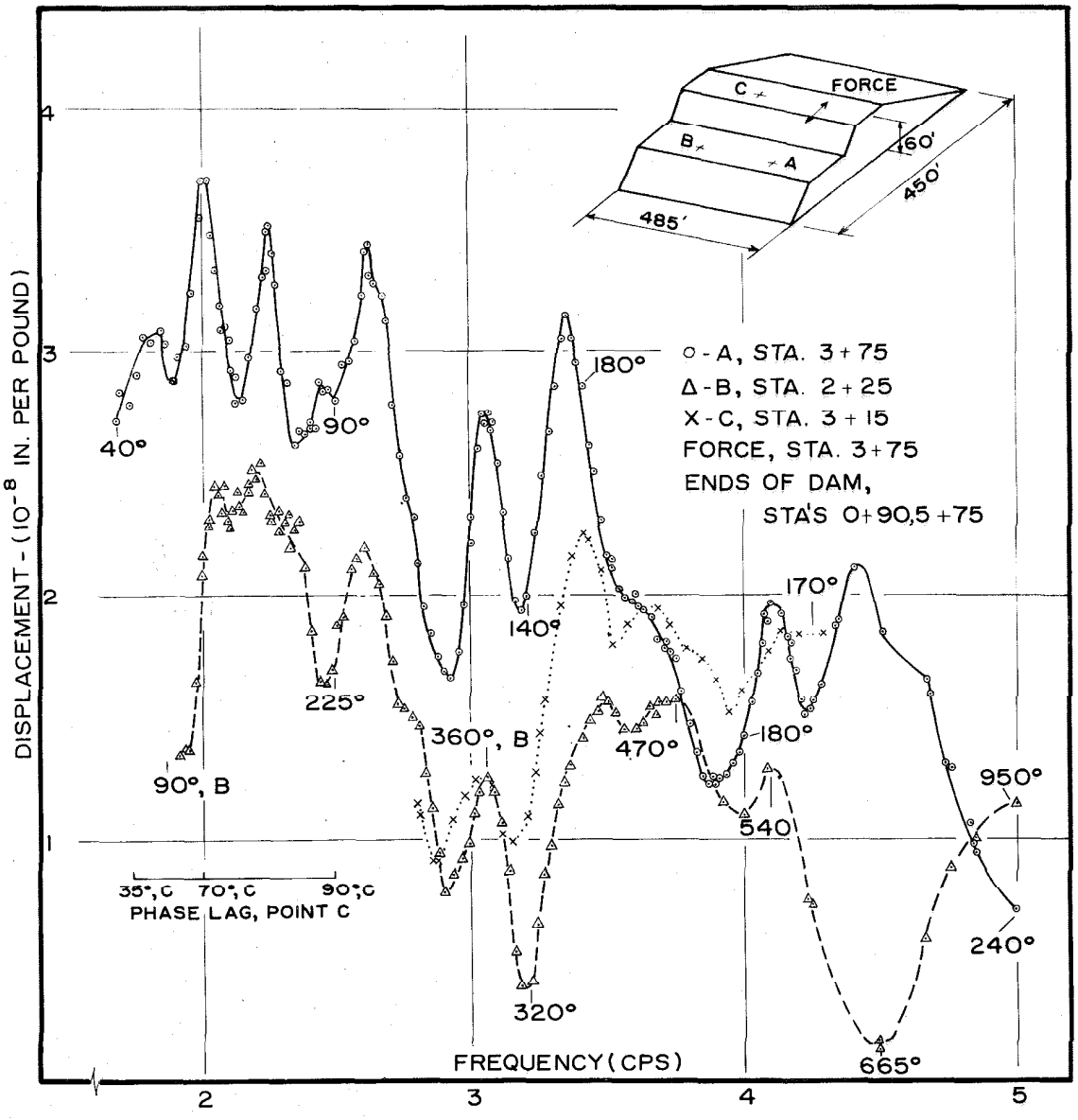

FIGURE 3.4
EXPERIMENTAL RESONANCE CURVES OF
DRY CANYON DAM

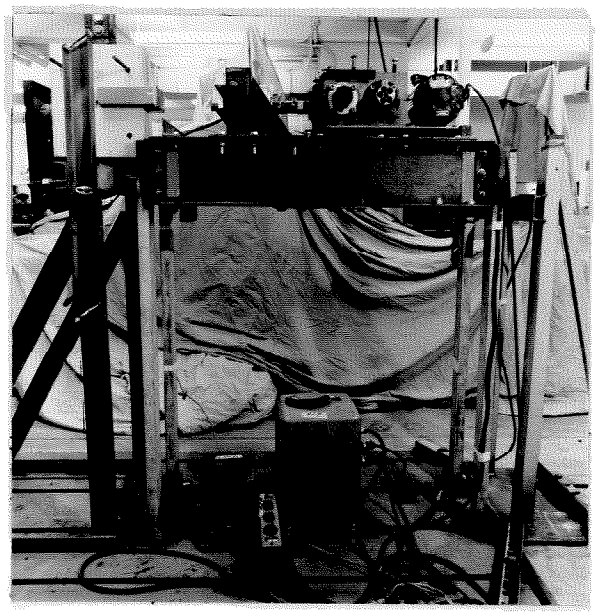

LABORATORY STRUCTURE, SOUTH SIDE

FIGURE 4.3

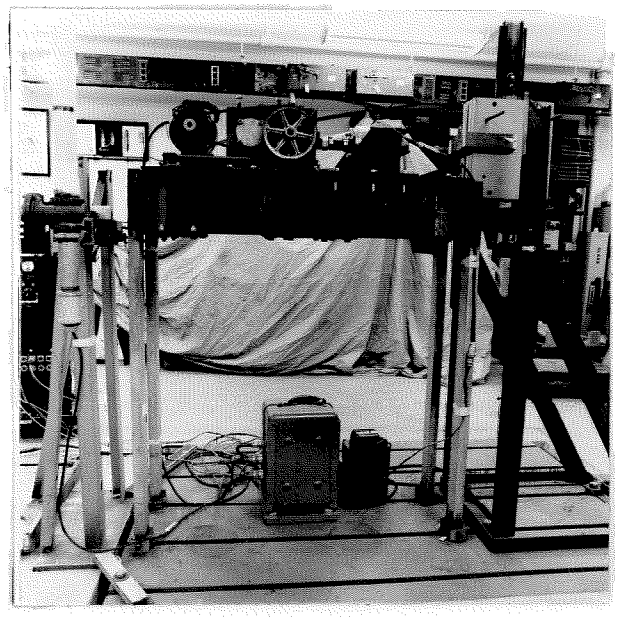

LABORATORY STRUCTURE, NORTH SIDE

FIGURE 4.4

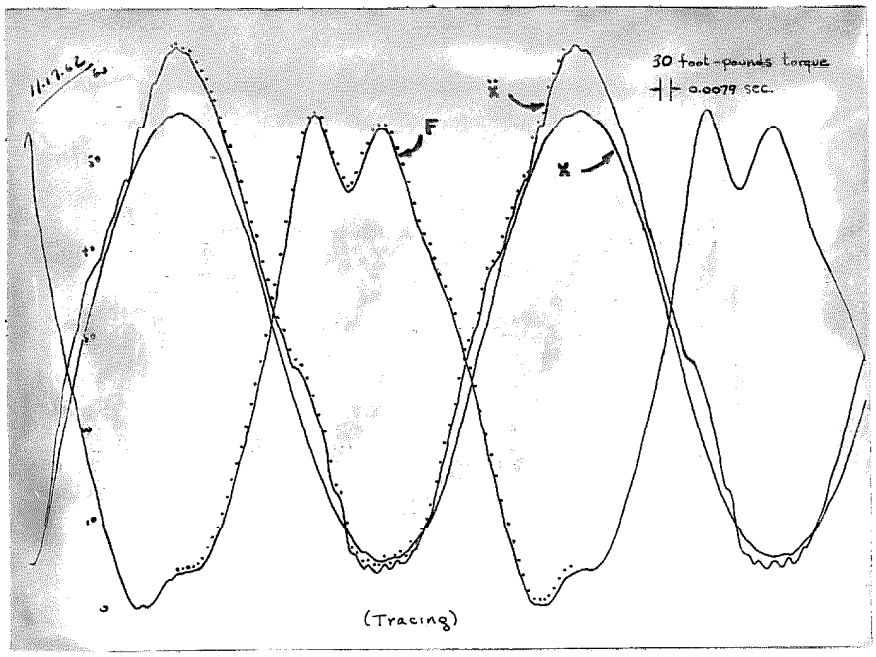

OSCILLOGRAM, 30 FOOT-POUNDS BOLT TORQUE

FIGURE 4.5

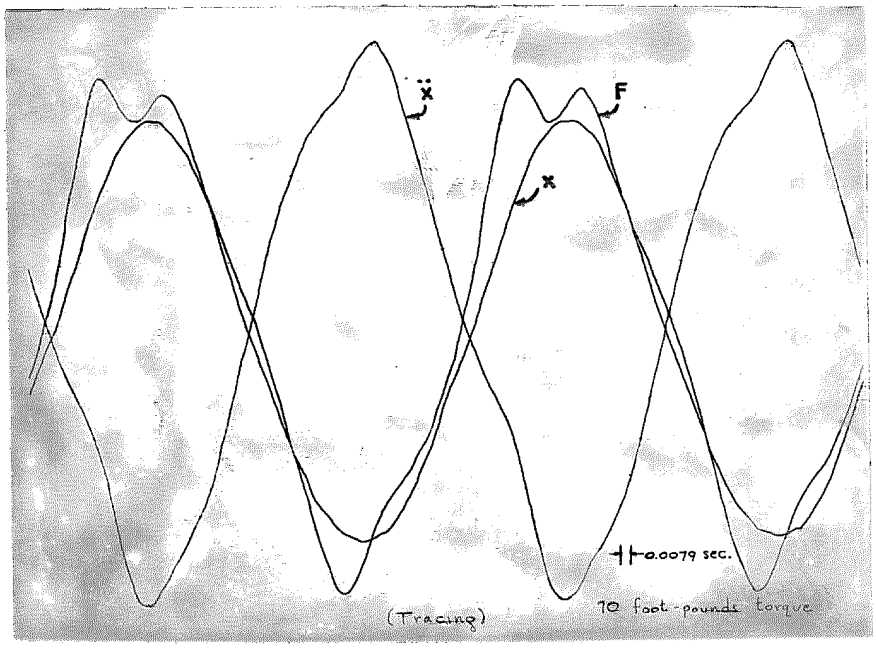

OSCILLOGRAM, 70 FOOT-POUNDS BOLT TORQUE

FIGURE 4.6

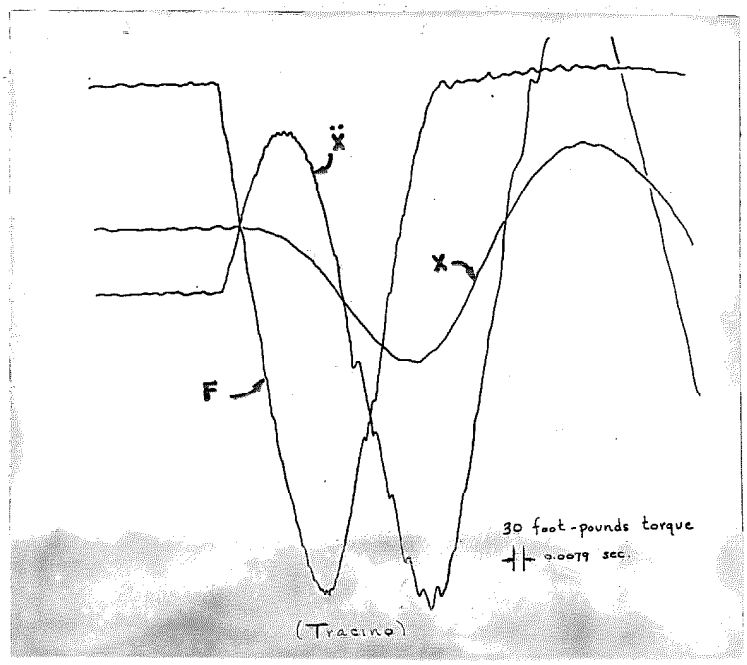

OSCILLOGRAM, PENDULUM IMPULSE

FIGURE 4.10